

COAL STRUCTURE AND COAL SCIENCE: OVERVIEW AND RECOMMENDATIONS

Richard C. Neavel

Exxon Research and Engineering Co., P.O. Box 4255, Baytown, Texas 77520

Coal is a sedimentary rock accumulated as peat and composed principally of macerals, subordinately of minerals, and containing water and gases in submicroscopic pores. Macerals (mas' er - als) are organic substances derived from plant tissues and exudates that have been variably subjected to decay, incorporated into sedimentary strata, and then compacted, hardened, and chemically altered by natural (geological) processes.

Coal is not a uniform mixture of carbon, hydrogen, oxygen, sulfur, and minor proportions of other elements; nor is it, as is often implied, simply a uniform, polyaromatic, "polymeric" substance. Rather, it is an aggregate of microscopically distinguishable, physically distinctive, and chemically different macerals and minerals.

Coal is analogous to a fruitcake, formed initially as a mixture of diverse ingredients, then "baked" to a product that is visibly heterogeneous. The heterogeneous nature of coal is evident in Figure 1, a photomicrograph of a polished surface of a piece of typical coal. The different macerals reflect different proportions of incident light and are therefore distinguished as discrete areas exhibiting different shades of gray. It should be evident that any attempt to characterize the chemical structure of this coal without recognizing the organization of the elements and molecules into discrete substances would be like trying to describe the essence of a fruitcake by grinding it up and analyzing its elemental composition.

The heterogeneity of coal, exemplified by Figure 1, is inherited from the diversity of source materials which accumulated in a peat swamp. Coals may be compared, contrasted and classified on the basis of variations in the proportions of these microscopically identifiable components. Such a classification is referred to as a classification according to type. Coals may also be classified according to how severely geological alteration processes, referred to collectively as metamorphism, have affected their properties. This is classification according to rank. These two classification methods are independent and orthogonal; therefore, within certain limits, any type of coal can be found at any rank.

Classification according to type involves the relative proportions of both the inorganic substances and the different organic substances. Because only the organic material is altered by metamorphic processes, rank classification is independent of inorganic content. Inorganic material is significant in commercial uses of coal, and its presence must be accounted for in scientific studies. The present discussion, however, concentrates on the properties of the organic substances, because only the organic macerals make coal the valuable material that it is.

In Figure 1, selected areas are identified as vitrinite, liptinite, and inertinite. These terms refer to the three major classes of macerals recognizable in all ranks of coal except those of the highest ranks. A few of the more significant features of these major classes of macerals and of their more important subclasses are summarized in Figure 2. It can be seen from Figure 2 that the differentiation of coals according to type, viz. according to the content of materials assignable to each of the maceral classes, is really a differentiation according to the ingredients which initially accumulated as peat to form that coal. Although the rank scale according to ASTM has been arbitrarily divided, and

specific segments have been identified by an epithet (i.e., lignitic, bituminous, anthracitic coals), there are no such well-recognized classes of coal types.

In this sense, there is essentially a continuous series of coals of different types, defined by microscopic quantification of their maceral (and mineral) contents. Particles of crushed coal, when cemented together as a solid block with a catalytically solidified resin or plastic, can be polished and examined microscopically. Individual particles derived from different layers of a coal seam, may differ significantly in maceral and mineral contents. Recognition of this feature has led to the concept of the microlithotype, wherein each particle can be classified according to its maceral content. In this procedure, arbitrary classes of particles are recognized according to specific maceral proportions as shown in Table 1. It is important that the scientist or technologist recognize that particles of the different microlithotypes are likely to perform quite dissimilarly when analyzed or processed; therefore, coals must be sampled carefully to prevent the selection of non-representative particles.

Each of the materials recognized as belonging to a specific maceral class (according to the criteria shown in Figure 2) has physical and chemical properties that depend upon its composition in the peat-swamp and the effects of subsequent metamorphic alteration. Thus, for instance, in all coals there is material derived from the structural tissues ("wood") of plants. These "woody" substances (lignin, cellulose) are the dominant components of plants, and hence their derivatives dominate in typical coals. In the peat swamp, some of the woody tissues may have been pyrolyzed by fire, forming a carbon rich char recognized as fusinite in the coal. In some coal layers, this may be the dominant maceral, and such layers would be referred to as fusinite-rich types of coal.

Much more commonly, though, the woody tissues accumulated below a water covering where imperfectly understood, largely microbiological processes converted them to humic substances of somewhat variable composition. These humic substances were subsequently altered by metamorphic processes (heat, pressure) into substances classifiable as one of the vitrinite macerals. Therefore, the physical and chemical properties of the vitrinitic materials in a specific coal were largely conditioned by the magnitude of temperature and pressure to which they were subjected after burial. Thus, one could say that the properties of the macerals in a given coal reflect the rank of the coal; or more correctly, one should say that the rank of the coal reflects the properties of macerals as conditioned by the severity of the metamorphic processes to which the coal was subjected.

One of the properties of macerals that changes progressively with metamorphic severity is the microscopically measurable reflectance of polished surfaces. Using a sensitive photomultiplier cell mounted on a microscope, it is possible to measure objectively the absolute percentage of incident light reflected from very small areas (5 μ m diameter) of polished coal surfaces. In Figure 3 is shown a series of reflectance distributions, each representing a sampling of the material in a coal of the rank indicated. These distributions are arbitrarily constructed to show what would happen to a given peat if it were to be subjected to increasingly more severe metamorphism. Recognize, of course, that these are "slices" through a continuum, and that no jump from rank to rank is implied. Properties such as carbon content, oxygen content, degree of aromaticity, and many others, could be substituted for the reflectance scale and a similar sort of picture would emerge. In Table 2, some typical values are shown for selected properties of vitrinite macerals in different rank coals. In Table 3, a number of the properties of non-vitrinite macerals are compared to those of vitrinite from coal of the same rank.

Typical U.S. coals are relatively vitrinite-rich, therefore analyses of whole coals, when appropriately corrected for inorganic content, reflect, to a first approximation, the composition and properties of the included vitrinite. For this reason, the parameters employed to classify coals according to rank, reflect the

rank (stage of metamorphic development) of the vitrinite. Calorific values or fixed carbon yields are calculated to a so-called mineral-matter-free basis for use in the ASTM classification of coals according to rank (1). It is essentially impossible to obtain inorganic-free samples; therefore, to represent organic matter accurately in comparative studies of any of the organic properties of coal, analytical data must be converted to an inorganic-free basis. Commonly, a dry, ash-free (DAF*) basis is employed. It is preferable, however, to convert to a dry, mineral-matter-free (DMMF) basis, as discussed by Given and Yarzab (2). In fact, the most meaningful assessment of coal rank or of the properties of coals of different ranks should be done with samples of concentrated vitrinite or on samples where the vitrinite comprises more than about 80% of the organic fraction. Because reflectance is closely correlative with many rank-sensitive properties and its determination can be made on vitrinite alone, it has become a widely accepted parameter to designate the rank of a coal (see Figure 4). Unfortunately, even when a reflectance value is available, it may not be reported in scientific publications. I strongly recommend that petrographic analyses and vitrinite reflectance be reported for samples on which structural studies are conducted.

Although many properties of vitrinites appear to change in a more or less parallel fashion as a result of metamorphism, there is considerable scatter in their correlation. Figure 5 is offered as evidence of this contention. The data plotted in Figure 5 are from coals containing more than 80% vitrinite on a DMMF basis (3). It is obvious that the progression from high to low H/C and O/C values reflects the influence of more severe metamorphic alteration; in other words coals toward the lower H/C and O/C end of the band are higher rank. However, the fact that the data do form a band, rather than a linear progression, implies that there is not a simple scale which defines the rank progression. As Given and his co-workers have so eloquently shown, the geological/geographical disposition of U.S. coals appears to exert some, as yet undefined, influence on the intercorrelations of coal properties (4).

Clearly, neither geology nor geography are coal properties and hence cannot be "measured". Different source materials, depositional conditions (including especially sulfur availability), and time/temperature/pressure conditions during metamorphism, interacted so as to provide a multitude of potential paths which different coals (or even vitrinites in different coals) followed to their present condition. In other words, the concept of a single rank progression is more fallacy than fact.

As unifying, underlying concepts, type and rank certainly can be validly employed to envision why coals have the properties that they do. However, it is time for a re-evaluation of coal classification concepts. How can we measure rank when we analyze coals of different types and when there is no simple rank progression even when vitrinite or vitrinite-rich coals are compared? And how can we assess type when maceral identification criteria are highly subjective, except for reflectance measurements that routinely are not even applied to the liptinite and highly variable inertinite macerals? And, finally, how can coals be classified scientifically when empirical and derived properties like calorific value and fixed carbon yield are employed as classifying parameters?

A scientific classification should be based first on the fundamental properties of the vitrinite in coals. This means, at the very least that element concentrations and molecular structure configurations must be assessed. The structural properties of most importance to classification and process responses

*Not 'MAF', which is often unfortunately used as an abbreviation for moisture-and-ash-free.

appear to be: (1) the nature of hydrogen bonding and physical entanglement that cohere molecular moieties, (2) the nature of cyclical structures (e.g., ring condensation index, aromaticity, heteroatoms), (3) amount and distribution of hydro-aromatic hydrogen, (4) scissle bridging structure (e.g., ether, sulfides, polymethylenes), (5) functional group characteristics (esp. oxygen- and sulfur-containing), and (6) organic/inorganic interactions. To develop the basis of a scientific classification, these determinations need to be made on a large number of vitrinite-rich coal samples spanning a wide range of rank. Because coals are sensitive to oxidation and moisture changes during handling, these samples must be carefully collected, prepared and preserved.

It is fairly evident that because of the complex interactions of depositionally-influenced and metamorphically-influenced properties, the fundamental chemical/structural properties will need to be related to each other in a complex statistical fashion. A multivariate correlation matrix such as that pioneered by Waddell (5) appears to be an absolute requirement. However, characterization parameters far more sophisticated than those employed by Waddell are required. One can hope that, as correlations between parameters become evident, certain key properties will be discovered which will allow coal scientists and technologists to identify and to classify vitrinites uniquely. Certain optical properties might prove valuable in this respect. It would then not be necessary for every laboratory to have super-sophisticated analytical equipment at its disposal in order to classify a coal properly. By properly identifying/classifying the vitrinite in a coal, one could then estimate accurately the many other vitrinite properties available in the multivariate correlation matrix.

Of course, elucidation of vitrinite properties and establishment of unique vitrinite class identifiers would not solve all of the problems of coal classification. Further work needs to be done to characterize the inorganic materials in coals, especially developing simple tests for quantification of inorganic species.

Once vitrinites could be properly identified and classified, then it would be necessary to characterize and to identify uniquely the members of the other maceral classes. It is probable that liptinite properties change in some fashion correlative with the changes wrought by metamorphism on vitrinite. Therefore, classification of vitrinite would automatically classify liptinite. Whether inertinite changes with rank is uncertain; but it is certain that far better differentiation of fusinites needs to be employed for it is evident that fusinite reflectance values span wide ranges in a given coal.

A multivariate vitrinite classification, supplemented by information about the inorganic matter and the proportions and properties of associated macerals, would be of little value if it could not be used to predict the response of a given coal in a processing system and thereby provide an estimate of the value of that coal. Consequently, it will be necessary to relate the scientific classification to the responses of coals in such processes as pyrolysis, liquefaction, gasification, combustion, and coke-making. This can only be done by relating the fundamental, classifying properties to empirically determined processing responses on a substantial number of samples. Again, they should be vitrinite-rich and cover a broad range of ranks.

Only through the conduct of an integrated program more or less along the lines that I have outlined is Coal Science ever going to move out of the era of the 1950's where it is now mired. The scattered probes of coal structural properties on a bewildering range of poorly selected, poorly collected, poorly prepared, poorly preserved and poorly characterized coal samples will lead us only into further confusion. Progress in Coal Science can only be made when scientific and technological investigations on coal result in a comprehensive integration and synthesis of data and information. The essence of science is

"the reduction of the bewildering diversity of unique events to manageable uniformity within one of a number of symbol systems" (6). Present investigations of coal structure hardly conform to that definition today, and therefore hardly deserve the epithet of Coal Science.

References

1. Annual Book of ASTM Standards, Designation D388, standard specification for the classification of coals by rank.
2. Given, P. H., R. F. Yarzab, Problems and solutions in the use of coal analyses, Coal Res. Sect., Penn. State Univ., Tech. Rpt. No. FE 0390-1, 1975.

Given, P. H., The use of daf and dmmf ultimate analyses of coals, Fuel, 55, 256, 1976.

Given, P. H., W. Spackman, Reporting of analyses of low-rank coals on the dry, mineral-matter-free basis, Fuel, 57, 219, 1978.
3. Spackman, W., and others, Evaluation and development of special purpose coals; final report, Coal Res. Sect., Penn. State Univ., Tech. Rpt. No. FE 0390-2, 1976.
4. Abdel-Baset, M. B., R. F. Yarzab, P. H. Given, Dependence of coal liquefaction behavior on coal characteristics. 3. statistical correlations of conversion in coal-tetralin interactions, Fuel, 57, 89-94, Feb. 1978.
5. Waddel, C., A. Davis, W. Spackman, J. C. Griffiths, study of the inter-relationships among chemical and petrographic variables of United States coals, Coal Research Section, Penn. State Univ., Tech. Rpt. FE-2030-9, 1978.
6. Huxley, Aldous, Education at the non-verbal level, Daedalus, spring 1962.

TABLE 1. CLASSIFICATION OF MICROLITHOTYPES

	<u>Micro lithotype</u>	<u>Maceral</u>	<u>Volume Percent</u>
Monomaceralic	Vitrite	Vitrinite (V)	> 95%
	Liptite	Liptinite (L)	> 95%
	Inertite	Inertinite (I)	> 95%
Bimaceralic	Clarite	V + L	> 95%
	Vitrinerite	V + I	> 95%
	Durite	I + L	> 95%
Trimaceralic	Duroclarite	V + I + L	V > (I + L)
	Clarodurite	V + I + L	I > (L + V)
	Vitrinertoliptite	V + I + L	L > (I + V)
	Carbominerite	V, L, I and Mineral Matter (MM)	MM > 20%, < 60%

TABLE 2. SELECTED PROPERTIES OF VITRINITES IN
COALS OF DIFFERENT RANKS

	<u>Liq.</u>	<u>Sub-Bit.</u>	<u>Bit.</u>	<u>Anth.</u>
Moisture Capacity, Wt. %	40	25	10	< 5
Carbon, Wt. % DMMF	69	74.6	83	94
Hydrogen, Wt. % DMMF	5.0	5.1	5.5	3.0
Oxygen, Wt. % DMMF	24	18.5	10	2.5
Vol. Mat., Wt. % DMMF	53	48	38	6
Aromatic C/Total C	0.7	0.78	0.84	1.0
Density (He, g/cc)	1.43	1.39	1.30	1.5
Grindability (Hardgrove)	48	51	61	40
Btu/lb, DMMF	11,600	12,700	14,700	15,200

DMMF = Dry, Mineral-matter-free basis. These are typical values for rank classification. Sulfur and nitrogen are rank-independent and not shown.

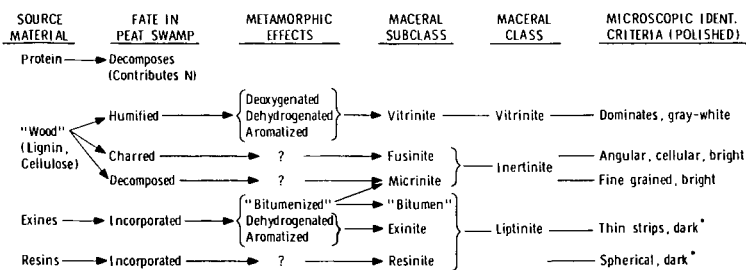
TABLE 3. PROPERTIES OF MACERALS COMPARED TO VITRINITE IN SAME COAL
(Subbituminous and High-Volatile Bituminous Only)
Magnitude of property greater than (>), less than (<), or
equal to (=) that of associated vitrinite.

	<u>Inertinite</u>			
	<u>Semi-Fusinite</u>	<u>Fusinite</u>	<u>Micrinite</u>	<u>Exinite</u>
<u>Optical Properties</u>				
Reflectance	>	> >	>	<
Fluorescence				>
<u>Chemical Structure</u>				
Basic carbon structure				=
Molecular weight				>
H/C ratio	<	< <	=	>
H aliphatic/H total;-CH ₂ ; hydroaromaticity				>
Fraction aromatic C; rings/unit		>	>	<
Oxygen _{OH} /Oxygen _{Total}		<		<
Unpaired spins by ESR		>		<
Unpaired spins of fusinite with same carbon as vitrinite		>		
<u>Reactivity</u>				
Methane sorption		>		
Decomposition temperature				<
Oxidizability				<
Reduction with Li in EtDA		<	=	<



Figure 1. Photomicrograph of polished surface of a high-volatile bituminous coal.
 Vit. = Vitrinite; Inert. = Inertinite; Liptin. = Liptinite

FIGURE 2. PRINCIPAL MACERAL CLASSES



* In Low-Vol Bituminous and Anthracites, Liptinite Indistinguishable from Vitrinite

FIGURE 3. REFLECTANCE DISTRIBUTION OF MACERALS IN TYPICAL COALS

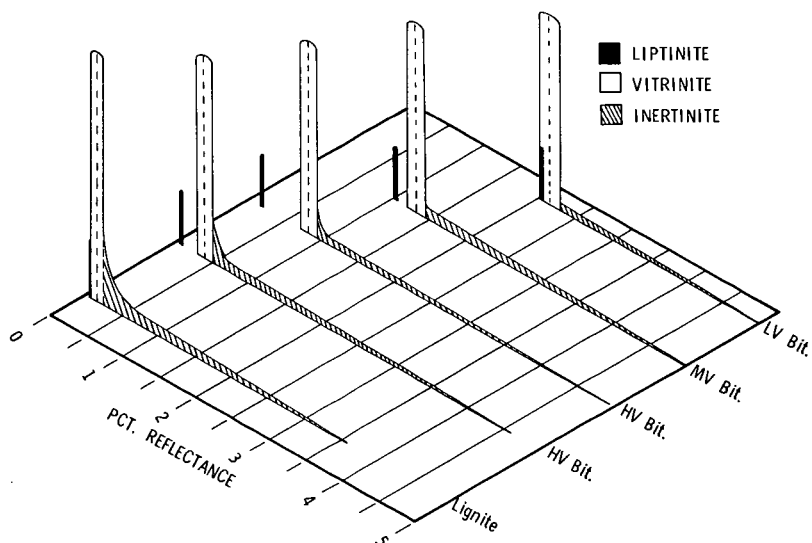


FIGURE 4. CORRELATION OF REFLECTANCE OF VITRINITE
AND CARBON CONTENT OF COALS. DATA FROM REF. 3

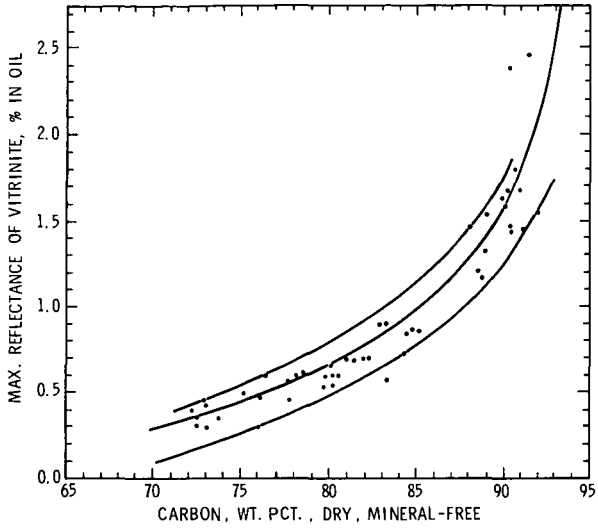
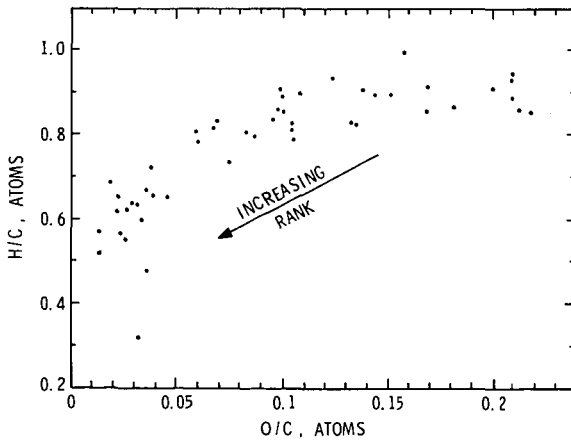


FIGURE 5. CORRELATION OF ATOMIC H/C AND O/C FOR
COALS OF DIFFERENT RANKS. DATA FROM REF. 3



NATURE OF THE FREE RADICALS IN COALS, PYROLYZED COALS,
AND LIQUEFACTION PRODUCTS

H. L. Retcofsky, M. R. Hough

Pittsburgh Energy Technology Center, U. S. Department of Energy
4800 Forbes Avenue, Pittsburgh, PA 15213

R. B. Clarkson

Varian Associates, Instrument Division
611 Hansen Way, Palo Alto, CA 94303

Electron spin resonance (ESR) spectrometry has been the favored instrumental tool to probe the nature of the free radicals in coals and materials derived from coal (1). Recently, it was shown that these free radicals are also amenable to study by electron nuclear double resonance (ENDOR) spectrometry (2,3). The ENDOR technique is becoming increasingly popular in free radical studies because frequently the resulting spectra are much more highly resolved than corresponding ESR spectra of the same materials (4).

As a first step toward elucidating the role of free radicals in the liquefaction of coal, the stable radicals present in coals, pyrolyzed coals, and liquefaction products require characterization. In the present characterization study we have applied both the ESR and ENDOR techniques. For many of the samples examined, it was found that great care must be taken during sample preparation to ensure reliability of the spectral data.

Coals. ESR measurements on non-anthracitic and young anthracitic coals can be made with little difficulty. It is best to evacuate the samples since it has been shown that the ESR spectra of fusains, petrographic constituents found in nearly all coals, are quite sensitive to the presence or absence of air (oxygen) in the sample (5). Contrary to other evidence in this report (5), high rank anthracites and meta-anthracites do require dilution of the samples with a non-conducting medium to prevent errors in ESR measurements due to microwave skin effects. For example, the ESR intensity of a meta-anthracite from Iron County, Michigan increased significantly rather than decreased after the sample was diluted with KBr.

For non-anthracitic coals, the observed variation of the ESR g value with coal rank suggested that the naturally occurring radicals in coals become more "hydrocarbon-like" as coalification progresses (6). Evidence supporting this hypothesis is depicted in Figure 1. The plot of ESR g values vs oxygen contents of the coals suggests that the unpaired electrons in low rank coals interact with oxygen atoms in the sample. Statistical treatment of the data revealed that the g values of only two of the coals fall outside the area bounded by the dashed lines drawn \pm twice the standard error of estimate from the linear regression line. These two coals are somewhat unique in that they contain an unusually high content of organic sulfur (7). In the second plot of Figure 1, the abscissa has been changed to reflect the sum of the oxygen and sulfur contents of the coals, (each element being weighted according to its spin-orbit coupling constant). This latter plot exhibits much better statistics, suggesting that the unpaired electrons interact with sulfur as well as with oxygen. Attempts to extend the statistical treatment to nitrogen in the samples were inconclusive.

Pyrolyzed Coals. A number of investigators have applied ESR techniques to pyrolyzed coals (1). At least two groups of investigators (8,9) have reported g values less than that of the free electron for certain coals heated to commonly used liquefaction temperatures. One group (9) attributed these low g values to the

presence of sigma radicals. During the present investigation, we observed a similar g value dependence with heat-treatment temperature for hvAb coal from the Ireland Mine (Pittsburgh bed) in West Virginia.

It had been shown previously (10) that incorrect ESR g values were obtained for heat-treated sucrose if proper dispersal techniques were not used. With this in mind, we measured the effect of sample dilution on the apparent g value of Ireland Mine coal heat-treated to 450°C. The results, shown in Figure 2, show that the true g value of the sample in question is actually higher than that of the free electron. This suggests that great care must be exercised when applying ESR techniques to heat-treated coals. This problem will undoubtedly present some obstacles to the in situ ESR studies of coal pyrolysis and coal liquefaction planned by many laboratories.

Liquefaction Products. A few ESR studies of liquefaction products from coal have been reported (6,11,12). One group of investigators (6) concluded from ESR studies of coal-derived asphaltenes that charge-transfer interactions are relatively unimportant binding forces between the acid/neutral and base components.

ESR results from our on-going efforts to elucidate the changes in chemical structure that occur during coal liquefaction are given in Table 1. The samples examined were obtained from a liquefaction run in the Pittsburgh Energy Technology Center's 10 lb coal/hr process development unit (13). The run was made without added catalyst. The samples included the process coal and its pyridine extract, and the preasphaltenes, asphaltenes, and oils separated from the centrifuged liquid product. It can be seen that the free radical contents change in the order: process coal < preasphaltenes >> asphaltenes > oils. The g values suggest the presence of "hydrocarbon-like" radicals with perhaps some interaction between the unpaired electrons and heteroatoms in the asphaltene and oil fractions. The line widths appear to increase (at least crudely) with increasing hydrogen contents of the samples.

ENDOR Studies. In contrast to the ESR spectra of coals, which generally consist of a single line devoid of any resolvable fine structure due to hyperfine interactions, the ENDOR spectra (at least in the present study) are rich in detail (Figure 3). These results are quite surprising in light of spectra published several months ago which showed only a single band at the so-called free proton frequency (2). In an attempt to experimentally deduce the reasons for this apparent discrepancy of results, we found a reversible effect of air (oxygen) on the ENDOR spectrum, i.e., the hyperfine lines were observed for evacuated samples, but disappeared upon admission of air to the samples.

The fact that an ENDOR spectrum is observed under the experimental conditions employed is unambiguous proof that the unpaired electrons in the coal couple with nuclear spins, undoubtedly protons, in the sample. This provides additional support for the free radical interpretation of the ESR spectrum. The magnitude of the hyperfine interactions, i.e., none greater than 10 gauss, indicates that none of the radicals has a high unpaired electron spin density at a particular carbon atom.

Table 1. MAF analyses, carbon aromaticities, and electron spin resonance data for materials produced from the liquefaction of West Virginia (Ireland Mine) hvAb coal in the Pittsburgh Energy Technology Center's 10 lb coal/hr process development unit.

	COAL		PREASPHALTENES	ASPHALTENES	OILS
	Solid Coal	Pyridine Extract			
<u>MAF Analysis, %</u>					
C	78.5	81.7	86.9	87.3	86.6
H	5.6	5.9	5.1	6.3	8.2
O	9.7	8.0	4.8	3.6	3.3
N	1.2	1.9	2.2	2.0	1.2
S	4.9 _i	2.6	0.9	0.9	0.7
f _a	0.76 ^{1/}	0.73 ^{1/}	0.84 ^{1/}	0.77 ^{2/}	0.63 ^{2/}
<u>ESR Data</u>					
Free Spins/Gram	1.4x10 ¹⁹	9.0x10 ¹⁸	2.0x10 ¹⁹	2.4x10 ¹⁸	9.4x10 ¹⁷
g value	2.0027 ₇	2.0031 ₂	2.0027 ₉	2.0032 ₉	2.0030 ₇
Linewidth, gauss	5.9	5.7	6.6	7.3	8.7

^{1/}f_a determined by cross-polarization ¹³C NMR.

^{2/}f_a determined by high-resolution ¹³C FT NMR.

REFERENCES

1. For reviews of the early literature see (a) H. Tschamler and E. De Ruiter, "Chemistry of Coal Utilization", Suppl. Vol. H. H. Lowry, Ed., Wiley, New York, 1963, p. 78; (b) W. R. Ladner and R. Wheatley, Brit. Coal Util. Res. Assoc. Monthly Bull., 29, 202 (1965); and (c) D. W. Van Krevelen, "Coal", Elsevier, Amsterdam, 1961, p. 393.
2. S. Schlick, P. A. Narayana, and L. Kevan, J. Am. Chem. Soc., 100, 3322 (1978).
3. H. L. Retcofsky and M. R. Hough, "Electron Spin Resonance Studies of Coals and Coal Liquefaction", Paper presented at the 29th Pittsburgh Conference on Analytical Chemistry and Applied Spectroscopy, Cleveland, Ohio, February 27-March 3, 1978.
4. L. Kevan and L. D. Kispert, "Electron Spin Double Resonance Spectroscopy", Wiley, 1976, p. 2.
5. H. L. Retcofsky, J. M. Stark, and R. A. Friedel, Anal. Chem., 40, 1699 (1968).
6. H. L. Retcofsky, G. P. Thompson, M. Hough, and R. A. Friedel, Chapter 10 in "Organic Chemistry of Coal", John W. Larsen, Ed., ACS Symposium Series, No. 71, 1978, p. 142.
7. R. M. Eloffson and K. F. Schulz, Preprints, Am. Chem. Soc. Div. Fuel Chem., 11, 513 (1967).
8. S. Toyoda and H. Honda, Carbon, 3, 527 (1966).
9. L. Petrakis and D. W. Grandy, Anal. Chem., 50, 303 (1978).
10. L. S. Singer, Proc. Fifth Carbon Conf., 2, Pergamon Press, 1963, p. 37.
11. D. L. Wooten, H. C. Dorn, L. T. Taylor, and W. M. Coleman, Fuel, 55, 224 (1976).
12. T. F. Yen, Private Communications.
13. P. M. Yavorsky, S. Akhtar, J. J. Lacey, M. Weintraub, and A. A. Reznik, Chem. Eng. Prog., 71, 79 (1975).

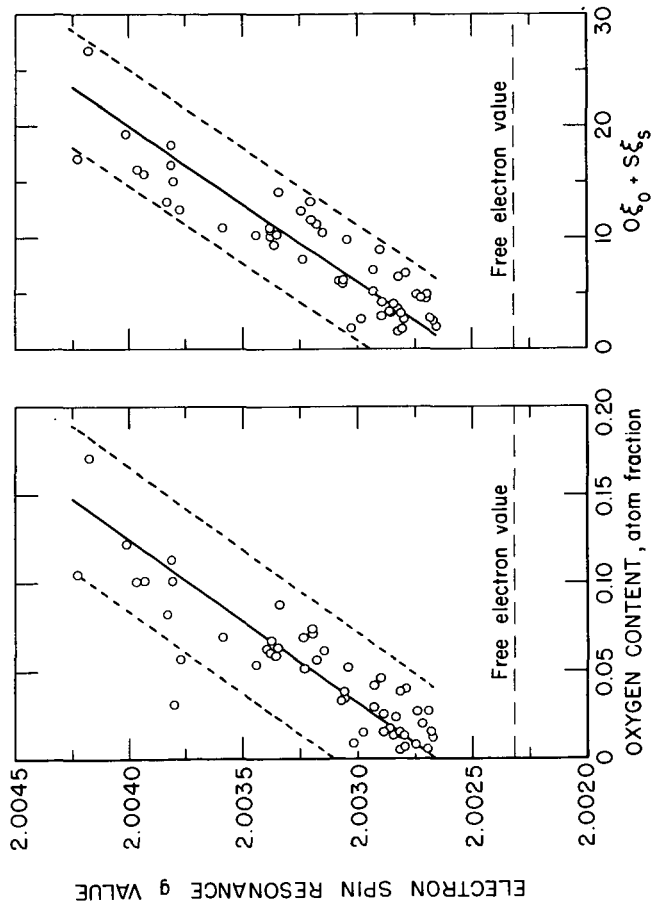


Figure 1. Functional dependences of the electron spin resonance g values of vitrains from selected coals.

11-4-77 L-15681

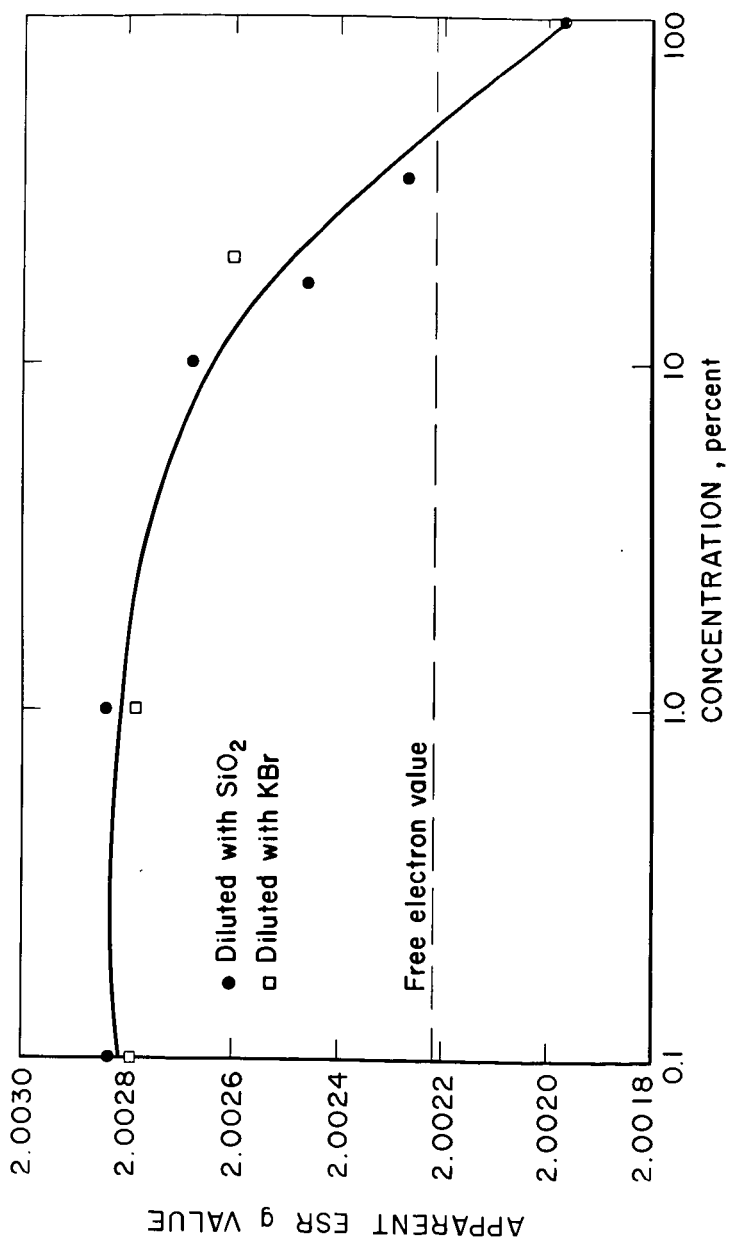


Figure 2. The effect of sample dilution on the apparent electron spin resonance g value of Ireland Mine hvAb coal heat-treated to 450°C.

11-29-78 L-16340

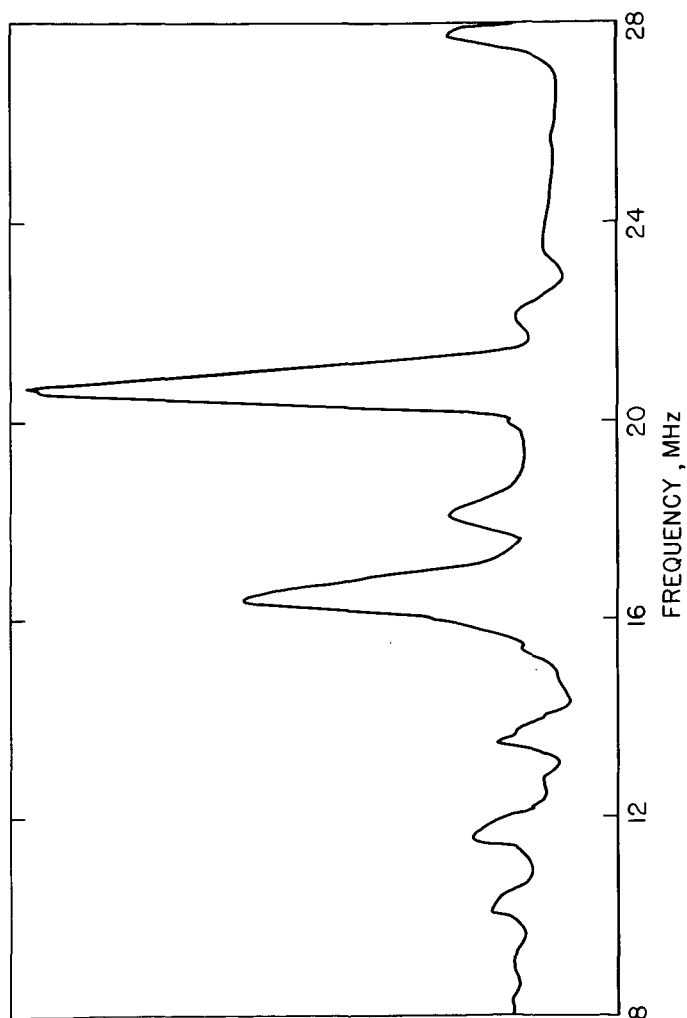


Figure 3. Electron nuclear double resonance (ENDOR) spectrum of vitrain -
rich Pittsburgh coal.

2-7-78 L-15839

A Tentative Identification of Average Aromatic Ring Size in an Iowa Vitrain and a Virginia Vitrain

B. C. Gerstein, L. M. Ryan, and P. Dubois Murphy

Ames Laboratory, U. S. Department of Energy, and
Department of Chemistry, Iowa State University
Ames, Iowa 50011

Introduction

A knowledge of the average aromatic ring size in coals is useful not only in indicating the appropriate chemistry one might use for conversion to fuel oil, but also as an indicator of possible physiological effects of contact with coals and coal products. In principle, NMR offers the capability of a direct determination of average ring size via an identification of the fractions of ^{13}C and ^1H in coals. Three factors prevent use of conventional NMR for this purpose in solid coals. The first is the effect of homonuclear and heteronuclear dipolar interactions which lead to linewidths of hundreds of ppm for both ^1H and ^{13}C in solid coals^(1a,b). The second is the fact that even in the absence of dipolar broadening, chemical shift anisotropies of ^1H can be as large as 34 ppm⁽²⁾ for, e.g. the single species ^1H in $\text{H}_2\text{O}(\text{s})$, such that a randomly oriented solid sample containing many protons in different chemical environments would exhibit an NMR spectrum in which individual protons could not be easily identified. A similar statement applies to NMR spectra of ^{13}C in solids. A third factor peculiar to coals is the possibility of an enormous number of chemically shifted species of a given nucleus, leading to NMR spectra which are still severely overlapping in the absence of broadening due to dipolar and chemical shift interactions.

In the present work, cross polarization to enhance sensitivity⁽³⁾ combined with strong heteronuclear decoupling⁽⁴⁾ and magic angle spinning⁽⁵⁾ to remove heteronuclear dipolar broadening and chemical shift anisotropy broadening are used to distinguish aliphatic from aromatic ^{13}C in Pocahontas #4 vitrain, and Star vitrain. Combined rotation and multiple pulse (NMR) spectroscopy (CRAMPS)⁽⁶⁾ are similarly used to narrow NMR spectra of ^1H in these coals. The ratios of aliphatic to aromatic ^1H and ^{13}C thus inferred are used to estimate an average aromatic ring size in the samples investigated.

Experimental

The NMR spectrometer used for determinations of spectra of both ^1H and ^{13}C has previously been described, (1a) as have the probes used for magic angle spinning^(7, 8). The Virginia coal "Pocahontas #4" was supplied by H. L. Retcofsky of the Pittsburgh Energy Research center of the U.S. Department of Energy. A vitrain portion of the Iowa coal "Star" was supplied by Dr. D. L. Biggs of the Iowa State University Department of Earth Sciences and the Ames Laboratory of the U. S. Department of Energy. The coals were analyzed for major constituents and free radical content as previously reported.⁽¹⁾ Results of these analyses are given in Table I.

Results

The high resolution solid state spectra of ^{13}C in both coals are shown in Figure 1. The high resolution solid state spectrum of ^1H in 2,6 dimethylbenzoic acid is shown in Figure 2, as an indication of the resolution available with equipment used in the present experiments. The high resolution solid state spectra of ^1H in both coals are

shown in Figures 3 and 4. Also indicated in Figures 2 - 4 are the Lorentzian lines used to approximate the total experimental spectra, indicated by crosses (+), and the sum of these lines indicated by the smooth curve through the experimental points.

The mole ratios of aromatic hydrogen to aromatic carbon implied by the elemental analyses given in Table I, and the fractions of aromatic to total hydrogen and carbon calculated from the results of estimating the integrated areas associated with these species as shown in Figures 2 - 4 yield the following values for (H_{Ar}/C_{Ar}): Pocahontas #4, 0.53; Star, 0.40. At first thought, these numbers seem a bit surprising, because Pocahontas, having the higher carbon content, is an older coal, and one would expect a larger ring size to correspond to the more "graphitized" material. A bit of reflection, as illustrated by the entries in Table II, might help to remove the ambiguity.

TABLE I

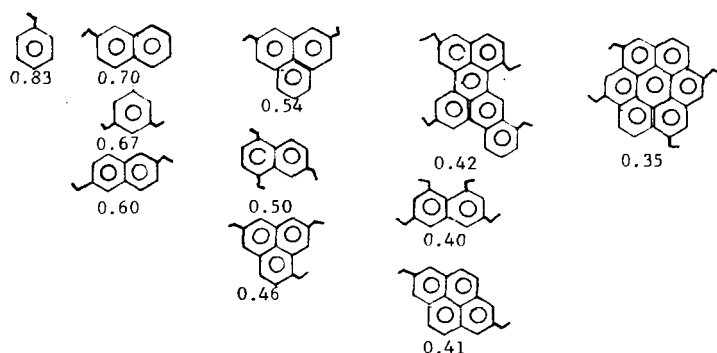
Elemental analyses, Wt% (maf), free radical concentration, and fractions of aromatic hydrogen and carbon.

SAMPLE	% C	%H	%N	%S	$[e^-]$, spins $g^{-1} \times 10^{-19}$ a	$\frac{Ar}{f_C}$	$\frac{Ar}{f_H}$
Pocahontas #4 Vitrain	90.3(2)	4.43(4)	1.28	0.85	4	0.86	0.77
Star Vitrain	77.0(1)	6.04(4)	1.17(14)	5.02	1.6	0.71	0.31

^a Determination made on unheated sample

Table II

Average aromatic ring size as a function of H_{Ar}/C_{Ar} and connectivity



The point to be made from Table II is that the average aromatic ring size inferred from the aromatic hydrogen to carbon ratios depends a good deal upon the number of side chains, or functional groups, indicated by the symbol \wedge in Table II, connected to the ring in question. We see that a value of 0.53 for this ratio is not inconsistent with an average ring size of three, with two connections per polyaromatic ring. On the other hand, a value of 0.40 is not inconsistent with an average ring size of two, with four connections per polyaromatic ring (but is also not in disagreement with an average ring size of four to six, as indicated in the fourth column of Table II). Our present prejudice is that the average polyaromatic hydrocarbon ring size in the older coal should be greater than that in the younger. With what we feel are reasonable values for connectivities, we thus infer that the average polyaromatic hydrocarbon ring size in Pocahontas #4 is no greater than three, and that in Star no greater than two, the values thus inferred being dependent upon the assumption that on the average, the younger coal has more aliphatic chains attached to the rings. Inference from ^{13}C spectra alone yield similar values⁽⁹⁾.

One source of error in the above inferences is the fraction aromatic carbon, since it is known that not all carbon are polarized in cross polarization experiments⁽¹⁰⁾. A second most obvious source of error is the accuracy of resolving the high resolution solid state spectra of protons in these coals. The former error would tend to increase the ring size on the average, since it is quite probable that the carbons not seen in cross polarization experiments are in the neighborhood of stable free radicals, characterized by relatively large polyaromatic hydrocarbon rings. Relaxation times of protons under the spin locking conditions of the cross polarization experiments⁽¹¹⁾ may be sufficiently short to obviate effective cross polarization. Spin counting of protons with, and without strong homonuclear decoupling indicates that at least 95% of the protons in the present samples are being detected under the high resolution solid state techniques used in the present work.

ACKNOWLEDGEMENT

This work was supported by the Office of Chemical Sciences of the Division of Basic Energy Sciences of the U.S. Department of Energy.

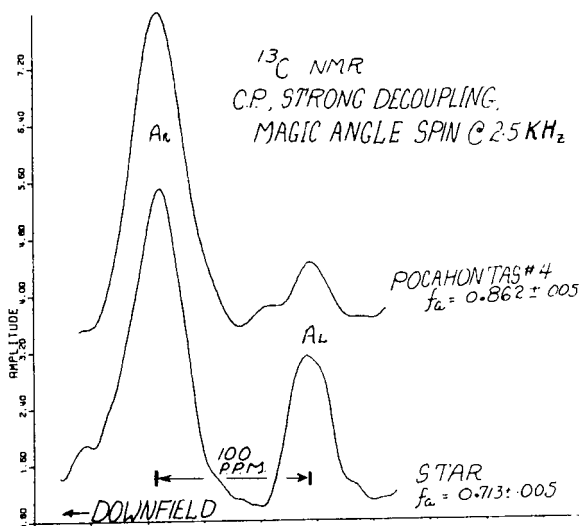


Figure 1.

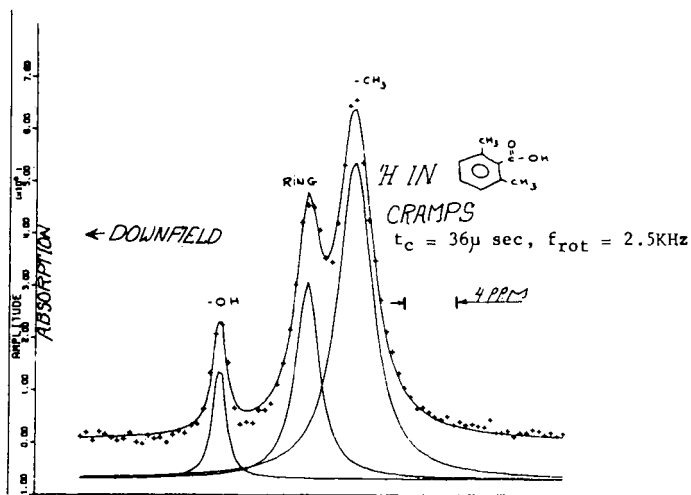


Figure 2.

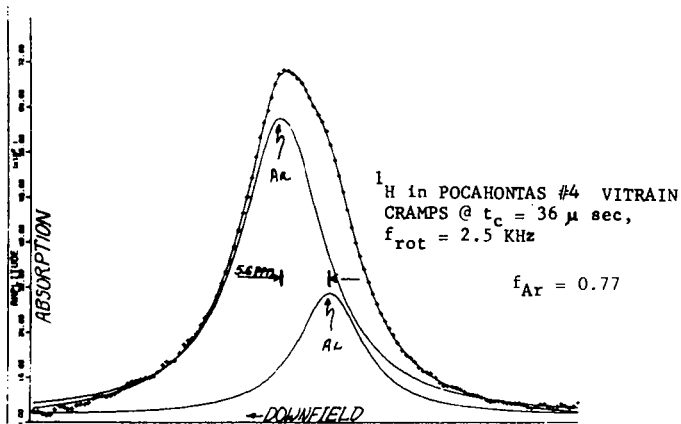


Figure 3.

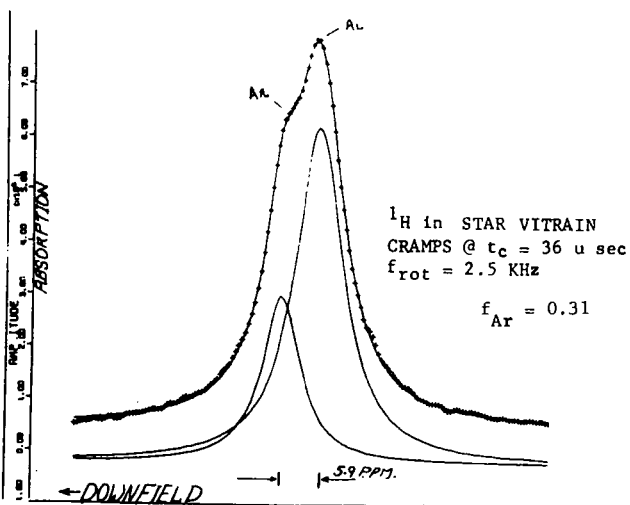


Figure 4.

References

1. a) B. C. Gerstein, C. Chow, R. G. Pembleton, and R. C. Wilson, J. Phys. Chem. 81, 565-70 (1977).
 b) H. L. Retcofsky and R. A. Friedel, J. Phys. Chem. 77, 68-71 (1973)
2. L. M. Ryan, R. C. Wilson, and B. C. Gerstein, Chem. Phys. Lett. 52, 341-4 (1977).
3. S. R. Hartman and E. L. Hahn, Phys. Rev. 128, 2042-53 (1962).
4. A. Pines, M. G. Gibby, and J. S. Waugh, J. Chem. Phys. 59, 569-95 (1973)
5. E. R. Andrew, in "Progress in Nuclear Magnetic Resonance Spectroscopy" Vol. 8, Part 1, Ed. J. W. Emsley, J. Feeney, and L. H. Sutcliffe, Pergamon Press (1971).
6. B. C. Gerstein, R. G. Pembleton, R. L. Wilson, and L. M. Ryan, J. Chem. Phys. 66, 361-2 (1977).
7. R. G. Pembleton, L. M. Ryan, and B. C. Gerstein, Rev. Sci. Instr. 48, 1286-9 (1977).
8. P. D. Murphy and B. C. Gerstein, Report #IS-4388, Iowa State University, (1978).
9. H. L. Retcofsky and D. L. VanderHart, Fuel 57, 421 (1978).
10. D. L. VanderHart and H. L. Retcofsky, Fuel 55, 202 (1976).
11. B. C. Gerstein "Fingerprinting Solid Coals Using Pulse and Multiple Pulse Nuclear Magnetic Resonance", Chapter 52, in Vol 3, Analytical Methods for Coal and Coal Products, Ed. Clarence Karr, Jr., Academic Press (circa 1979).

Temperature Dependence of ^1H NMR Absorption in Coal and Pitch

Kunio Miyazawa, Tetsuro Yokono, Yuzo Sanada

Coal Research Institute, Faculty of Engineering,
Hokkaido University, Sapporo, 060, Japan

Introduction

Many kinds of reactions such as pyrolysis, depolymerization, condensation occur simultaneously in complicated way when coal and tar pitch are heated over temperature range from 350°C to 500°C. In order to understand the processes of coal liquefaction and coal carbonization, it is important to clarify the characteristics of reaction behaviors for coal and tar pitch over the temperature range.

It is well known that pitch, solvent refined coal (SRC) and coking coal produce various kinds of mesophase at the early stages of carbonization [1-3]. The mechanisms of many chemical reactions and physical transformations relating to mesophase formation are studied by quenching techniques. Such research techniques as polarized light-microscopy and so on can be extremely fruitful. On the other hand, direct observation of phenomena at reaction temperatures may yield more easily interpretable or more relevant results. Line shape of NMR corresponding to mobility of molecule and/or segment in coal and tar pitch have been measured at the temperature range of mesophase formation.

No report has been appeared on direct measurement of change of hydrogen aromaticity (f_{Ha}) at higher temperature occurring pyrolysis and carbonization. This paper deals with observation of resolved NMR spectra corresponding to aromatic and aliphatic protons at high temperatures in a tar pitch. High resolution NMR spectra for thermally decomposed polyvinyl chloride were observed by S. Shimokawa et al. [4] over the temperature range from 350°C to 450°C using the same apparatus at Hokkaido University.

Experimental

The experiments were done by using a Bruker Sxp 4-100 pulsed Fourier transform (FT) spectrometer with a high temperature probe and an improved JEOL 3H electromagnet (0.88T) with a 60 mm gap operating at 36.4 MHz for the ^1H NMR. In order to improve the resolution of a spectrum at high temperatures, a home-built shim system was used [4]. Outlines of the high temperature probe and flowing gas system are illustrated in Fig. 1. The samples as received were heated in the high temperature probe and NMR spectra were obtained simultaneously. No heat-treatment was done before measurements. Kureha pitch was heated at 10°C min⁻¹ and the others were heated at 5°C min⁻¹ to various given temperatures under nitrogen gas flushing. In the case of the resolved NMR spectra for ethylene tar pitch, the heating rate employed was 2°C min⁻¹. Characteristics of all samples so far studied are shown in Table 1.

Results and discussion

Temperature dependence of molecular and/or segmental motion

Representative proton NMR spectra for coals and solvent extracts from coal are shown in Fig. 2. Apparently, there is no structure in the lines. Increasing temperature produces changes in the spectra. In order to discuss the broadening behavior quantitatively, the values of the line widths at half-height ($\Delta H_{1/2}$) were utilized. Temperature dependence of $\Delta H_{1/2}$ is shown in Fig. 3. It is obvious that there are three different groups with respect to temperature dependence of $\Delta H_{1/2}$. The value of $\Delta H_{1/2}$ of the first group to which Taiheiyo coal belongs decreases and then increases rapidly with increasing temperature. The behavior of $\Delta H_{1/2}$ of the second group, Yubarishinko coal and β -component (pyridine soluble, chloroform insoluble fraction of a coal [5]) of Yubarishinko coal, resembles that of the first group, but the curve of $\Delta H_{1/2}$ is shifted to higher temperatures. The third group, which includes γ -component (pyridine soluble, chloroform soluble fraction of a coal [5]) of Yubarishinko coal, coal tar pitch and ethylene tar pitch, indicates that the values of $\Delta H_{1/2}$ remain small over

a wide temperature range. This suggests that the molecules and/or segments in them are mobile throughout the temperature range.

The carbonization process at low temperatures has been studied by the method of polarized-light microscopy. The formation of low temperature carbons by solidification from a liquid phase proceeds through the separation of an optically anisotropic mesophase.

Optically anisotropic textures of mesophase from the samples heat-treated at the early stages of carbonization are classified into five types corresponding to isotropic, fine mosaic, coarse mosaic, fibrous and domain. It has been found that there is a close relation between the spin-lattice relaxation time, T_1 , observed with pulsed FT NMR at room temperature and microstructure of mesophase, transformed from the parent matrix of coal. That is, the longer the relaxation time is, the more sufficient the growth of mesophase from the matrix occurs as shown in Table 1. The parent materials, which give the fibrous/domain texture at the early stages of carbonization, have the longest relaxation time so far as being described in the table. There is also an excellent relation between the microstructure of mesophase and the temperature dependence of $\Delta H_{1/2}$. The minimum value of the line width at half-height with respect to the temperature dependence of $\Delta H_{1/2}$ is expressed as $\Delta H_{1/2, \min}$ and used for characterization of mesophase texture. $\Delta H_{1/2, \min}$ of isotropic mesophase is larger than that of coarse or fibrous/domain mesophase and the temperature of isotropic mesophase corresponding to $\Delta H_{1/2, \min}$ is lower than that of fine mosaic mesophase. The values of $\Delta H_{1/2}$ in coarse mosaic or fibrous mesophase keep small over a wide temperature range (see Fig. 3). But no distinction was observed between coarse mosaic and fibrous textures concerning the broadening behavior of NMR.

Regarding the concentration of free radicals and the line width, these values remain almost constant up to about 400°C for coals of different rank [6]. Therefore, it seems that the contribution of free radicals on the NMR line width is not so important as that of the proton dipole-dipole interaction.

At higher temperatures we estimate the value of T_1 following equation,
$$t = T_1 \ln 2$$

where t is the time at the amplitude of the Free Induction Decay (FID) following the 90° pulse being equal to zero. Pulse sequence used was 180°- τ -90° in this experiment.

Fig. 4 shows the relation between the T_1 of ethylene tar pitch and the inverse of temperature. T_1 of ethylene tar pitch has the value of 400 ms at room temperature. It decreases with the increase of temperature, and reaches a minimum value at about 150°C. As is shown in the figure, T_1 has a maximum value of 190 ms at 340°C, and decreases rapidly with the increase of temperature.

It is clearly marked that the aromaticity of ethylene tar pitch increases with increase of temperature at 340°C and the formation of mesophase for the sample heat-treated becomes observable by an optical microscope. Rotational correlation time for aromatic lamellae, which are stacking parallel each other in the mesophase, is long due to being in rigid state. Accordingly T_1 becomes short. However, more detailed discussion will be made with further experiments.

NMR line simulation by means of computer

A proton NMR spectrum from Kureha pitch at 450°C (15 min) (a) and a comparison of the experimentally observed spectrum with a computer simulated spectrum (b) are illustrated in Fig. 5. The spectrum (a) contains considerable intensity in the wings of the line, and the ratio of the width at one-eighth height to that at one-half height, indicated by the symbol $R(8/2)$, is 6.4. The ratio for a pure Lorentzian line is 2.64 and for a pure Gaussian line is 1.73 [7]. By means of computer simulation the NMR line for the mesophase in Kureha pitch is composed of at least three different components, i.e. one Gaussian component with value of proton spin-spin relaxation time $T_2 = 7$ microseconds and two Lorentzian components with those of $T_2 = 210$ and 636 microseconds at 36.4 MHz, respectively. The fractions are also estimated as 0.85, 0.05 and 0.10, respectively. Kureha pitch at the early stages of carbonization contains 85 percent rigid structures from the view point of general NMR behavior [8].

In some liquid crystal systems broad partially resolved spectra with little structure attributed to proton dipole-dipole interaction have been observed [9-11]. On the other hand, such spectra were not observed in this study, so that the

ordering parameters of the samples employed would be expected to be very small. This result is compatible with that of ESR study reported by Yamada et al. [12].

Resolved NMR spectra at thermal decomposition temperature

In order to improve the resolution at higher temperature, a home-built shim system was attached with the magnet of NMR spectrometer. Typical ^1H NMR spectra for ethylene tar pitch are shown in Fig. 6. On heating at about 84°C , a broad resonance with no resolved structure becomes observable. And then at about 123°C , the NMR spectrum shows two discrete lines apparently, 200 Hz apart. That is, the lines correspond to the resonance due to aromatic and aliphatic protons. Assignment of the two peaks was done by comparing with the ones of a pure compound, acenaphthylene, which has the value of 0.75 hydrogen aromaticity (f_{Ha}). At about 208°C , the NMR spectrum becomes narrow and separately due to the rapid tumbling of molecule in ethylene tar pitch. This suggests that the molecules exhibit the random motion similar to that in isotropic solution and the value of the dipolar tensor over all orientation in them is almost zero in the vicinity of this temperature. However, fine structures due to the protons attached to α , β and γ carbons refer to aromatic rings were not able to observe at the higher temperatures, because of superposition of protons having various chemical shifts.

The intensity of aliphatic protons is higher than that of aromatic ones up to 208°C , at which the intensity change is observable. The values of f_{Ha} are able to elucidated from the intensity of the splitted spectra. However, two lines merge and broaden raising at about 430°C . Heating of the specimen at higher temperatures accelerates the degree of broadening of the spectrum. Therefore, it is difficult to observe the spectrum in the range of a usual high resolution NMR sweep width.

The spectrum obtained with a wider sweep width (25kHz) are shown in Fig.

7. For the spectrum in the figure, the ratio of the width at one-eight height to that at one-half height, indicated by the symbol $R(8/2)$, is 7.0. This line shape is designated as "Super Lorentzian" [13] which contains considerable intensity in the wings of the line. After the measurement of the NMR spectra at 470°C , the sample was immediately quenched to room temperature and observed by polarized light-microscopy. And it was confirmed that the bulk mesophase was produced at 470°C .

When a magnetic field is applied, it is known that the direction of alignment of c-axes of mesophase spherules is aligned perpendicular to that of the magnetic field by interacting magnetic anisotropy of polycondensed aromatic molecules with the magnetic field applied [14]. On heating of ethylene tar pitch beyond 430°C in a magnetic field, a dipolar tensor is only partially averaged due to less chaotic molecular motion in a magnetic field. Resulting line becomes broad but is not as broad as solid. The structure of the mesophase produced in an NMR magnetic field is more rigid than that of isotropic liquid.

Table 2 summarizes range of sweep width for various NMR type at 36.4 MHz of resonance frequency. Generally, the sweep width of broad line NMR is the order of $10^5 \sim 10^6$ Hz, while that of high resolution NMR is about 10^3 Hz at 36.4 MHz for a proton. But the NMR spectrum of the mesophase obtained from ethylene tar pitch shown in Fig. 7 was swept over 2.5×10^4 Hz. Thus, the sweep width of the NMR spectrum for the carbonaceous mesophase is intermediate between those of broad line NMR and high resolution NMR. It seems that the result is supported by that obtained by J. J. Fink et al. [15]. They have measured the line width of 2.3×10^{-4} to 3.1×10^{-4} T for conventional nematic and smectic liquid crystals.

Conclusion

It could be concluded from the above results that the materials which give spherical mesophase on heating show a narrowing of the NMR with increasing temperature which corresponds to so-called softening and plastic stages. Moreover, the degree of motional narrowing of the proton NMR spectra reflects the degree of fluidity at the plastic stage. The temperature dependence of hydrogen aromaticity would be monitored directly by using the NMR high temperature technique.

Chemical reactions such as pyrolysis, depolymerization, condensation could be clarified. Moreover, application of the technique seems to be promising in the mechanism of coal liquefaction as well as that of mesophase formation.

Acknowledgement

The authors express their sincere thanks to Messrs. S. Shimokawa and E. Yamada for the experimental assistance and helpful discussion.

References

- [1] J. D. Brooks and G. H. Taylor, *Carbon*, **3**, 185 (1965)
- [2] H. Honda, H. Kimura, Y. Sanada, S. Sugawara and T. Furuta, *Carbon*, **8**, 181 (1970)
- [3] J. Dubois, C. Agache and J. L. White, *Metallography*, **3**, 337 (1970)
- [4] S. Shimokawa and E. Yamada, *J. Phys. Chem.*, submitted
- [5] R. V. Wheeler and M. J. Burgess, *J. Chem. Soc.*, 649 (1911)
- [6] J. Smidt and D. W. van Krevelen, *Fuel*, **38**, 355 (1959)
- [7] C. P. Poole, Jr. and H. Farach, *The Theory of Magnetic Resonance*. John Wiley & Sons, Inc. (1972)
- [8] A. Abragam, *The Principles of Nuclear Magnetism*, Clarendon Press, Oxford (1961)
- [9] A. Saupe and G. Englert, *Phys. Rev. Letters*, **11**, 462 (1963)
- [10] K. R. K. Easwaran, *J. Mag. Res.* **9**, 190 (1973)
- [11] J. C. Rowell, W. D. Phillips, L. R. Melby and M. Panar, *J. Chem. Phys.*, **43**, 3442 (1965)
- [12] Y. Yamada, K. Ouchi, Y. Sanada and J. Sohma, *Fuel*, **57**, 79 (1978)
- [13] K. D. Lawson and T. J. Flautt, *J. Phys. Chem.*, **72**, 2066 (1968)
- [14] L. S. Singer and R. T. Lewis, 11th Biennial Conference on Carbon, Gatlinburg, Tennessee, Prepring, CG-27 (1973)
- [15] J. J. Fink, H. A. Moses and P. S. Cohen, *J. Chem. Phys.*, **56**, 6198, 1972
- [16] T. Yokono, K. Miyazawa and Y. Sanada, *Fuel*, **57**, 555 (1978)
- [17] T. Yokono and Y. Sanada, *Fuel*, **57**, 334 (1978)

Table 1
Characteristics of samples used

Sample	weight % (d.a.f.)					f_a 1)	T_1 (ms) ²⁾	Optical texture in carbonized coal
	C	H	N	S	O			
Taiheiyō coal	77.0	6.0	1.4	0.1	15.5	0.70	18	isotropic
Hongei coal	93.1	3.2	1.0	2.7	-	0.70	58	isotropic
Miike coal	83.5	6.2	1.2	1.8	7.3	-	421	fine mosaic
Yubarishinko coal	86.6	5.9	2.0	0.3	5.2	0.80	438	fine mosaic
β-component of Yubarishinko coal	82.2	5.7	2.2	-	-	0.78	531	fine mosaic
γ-component of Yubarishinko coal	87.8	7.0	1.5	-	-	0.80	719	coarse mosaic
Kureha pitch	95.2	4.2	0.1	0.2	0.3	0.86	952	fibrous/domain
Ethylene tar	94.3	5.5	0	0.1	0.1	0.78	1103	fibrous/domain
Coal tar pitch	92.1	4.8	1.3	0.3	1.5	0.83	1560	fibrous/domain

1) values obtained from proton spin-spin relaxation time at -100°C [16]

2) proton spin-lattice relaxation time [17]

Table 2
Range of sweep width for various NMR at 36.4 MHz of
resonance frequency [$H_0=0.88T$]

NMR	Range of sweep width (Hz)
High resolution	10^3
Intermediate	10^4
Broad line	$10^5 \sim 10^6$

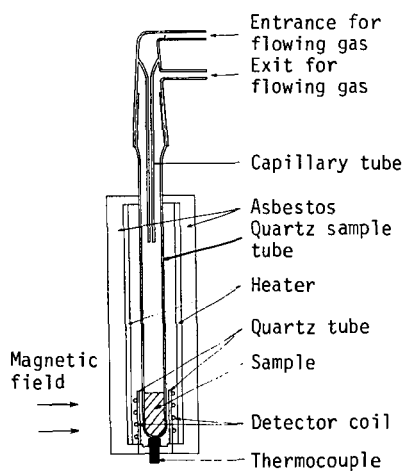


Fig. 1 Outlines of the high temperature probe and flowing gas system.

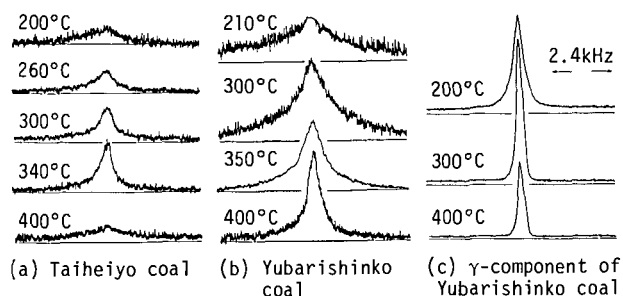


Fig. 2 Proton NMR spectra of Taiheiyō coal (a), Yubarishinko coal (b) and γ -component of Yubarishinko coal (c) at high temperatures.

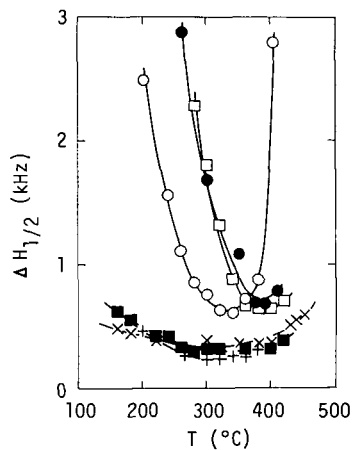


Fig. 3 Temperature dependence of the line width at half-height ($\Delta H_{1/2}$):
 ○ Taiheiyō coal, ● Yubarishinko coal,
 □ β -component of Yubarishinko coal,
 ■ γ -component of Yubarishinko coal,
 + Coal tar pitch and × Ethylene tar pitch.

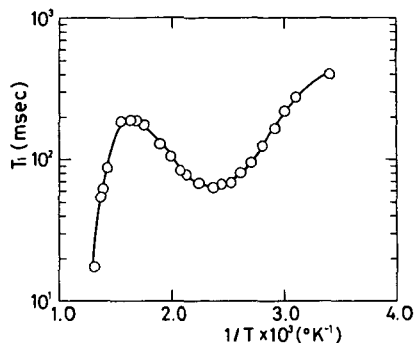


Fig. 4 Temperature dependence of spin-lattice relaxation time (T_1) of ethylene tar pitch.

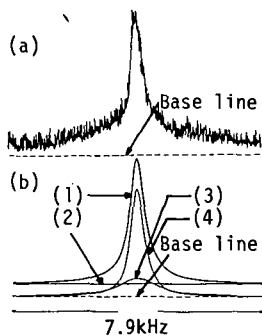


Fig. 5 A proton NMR spectrum of Kureha pitch at 450°C (for 15 min) (a) and a comparison of the experimentally observed spectrum with a computer simulated spectrum (b): (1) Total simulated curve, (2) Gaussian component with $T_2=7 \mu s$, (3) Lorentzian component with $T_2=210 \mu s$ and (4) Lorentzian component with $T_2=636 \mu s$.

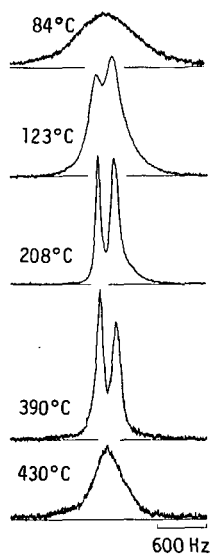


Fig. 6 Proton NMR spectra of ethylene tar pitch at high temperatures.

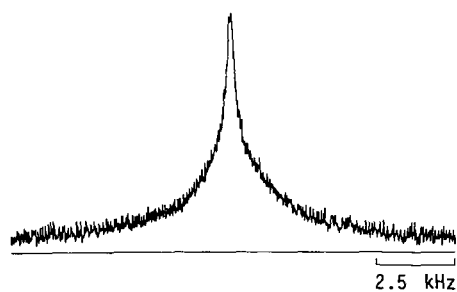


Fig. 7 A proton NMR spectrum of ethylene tar pitch at 470°C.

MAGNETIC RESONANCE STUDIES OF LABELED GUEST MOLECULES IN COAL

L. B. Ebert, R. B. Long, R. H. Schlosberg, and B. G. Silbernagel

Corporate Research Laboratories, Exxon Research and Engineering Co.
P.O. Box 45, Linden, NJ 07036

We have used magnetic resonance techniques to probe the time scales of motion for a series of labeled guest molecules imbibed in subbituminous Wyodak and bituminous Illinois #6 coals. Nuclear magnetic resonance (NMR) was used to study a suite of such guests which were either deuterated or fluorinated, while electron spin resonance (ESR) was used to examine paramagnetic TEMPOL spin labels. These labeled guest molecules can be observed directly with a minimum amount of interference from the nuclei and paramagnetic species naturally occurring in the coal. By choosing a variety of differently labeled species, a broad range of time scales for molecular motion can be examined. The rate and nature of the motion provides information about the environment of the guests in the coal structure.

Dry coal samples (10-20 mesh) were exposed to various solvent vapors while contained in closed jars. The solvent uptake was monitored by periodic weighing of the sample during the exposure period. As shown for C_6H_6 and C_5H_5N in Illinois #6 coal (Figure 1), the uptake pattern depends upon the choice of solvents: benzene uptake approaches an asymptotic value in roughly one week while pyridine continues to be included over a much longer time period. The amounts of imbibed labeled molecules in the coals used for the present study, shown in Table 1, range from ~ 0.1 to ~ 10 m mole of solvent/gm of coal.

In most liquids, rapid molecular motion causes averaging of the interactions between nuclear and electronic spins and their environment. If the rate of motion becomes sufficiently slow, these interactions are no longer averaged and a change in the magnetic resonance signal, typically a broadening, is observed. This averaging process has been studied in many liquids and solids and relatively simple theories have been developed which predict the characteristic times for motion required for the onset of averaging for different electronic and nuclear spins (1). For example, in 2-fluoropyridine the ^{19}F NMR is broadened by dipolar interactions, principally with protons on the same molecule, and motion on a time scale shorter than 250μ sec is needed to average the interaction. For the $-CF_3$ components of hexafluoropropanediamine, this characteristic time is $\sim 100 \mu$ sec. The 2H nuclei in deuterated labels are broadened by the stronger nuclear electric quadrupolar interaction and more rapid motion ($\sim 5 \mu$ sec) is required for averaging. Interactions of the much larger electronic moments in the paramagnetic TEMPOL spin labels require times on the order of 10^{-8} sec to be averaged. A combination of these labels allows us to survey rates of motion which vary by over a factor of one million.

The derivative of the ^{19}F NMR absorption of 2-fluoropyridine in Illinois #6 coal is shown in Figure 2. A narrow NMR line is seen at 300K, with no evidence for the broad component which would indicate molecules moving more slowly than 250μ sec. No broad 2H NMR line is seen in coal samples containing D_2O . However both broad and narrow components are seen in coals with C_6D_6 and C_5D_5N guests. The derivative of the 2H NMR for C_6D_6 in Illinois #6 is shown in Figure 3. The same data is displayed at two levels of gain to show the two satellites which occur on either side of the intense central component. Very roughly, comparable numbers of nuclei contribute to the narrow and broad components. The C_6D_6 molecules contributing to the central absorption are moving on time scales shorter than 5μ sec and the 2H quadrupole interaction is completely narrowed. The satellite splitting for the broad C_5D_5N component is twice as large as in the C_6D_6 case. From the

magnitudes of these broad spectra (2) we infer that the C_6D_6 molecules are still spinning about their C_6 symmetry axis at times shorter than 5μ sec, while the C_5D_5N molecules are not. The restricted motion of this class of C_6D_6 molecules suggests that they may be sterically confined by the nearby coal matrix. The absence of rapid motion for this class of C_5D_5N molecules may reflect a chemical interaction between the molecules and the coal matrix.

ESR studies of the TEMPOL spin label also show this slowing down process in the coal. Immediately after adding a TEMPOL solution to a coal sample, a narrow triplet ESR signal from the TEMPOL in the liquid is super-imposed on the carbon radical signal in the coal (Figure 4A). The narrow TEMPOL lines broaden as time passes while the total EPR signal does not change, again implying the loss of averaging due to slower motion of the molecules (Figure 4B). The characteristic time of motion is therefore longer than 2×10^{-8} sec. The reduction of the narrow triplet signal intensity (Figure 4C) is proportional to $\exp(-\alpha t^{1/2})$ suggesting that this slowing of the motion reflects diffusion of the TEMPOL labels into the coal.

Pulsed NMR studies of the narrow component of the resonance line also show the change in motion of a molecule when introduced into the coal solid. The energy exchange between ^{19}F nuclei in 2-fluorophenol and their environment was determined in the free liquid and for molecules included in coal by using spin lattice relaxation (T_1) measurements. T_1 is frequency independent for both systems, but the relaxation time is much shorter for the guest molecules in coal: $T_1 = 13 \pm 3$ m sec, in comparison with $T_1 = 1.5 \pm 0.3$ sec for the free liquid at the same temperature (300K). These data imply characteristic times of motion for the guest species. A factor of 100 slower than for the free species.

In summary, a combination of labeled molecular probes and different observation techniques provides information on the environment and motion of molecular species in coal. The range of characteristic times of motion is indicated schematically in Figure 5. As illustrated in the case of the spinning C_6D_6 molecules, the type of the motion may also be deduced in some cases.

REFERENCES

1. This averaging phenomenon is discussed by A. Abragam, "Principles of Nuclear Magnetism" (Oxford, 1961), Chapter X.
2. See R. G. Barnes in "Advances in Nuclear Quadrupole Resonance", J. A. S. Smith, Ed. (Heydon and Sons, London, 1974), v. 1, p. 235 ff.

TABLE 1: MOLECULAR UPTAKE DURING THE SWELLING PROCESS

Coal Type	Imbibing Molecule	Millimoles Imbided/Gram of Coal
Wyodak:	D_2O	8.49
	C_5D_5N	8.93
	C_6D_6	1.26
Illinois #6:	D_2O	5.79
	C_5D_5N	6.21
	C_6D_6	2.08
	2-Fluorophenol	4.83
	4-Fluorophenol	1.88
	2-Fluoropyridine	6.09
	C_6F_6	0.47
	Hexafluoro Propane Diamine	0.29

Figure 1:
Examples
of the
Swelling
Process:

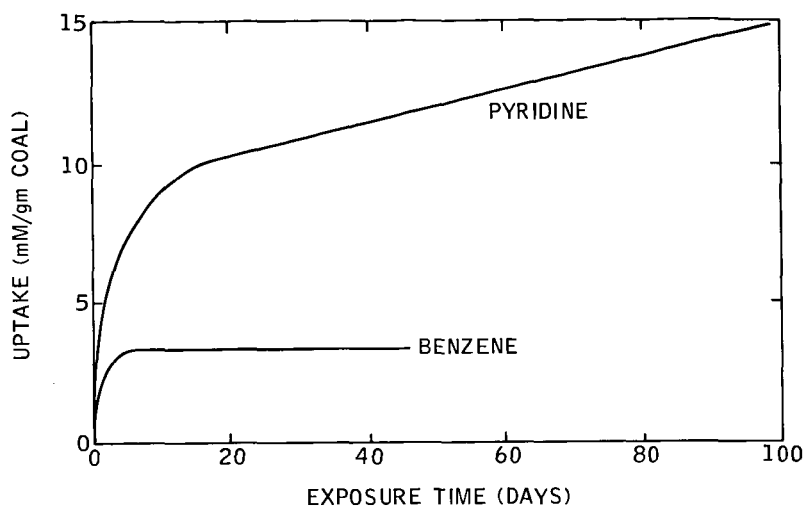


Figure 2: The ^{19}F
NMR of Illinois #6
Coal swelled with
2-fluoropyridine
shows only a narrow
component.

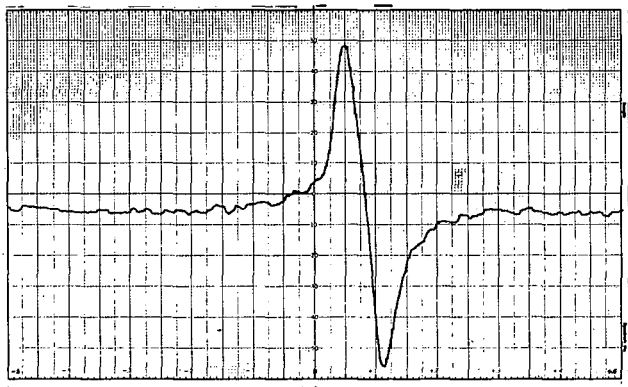


Figure 3: Both narrow
and broad ^{2}D NMR
signals are observed in
Illinois #6 coal
swelled with C_6D_6 .

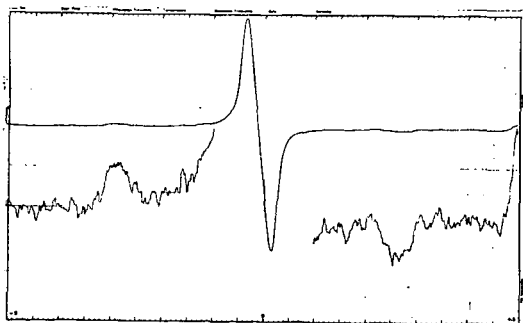
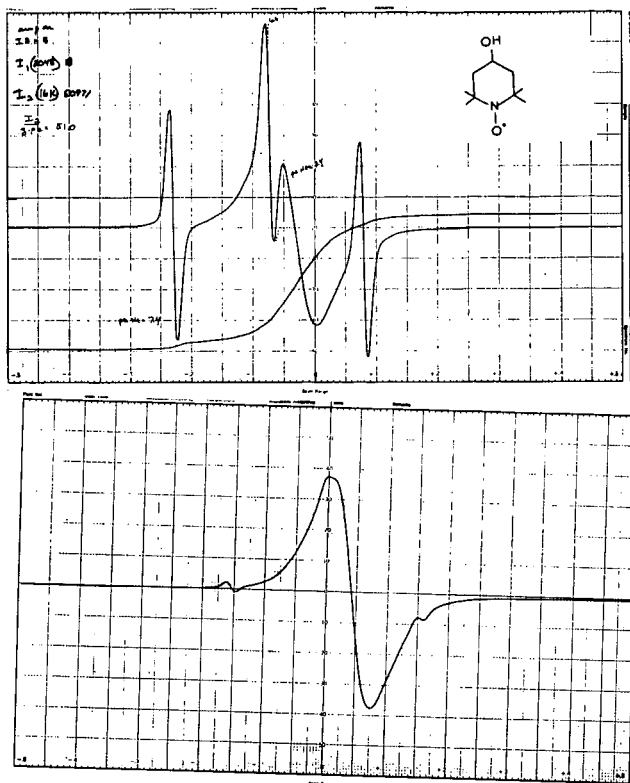


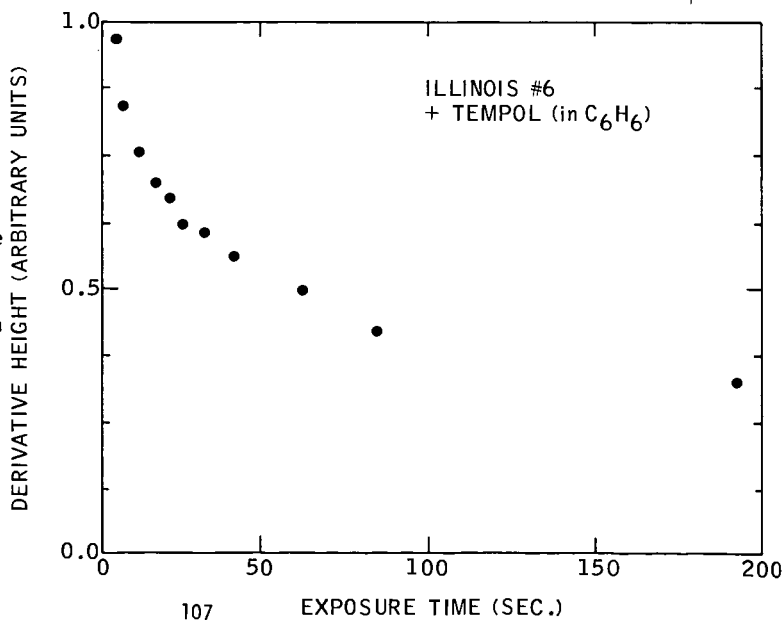
Figure 4: Coal Swelling with a paramagnetic spin label (TEMPOL)

A. Upon initial exposure of TEMPOL to coal, the narrow spin label triplet signal is superimposed upon the carbon radical signal from the coal.

B. At long times, only a trace of the triplet TEMPOL signal remains.



C. An example of the loss of TEMPOL signal intensity with time for Illinois #6 coal exposed to a solution of TEMPOL in benzene.



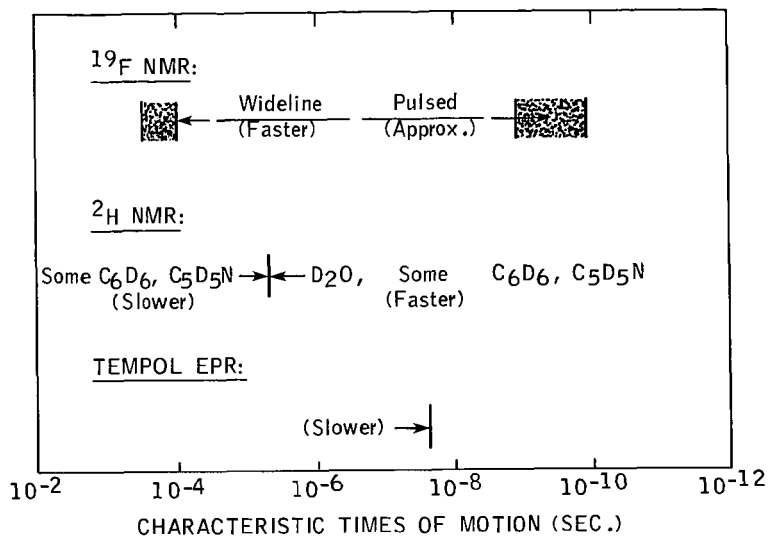


Figure 5: A survey of characteristic times of motion probed by the current labeled molecules.

CARBOXYLIC ACIDS AND COAL STRUCTURE. A. L. Chaffee, G. L. Perry and R. B. Johns.
School of Chemistry, University of Melbourne, Parkville, Victoria 3052, Australia.

The emphasis will be on fatty acids, particularly monocarboxylic and dicarboxylic acids as environmental indicators. Fatty acid data will be presented for a number of Lithotypes of Brown Coal from the LaTrobe Valley, Victoria, and a series of Australian Black Coals of varying rank. For the Brown Coal the relationship between fatty acids and Lithotype (which is believed to reflect the environment by deposition) will be discussed. The diagenetic changes which fatty acids in the coal structure undergo with depth of burial will also be discussed in relation to Lithotypes.

Structural Characterization of Coal: Lignin-Like Polymers in Coals

Ryoichi Hayatsu, Randall E. Winans, Robert L. McBeth,
Robert G. Scott, Leon P. Moore, and Martin H. Studier

Chemistry Division
Argonne National Laboratory, Argonne, Illinois 60439

INTRODUCTION

Although lignins are major constituents of vascular plants from which coals are derived, their roles in the coalification process and resulting coal structures have not been defined. On the basis of chemical and biological degradations, lignins are considered to be polymers of propylphenyl compounds, coniferyl alcohol and related alcohols (1-3). Because of their great abundance, high resistance to biological degradation and characteristic occurrence in land plants, isolation of coal degradation products related to these lignin compounds should shed some light on the roles, if any, played by lignins during coalification and in the final structure of coals. To date such studies have had only limited success.

Although fulvic and humic acids have been degraded successfully with alkaline solutions to produce lignin-related phenols (4-6), this method has not proved to be useful for coals. Reductive degradations of soil and coal-derived humic acids with sodium amalgam have been reported to produce a variety of phenolic compounds (9-10); however, several investigators have found that this procedure gives only a few phenols in very small amounts, because of the degradation of phenolic rings (11-12).

Many oxidative degradations have also been carried out to break coal down into simpler species; however, isolation and identification of phenols such as p-hydroxybenzene derivatives, vanillic and syringic groups, which are characteristic lignin oxidation products, have not been definitely confirmed yet. In general, commonly used oxidants destroy phenolic rings or give complex products (13-15). Some of the oxidants such as nitrobenzene produce reaction by-products that may interfere with the analysis of the oxidation products (16-18). To obtain lignin oxidation products from coals, we resorted to the alkaline cupric oxide oxidation method which has been successfully applied to analysis of lignins in plants (16), fulvic and humic acids (18-19), and land-derived marine sediments (16).

EXPERIMENTAL

Seven coals were used in this study (Table 1). To remove trapped organic materials (20-21), four coals (samples 1-4) were extracted with benzene-methanol (3:1, refluxing for 48 hours) and 2.5% aq.-NaOH (20-35°C for 16 hours) before oxidation. Since the alkaline extractable material was found to be negligible for samples 5-7 these coals were only extracted with benzene-methanol.

Each coal sample (5g) was oxidized with alkaline cupric oxide (51.9 g of $\text{CuSO}_4 \cdot 5\text{H}_2\text{O}$, 37.3 g of NaOH and 185 ml of H_2O) at 200°C for 8-10 hours* by the method of Greene et al. (22). After the reaction mixture had cooled, it was centrifuged. The alkaline supernatant was acidified with HCl to pH 2. After concentration of the acidic solution, the slushy residue was repeatedly extracted with benzene-ether (1:3). The residue was further extracted with methanol. Materials soluble in alkali only were also isolated from all samples. To recover non-oxidized coal, the alkaline insoluble residue was treated several times with concentrated HCl, and finally washed with water. A summary of the oxidation products is shown in Table 2.

Solid probe mass spectrometric analysis (20) showed that the benzene-ether extracts consist mainly of organic acids. Therefore, these extracts were derivatized with d₆-dimethylsulfate to yield d₃-methyl labelled derivatives. The derivatives were analyzed by GC-TOFMS and high resolution MS using techniques which have been previously described (20). Authentic samples of phenolic acids derivatized with d₆-dimethylsulfate or diazomethane were also analyzed by GCMS for reference.

Gas chromatograms of the derivatives obtained from samples 1 and 2 are shown in Fig. 1a and in Fig. 1b with numbered peaks identified in Table 3. The methanol extracts and fractions soluble in alkali only were found to consist essentially of humic acid-like materials by solid probe MS.

To obtain detailed information of the CuO-NaOH oxidation, control experiments with 15 model compounds and a polymer were carried out using the procedure employed for the coals. The results are shown in Table 4.

RESULTS AND DISCUSSION

As shown in Table 2 and in Table 3, most informative is the identification of large amounts of p-hydroxy and 3,4-dihydroxybenzoic acids in the oxidation products of samples 1 and 2. These are regarded as lignin oxidation products. It is interesting to note that, while no o- and m-hydroxybenzoic acids were found in the oxidation products of samples 1 and 2, all three isomers were identified in small amounts in other rank bituminous coals (samples 3, 5, 6). From sample 3, 3,4-dihydroxybenzoic acid was also isolated in small amount, however this compound was not detected in the oxidation products of other bituminous coals (samples 4-6).

It is interesting that bituminous (sample 4) gave organic acids qualitatively similar to those of lignite coal (see Table 2).

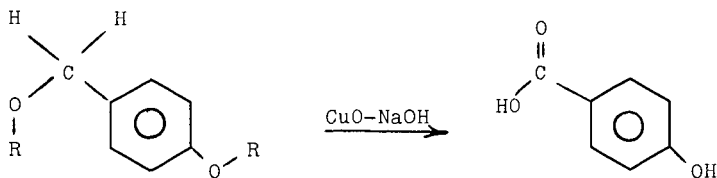
* In general, lignin, plant materials, fulvic and humic acids and marine sediments are oxidized at 170°C for 3-4 hours, however this condition has been found to be not strong enough to oxidize coals.

identified compounds were p-hydroxybenzoic acid, 4-hydroxy-1,3-benzenedicarboxylic acid, benzene di and tricarboxylic acids. No o- or m- isomer of hydroxybenzoic acid was detected. We have found that solvent extractable hydrocarbons obtained from this coal consist mainly of n-alkane (C_{11} to C_{31}). This is quite different from other results which showed that aromatic hydrocarbons were the major solvent extractable material of several bituminous and anthracite coals (20,23). Indeed, petrographic analysis shows that this coal has a high content of sporinite (14.3 wt %) and low content of vitrinite (30.2 wt %) (24). Anthracite coal (sample 7) did not yield any organic solvent extractable oxidation products.

Some acids not found in oxidation products of lignins, land plants and marine sediments were found in the oxidation products of coals. Among these were phenolic di and tricarboxylic acids and hydroxynaphthalenecarboxylic acids. From some soil fulvic and humic acids, phenolic polycarboxylic acids have been found in the oxidation products together with considerable amounts of fatty acids. Therefore, phenolic esters of fatty acids are considered to be present in these soil acids (5,18). However, little or no fatty acids were observed in the coal oxidation products.

Trihydroxybenzoic acid or its methoxy derivatives (syringic group) which are obtained from the oxidation of lignins, fulvic and humic acids and marine sediments were not found in any of our oxidation products. We have found that the authentic syringaldehyde and 2,6-dimethoxyphenol were largely degraded by the oxidation (Table 4). This may account for the fact that we did not observe them, however the syringic groups may have been degraded during coalification.

All phenolic acids identified were found as OCd_3 -derivatives. The mass spectra showed the complete absence of OCH_3 -group. It is confirmed that no isotope exchange of the H in OCH_3 with D occurred under our procedures. Although partial demethylation reaction during the oxidation cannot be excluded from the control experiment (see Table 4), it is probable that the phenolic acids found were derived mainly from the fission of ether linked aromatic systems as shown in the example below rather than from aryl methoxy units.



R = alkyl ($C \geq 2$), aryl

Indeed, it is known that very little or no methoxy groups are present in bituminous coals (25-26). In the lignite coal (sample 1) aryl methoxy groups are not present in significant amounts (26).

Nonhydroxy benzene, naphthalene, pyridine and thiophene carboxylic acids and humic acid-like materials found in the oxidation products might be derived from non-lignin or extensively transformed lignin polymers.

The oxidation of methyl groups of aromatic compounds has been found to be ineffective. Therefore, relatively large amounts of methyl-substituted phenolic and benzene carboxylic acids were isolated from the coal oxidation. Our control experiments also indicated that, while the CuO-NaOH oxidation of alcohol, aldehyde, ketone, quinone and ether is effective, methyl groups and methylene bridges are not oxidized significantly.

CONCLUSIONS

1. Although one cannot rule out the possibility that plant polyphenols (27) could be one of the important precursors for coal formation, the present work shows that lignin-like polymers have been incorporated into the macromolecules of coals, and are still identifiable in lower rank coals. Evidence for this is the identification of p-hydroxy- and 3,4-dihydroxy-benzoic acids which are known lignin oxidation products.

2. The lignin-like polymers contain more highly cross-linked structures increased in aromaticity compared with the original lignins. Phenolic polycarboxylic acids and hydroxynaphthalene-carboxylic acids which were identified are not found in the CuO-NaOH oxidation products of lignins and plant materials.

3. It is obvious that extensive transformation of lignin-like polymers occurred perhaps through reactions (28-29) such as demethylation, demethoxylation, dehydrogenation, oxidation, cleavage of ring structures, re-condensation, etc. during coalification from lignite to bituminous and anthracite coals. This is shown by the fact that (a) lower rank coals gave higher yields of the CuO-NaOH oxidation products; (b) higher phenolic acid/benzenecarboxylic acid ratio is shown for the lower rank of coals; (c) very little or no dihydroxybenzoic acid was identified in the oxidation products of higher rank coals (samples 3-6); (d) more naphthalene- and heterocarboxylic acids are found in the oxidation products of higher rank coals. Finally, major parts of lignin-like polymers are transformed into non-lignin type polymers at later stage of coalification. Indeed, the later coalification product, anthracite coal (sample 7) did not yield any phenolic acid by the oxidation.

4. In a previous paper (21) we characterized aromatic acids trapped in lignite coal, and have found that these acids are qualitatively quite similar to those obtained from the present oxidation of the same pretreated coal. This indicates that the trapped acids were derived mainly from the oxidative degradation of lignin-like polymers during the coalification. We have also observed that no trapped organic acid is isolated from the anthracite coal which no longer contains lignin-like polymers.

ACKNOWLEDGEMENT

This work was supported by the Division of Basic Energy Sciences of the Department of Energy.

REFERENCES

1. Freudenberg, K. and Neish, A. C., *Constitution and Biosynthesis of Lignin* (Springer Verlag, New York), 1968.
2. Bolker, H. I. and Brenner, H. S., *Science* 170, 173 (1970).
3. Grimshaw, J., *Rodd's Chemistry of Carbon Compounds*, S. Coffey, Ed., Vol. 3, Part D, Chapter 16, Elsevier Scientific Publ. Co., New York (1976).
4. Dubach, P., Mehta, N. C., Jakab, T., Martin, F., and Roulet, N., *Geochim. Cosmochim. Acta* 28, 1567 (1964).
5. Neyroud, J. A., and Schnitzer, M., *Canad. J. Chem.* 52, 4123 (1974).
6. Schnitzer, M., and Neyroud, J. A., *Fuel* 54, 17 (1975).
7. Pew, J. C., and Withrow, J. R., *Fuel* 10, 44 (1931).
8. Sharma, J. N., and Wilson, M. J. G., *Fuel* 40, 331 (1961).
9. Burges, N. A., Hurst, M. H., and Walkden, G., *Geochim. Cosmochim. Acta* 28, 1547 (1964).
10. Bimer, J., Given, P. H., and Raj, S., *ACS Symp. Series No. 71*, 86 (1978).
11. Stevenson, F. J., and Mendez, J., *Soil Sci.* 103, 383 (1967).
12. Schnitzer, M., DeSerra, M. I. O., and Ivarson, K., *Soil Sci. Soc. Am. Proc.* 37, 229 (1973).
13. Forrester, A. R., and Wardell, J. L., *Rodd's Chemistry of Carbon Compounds*, S. Coffey, Ed., Vol. 3, Part A, Chapter 4, Elsevier Scientific Publ. Co., New York (1971).
14. Musgrave, O. C., *Chem. Rev.* 69, 499 (1969).
15. Bearse, A. E., Cox, J. L., and Hillman, M., *Production of Chemicals by Oxidation of Coal*, Battelle Energy Program Report, Columbus, Ohio (1975).
16. Hedges, J. I., and Parker, P. L., *Geochim. Cosmochim. Acta* 40, 1019 (1976).
17. Bugur, K., Gaines, A. F., Guleg, A., Guger, S., Yurum, Y., and Olcay, Y., *Fuel* 52, 115 (1973).
18. Neyroud, J. A., and Schnitzer, M., *Soil Sci. Soc. Am. Proc.* 38, 907 (1974).
19. Griffith, S. M., and Schnitzer, M., *Soil Sci.* 76, 191 (1976).
20. Hayatsu, R., Winans, R. E., Scott, R. G., Moore, L. P., and Studier, M. H., *Fuel* 57, 541 (1978).
21. Hayatsu, R., Winans, R. E., Scott, R. G., Moore, L. P., and Studier, M. H., *Nature* 275, 116 (1978).
22. Green, G., and Steelink, C., *J. Org. Chem.* 27, 170 (1962).
23. Unpublished results.
24. Spackman, W., Davis, A., Walker, P. L., Lovell, H. L., Stefanko, R., Essenhigh, R. H., Vastola, F. J., and Given, P. H., *Evaluation of Development of Special Purpose Coals*, Final Report FE-0390-2, September 1976, ERDA.
25. Dryden, I. G. C., *Chemistry and Utilization of Coal*, Suppl. Vol., H. H. Lowry, Ed., Chapter 6, John Wiley, New York (1963).
26. Unpublished results from selective aq.-Na₂Cr₂O₇ oxidation of coals derivatized with d₆-dimethylsulfate.
27. Timell, T. E., Ed., *Proceeding of the 8th Cellulose Conference I. Wood Chemicals - A Future Challenge*, John Wiley & Sons, New York, 1975; see also Reference no. 3.
28. Flaig, W., *Coal and Coal-Bearing Strata*, D. Murchison and T. S. Westoll, Eds., Chapter 10, Oliver and Boyd, London 1968.
29. Swain, F. M., *Non-Marine Organic Chemistry*, The University Press, Cambridge (1970).

Table 1
Elemental Analysis of Samples* (maf %)

No.	Sample	C	H	N	S	O (by diff)	H/C
1	Lignite (Sheridan Wyoming)	66.4	4.8	1.5	1.1	26.2	0.87
2	Bituminous (IL. #2)	73.9	5.2	1.4	3.4	16.1	0.84
3	Bituminous (IL #6)	77.7	5.4	1.4	4.1	11.4	0.83
4	Bituminous (Ohio PSOC#297)	80.5	5.6	1.6	2.9	9.4	0.83
5	Bituminous (Pitt. #8)	82.0	5.5	1.4	3.7	7.4	0.70
6	Bituminous (Penn. PSOC#258)	86.5	4.8	1.3	2.6	4.8	0.67
7	Anthracite (Penn. PSOC#85)	91.0	3.8	0.7	1.2	3.3	0.50

* All samples were pretreated to remove solvent extractable trapped organic materials and were dried at 110-120°C for 16-18 hours under vacuum before oxidation.

Table 2
Summary of CuO-NaOH Oxidation Products

Wt % of fraction ^b / Sample No. ^a	1	2	3	4	5	6	7
Organic acid (Benzene-ether extract)	35.3	19.6	17.1	7.0	14.7	1.3	-
Humic acid A (Methanol extract)	54.3	61.0	46.2	9.3	39.5	69.5	-
Humic acid B (only aq. alkali soluble)	≤ 1.0	≤ 1.5	16.1	51.0	20.2	2.0	7.5
Non-oxidized coal ^c	11.0	21.0	22.2	30.4	26.5	32.0	95.0
Wt % of identified acids ^d							
Phenolic	66.6	54.1	14.6	41.0	8.3	5.8	-
Benzene carboxylic	26.0	36.2	69.4	50.2	62.7	76.7	-
Naphthalene carboxylic	2.0	3.3	6.2	5.5	22.9	10.6	-
Heterocyclic ^e	-	1.6	3.5	2.0	2.0	3.2	-
Aliphatic dibasic	2.6	1.0	1.4	-	≤ 1.0	≤ 1.0	-
Others	2.8	3.8	4.9	1.3	3.5	3.0	-
Ratio of Phenol/Benzene Acid	2.56	1.49	0.21	0.82	0.13	0.07	-

^aSee Table 1 for information.

^bWt % was obtained from coal sample on a dry, ash free basis.

^cSmall amount of insoluble Cu-salts are present.

^dWt % was obtained from each benzene-ether extract. Determination was made from the gas chromatograms of their methyl esters.

^eThiophene- and pyridine carboxylic acids for samples 2-6, and pyridine tricarboxylic acids for sample 1.

- Not found.

Table 3

Organic Acids Identified as Their d_3 -methyl Esters by GC-MS and
High Resolution MS

Peak No.	Compound
1	Succinic acid
2	C ₃ -dibasic acid
3	Benzoic acid
4	Methylbenzoic acid
5	p-Hydroxybenzoic acid
6	Hydroxytoluic acid
7	1,2-Benzenedicarboxylic acid
8	1,4-Benzenedicarboxylic acid
9	1,3-Benzenedicarboxylic acid
10	Methylbenzenedicarboxylic acid
11	Dihydroxybenzoic acid
12	Pyridinedicarboxylic acid
13	3,4-Dihydroxybenzoic acid
14	Dimethylbenzenedicarboxylic acid (naphthoic acid, minor)
15	Hydroxybenzenedicarboxylic acid (4-hydroxy-1,3-benzenedicarboxylic acid, largest peak)
16	Methylhydroxybenzenedicarboxylic acid
17	1,2,4-Benzenetricarboxylic acid
18	1,2,3-Benzenetricarboxylic acid
19	1,3,5-Benzenetricarboxylic acid
20	Methylbenzenetricarboxylic acid
21	Pyridinetricarboxylic acid
22	Naphthalenedicarboxylic acid
23	Hydroxybenzenetricarboxylic acid
24	1,2,4,5-Benzenetetracarboxylic acid
25	1,2,3,4-Benzenetetracarboxylic acid
26	1,2,3,5-Benzenetetracarboxylic acid
27	Methylbenzenetetracarboxylic acid
28	Dihydroxy-diphenyldicarboxylic acid (T)
29	Hydroxynaphthalenedicarboxylic acid
30	Benzenepentacarboxylic acid

T indicates that identification is tentative.

Table 4

CuO-NaOH Oxidation of Model Compound at 200°C for 8-10 Hours

Compound	Type of Reaction	Major Product ^a	Yield mol %
4-Methylbenzyl alcohol	$-\text{CH}_2\text{OH} \rightarrow -\text{COOH}$	4-Methylbenzoic acid	93
β -Naphthyl methylcarbinol	$-\text{CH}_2\text{OH} \rightarrow -\text{COOH}$	β -Naphthoic acid	77
Benzaldehyde	$-\text{CHO} \rightarrow -\text{COOH}$	Benzoic acid	95
4-Methoxybenzaldehyde	$-\text{CHO} \rightarrow -\text{COOH}$	4-Hydroxybenzoic acid	89(45)
2,6-Dimethoxyphenol	$-\text{OCH}_3 \rightarrow -\text{OH}$	b	-
Syringaldehyde	$-\text{CHO} \rightarrow -\text{COOH}$	3,4,5-Trihydroxybenzoic acid	4.5 ^c
Dibenzoylmethane	$-\text{CO}-\text{CH}_2- \rightarrow -\text{COOH}$	Benzoic acid	76
1,4-Naphthoquinone	$-\text{CO}-\text{C} \rightarrow -\text{COOH}$	Phthalic acid	91
Phenylacetic acid	$-\text{CH}_2-\text{CO}- \rightarrow -\text{COOH}$	Benzoic acid	68
Diphenyl ether	$-\text{O}- \rightarrow -\text{OH}$	Phenol	67
Dibenzyl ether	$-\text{H}_2\text{C}-\text{O}-\text{CH}_2- \rightarrow -\text{COOH}$	Benzoic acid	81
Diphenyl methane	$-\text{C}-\text{C}- \rightarrow -\text{COOH}$	Benzoic acid	11
Poly-(4-methoxystyrene)	$-\text{C}-\text{C} \rightarrow -\text{COOH}$	4-Hydroxybenzoic acid	6 ^d
1-Methylnaphthalene	$-\text{C}-\text{C}- \rightarrow -\text{COOH}$	1-Naphthoic acid	3
2,4-Dimethoxytoluene	$-\text{C}-\text{C}- \rightarrow -\text{COOH}$	2,4-Dihydroxybenzoic acid	5(58)
3,4-Dimethoxytoluene	$-\text{C}-\text{C}- \rightarrow -\text{COOH}$	3,4-Dihydroxybenzoic acid	7(52)

^aAll products were derivatized with d₆-dimethylsulfate or diazomethane, and analyzed by GCMS.

^bAbout 16.9 wt % of the oxidation product was obtained under the same conditions (170°C for 4 hours) employed for plant materials, humic acids and marine sediments. The product consisted mainly of polymerized material. Very small amount of trihydroxy compounds (2-3%) was detected by GCMS.

^cMost of syringaldehyde was degraded.

^dShown as wt %.

^eNumber in parenthesis shows % of demethylation from $-\text{OCH}_3$ group.

FIGURE CAPTION

Fig. 1a. Gas chromatogram of methyl esters of the organic acid fraction from lignite; Fig. 1b, from bituminous coal. The analysis was carried out on a Perkin-Elmer 3920B gas chromatograph interfaced to a modified Bendix model 12 time-of-flight mass spectrometer with a variable split between a flame ionization detector and the source of the mass spectrometer. The separation was made on a 15.2 m x 0.51 mm SCOT column coated with OV 17 and temperature programmed from 100-250°C at 4°C min⁻¹.

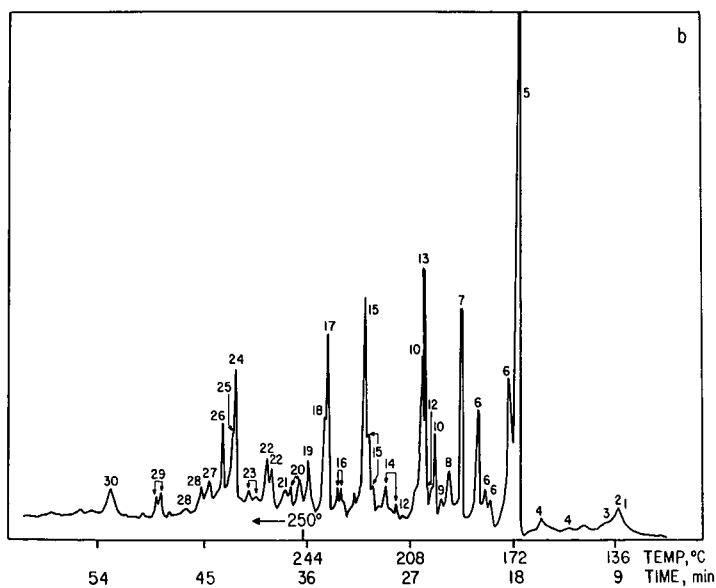
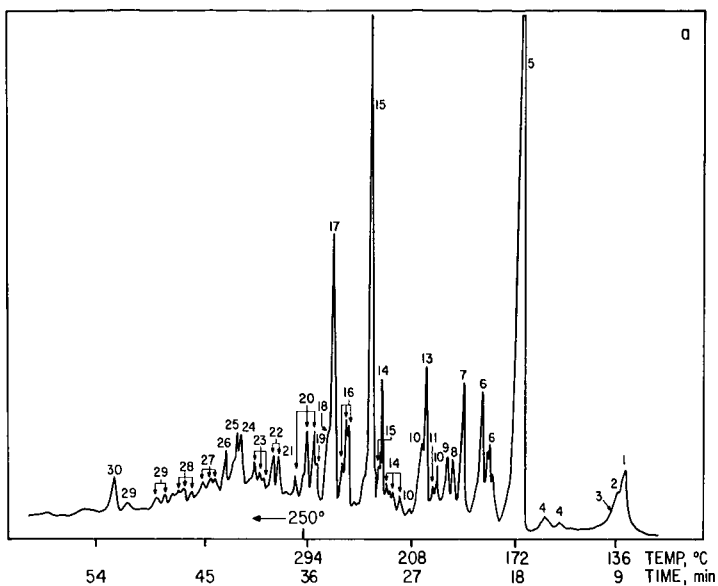


Figure 1

SHORT TIME REACTION PRODUCTS OF COAL LIQUEFACTION
AND THEIR RELEVANCE TO THE STRUCTURE OF COAL

Malvina Farcasiu

Mobil Research and Development Corporation
Central Research Division
P. O. Box 1025
Princeton, New Jersey 08540

INTRODUCTION

The subject of the chemical structure of coal is almost as controversial as it is complex. The complexity of this problem is partially due to the lack of homogeneity and solubility of coals, as well as to the large variety of organic rocks labeled as coals.

A fundamental question is whether we can even consider a chemical structure for a specific coal. Experimental data indicates that there are similarities in the physical properties of some groups of coal and in their behavior toward different chemical reactions; this at least allows us to speak of elements of structure in coal.

Traditionally, both physical and chemical data have been used to study coals. Both kinds of methods require a large amount of experimental work and highly specialized competence in the understanding and application of the method itself. This makes it quite difficult for any individual to master all the aspects of this kind of research. Fully aware of this reality, I will try to present some of our present concepts on coal structure. These concepts are based on data available in the literature as well as from our own experiments. The main idea is to use as much information as possible, which has been obtained by methods as different as possible, and to question all the data, especially those which can be proven by a single method only. One should mention that previous work by Given [1] and Wiser [2] was based on a similar approach. In this paper we will discuss some new data, which was not available to them when they proposed several representative coal average structures.

RESULTS AND DISCUSSION

The first step in the chemical analysis of a coal is the determination of its moisture-ash-free elemental composition. For example, for two coals which have been extensively studied for liquefaction behavior the elemental composition, calculated for 100 atoms is:

<u>Coal</u>	<u>Elemental Composition</u>
Illinois #6 (Monterey)	$C_{50.8}H_{43}O_{4.8}S_{0.8}N_{0.6}$
Wyodak	$C_{48.4}H_{42.4}O_{8.6}S_{0.07}N_{0.5}$

A look at the above data gives several hints about coal structure:

1. For each 100 atoms in coal over 90 are atoms of carbon and hydrogen. Stoichiometry dictates that the majority of the chemical bonds in coal will be carbon-carbon and carbon-hydrogen.
2. Oxygen is the main heteroatom and understanding its chemistry during any coal transformation is essential. For each reaction performed for the usual purpose of removing sulfur and nitrogen, understanding what happens to oxygen is very important, as well as how its reactivity affects those of N and S functions.

Looking at possible coal structures, two aspects are relevant:

- a) the chemical functions in which the heteroatoms appear,
- b) the carbon skeleton of the rest.

The most important chemical functionalities in coal are [3]: for oxygen: phenols, ethers, carboxylic acids, quinones; for nitrogen: pyrrole and pyridine derivatives.

These functionalities can be present in larger or smaller relative amounts in a given coal, but, qualitatively, all the coals contain the same kind of chemical functions.

The carbon skeleton of coal is perhaps the most controversial aspect of the research on coal structure. Three major questions are of interest in this field:

1. What is the percentage of aromatic carbons?
2. How condensed are the aromatic ring structures?
3. What is the carbon skeleton of the aliphatic portion of the coal?

The percentage of aromatic carbon can now be determined by solid-state ^{13}C -NMR. Alex Pines from the University of California at Berkeley made the quantitative measurements for the coals discussed in this paper.

To answer the other two questions related to the carbon skeleton, several approaches can be taken.

One of them is a careful structure determination of the short time reaction products of the thermal liquefaction of coal [4]. During the last four years we worked on a research project supported in part by the Electric Power Research Institute. One of the purposes of this project was to establish the chemical composition of short contact time thermal liquefaction products (including structure). We will now discuss how this data can be used to obtain information about coal structure.

In the short time of 2-5 minutes, coal dissolves in the presence of an H-donor; in the absence of an added catalyst only a few bonds are actually broken. Work at Mobil [4], Exxon [5] and Oakridge National Laboratory [6] indicates that none of the following reactions take place:

- Hydrogenation of aromatic polycyclic hydrocarbons,
- Destruction or formation of polycyclic saturated structures.

A corollary of this is: if these polyaromatic or polycyclic saturated structures are present in coal, they should be identified in the thermal liquefaction products.

Many of the chemical functionalities are also stable in these conditions, especially the O,S,N heterocyclic structures. Water formation by phenol dehydrogenation is also minimal. We found that in coal conversions even at long reaction times (up to 90 minutes) in the absence of an added catalyst, the -OH bonded to a monoaromatic ring is stable. In the same conditions, dehydroxylation of naphthenic phenols does occur [7].

The degree of ring condensation of the aromatic part can be semi-quantitatively determined in coal liquids [4]. It has been found that in the short time liquefaction products, the majority of the aromatic rings are as in benzene and naphthalene. These data are consistent with the data obtained by Hayatsu, Scott, Moore and Studier [9], using an oxidative method and with the uv-visible spectroscopy data reported by Friedel and Queiser [10]. I conclude then that in the subbituminous and bituminous coals studied by us and others, the aromatic carbons are not present in significant amounts as highly condensed rings.

Concerning the carbon skeleton of the aliphatic portion, there are no methods for direct identification. However, for a given formula if the total number of C and H is known, as well as the percentages of aromatic and aliphatic carbon and hydrogen a possible structure for the aliphatic part may be inferred.

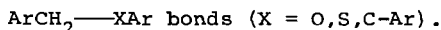
Possible average chemical structures present in short time reaction products have been determined by a methodology we have already reported [4,8]. Fractions with average molecular structures as in Figures 1-4 are consistent with the experimental data.

As shown in Figure 1 for a given molecular formula, there is a relationship between the degree of aromatic ring condensation and the degree of aliphatic ring condensation.

The relative number of aliphatic hydrogens and carbons is consistent with the presence of some polycondensed aliphatic structures. The number of the polycondensed aliphatic rings seems quite high in certain Wyodak coal liquids obtained in a thermal process at short reaction time (Figure 4). It is likely that such structures are also present in Wyodak coal. Other experimental data are also in favor of this explanation. For example, the oxidative method used by Deno et al. [11], gives selective oxidation of aromatic structures only if polycondensed aliphatic rings are not present. The results obtained by this method for Wyodak coal are nonreproducible and the oxidation products are difficult to analyze.

Another approach is a direct calculation of the possible number of the aliphatic rings. The calculation is based on the elemental analysis of the coal and the percent of aromatic carbon obtained by ^{13}C -NMR in solid state [4]. Based on this method, the Wyodak coal used in the liquefaction study to obtain data as in Figure 2 contained 44-50% aromatic carbon. This would be consistent with 2 to 8 aliphatic rings for 100 atoms of carbon. We should note that some other samples of Wyodak coal for which we measured the aromatic content were somewhat more aromatic (50-70% aromatic carbon).

The data we presented are based on the similarity of the elements of structure in coal and in the short contact time, noncatalytic liquefaction products. These elements of structure could be bound together with low energy thermally labile bonds. As described in the literature [4,6], these weak bonds could be:



An important practical consequence of knowing the coal structure and the structure of its short time liquefaction products is the understanding of the possible limits of reduction of H-consumption for the liquefaction of a particular coal. In Figure 5 we make such correlations. This aspect will be discussed more fully in the future.

ACKNOWLEDGMENTS

The work presented here was conducted under a program jointly sponsored by EPRI and Mobil Research and Development Corporation. Co-workers in this project are J. J. Dickert, T. O. Mitchell and D. D. Whitehurst. Technical assistance was provided by B. O. Heady and G. Odoerfer

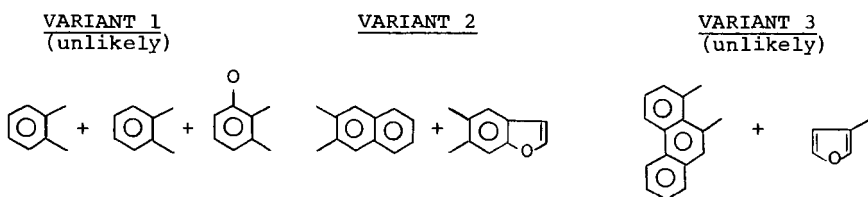
REFERENCES

1. P. H. Given, *FUEL*, **39**, 147 (1960).
2. W. Wiser, Storch Award Address, ACS Meeting, Miami, 1978.
3. W. Francis, "Coal", Edward Arnold Publishers, Ltd., London, 1961.

- 4a. D. D. Whitehurst, M. Farcasiu and T. O. Mitchell, "The Nature and Origin of Asphaltenes in Processed Coals," EPRI Report AF-252, First Annual Report Under Project RP-410, February 1976.
- 4b. D. D. Whitehurst, M. Farcasiu, T. O. Mitchell and J. J. Dickert, Jr., ibid, Second Annual Report, July 1977.
- 5a. T. Aczel, M. L. Gorbaty, P. S. Moa, R. H. Schlosberg, FUEL, 54, 295 (1975).
- 5b. T. Aczel, M. L. Gorbaty, P. S. Moa, R. H. Schlosberg, Preprints of the 1976 Coal Chemistry Workshop organized by EPRI, ERDA, NSF and SRI, Menlo Park, Calif., p. 165 (1976).
6. B. M. Benjamin, V. F. Raaen, P. H. Maupin, L. L. Brown and C. J. Collins, FUEL, 57, 269 (1978).
7. D. D. Whitehurst, M. Farcasiu, T. O. Mitchell, J. J. Dickert, Jr., "The Nature and Origin of Asphaltenes in Processed Coals," EPRI Project RP-410, Third Annual Report, to be published.
8. M. Farcasiu, FUEL, 56, 9 (1977).
- 9a. R. Hayatsu, R. G. Scott, L. P. Moore, M. H. Studier, Nature, 257, 378 (1975).
- 9b. R. Hayatsu, R. E. Winans, R. G. Scott, L. P. Moore and M. H. Studier, Preprints ACS-Division of Fuel Chemistry, Vol. 22, No. 5, p. 156 (Chicago 1977).
10. R. A. Friedel, J. A. Queiser, FUEL, 38, 369 (1959).
11. N. C. Deno, B. A. Greigger, S. G. Stroud, FUEL, 57, 455 (1978).

General Formula $C_{31}H_{27}O_2$
 Aromatic Moiety $C_{18}H_{10-11}$ (1H -NMR, ^{13}C -NMR)

Aromatic Structures Considered



Possible Average Structures

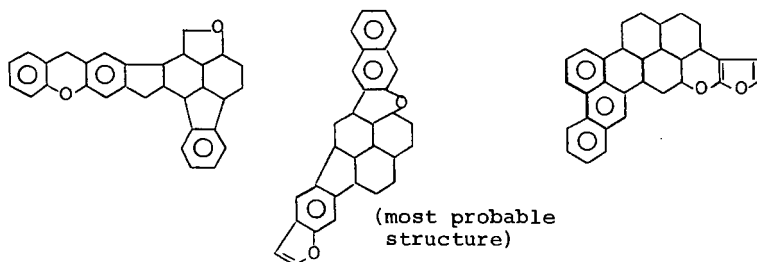


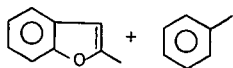
Figure 1: Possible Average Structure for a Short Contact Time Fraction SESC-3 of Monterey Coal.

General Formula $C_{43}H_{38}O_2$

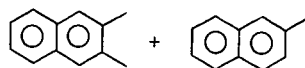
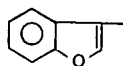
Aromatic Moiety $C_{26}H_{18}$ (1H -NMR, ^{13}C -NMR)

Aromatic Structures Considered:

VARIANT 1



VARIANT 2



Possible Average Structures:

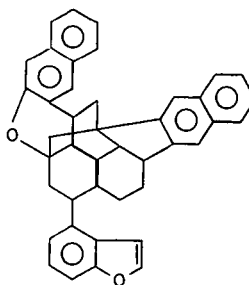
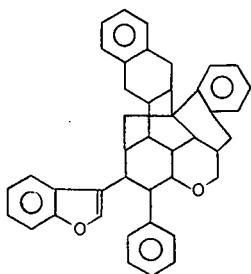
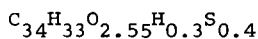


Figure 2: Possible Average Structures for Wyodak SESC-3 Short Contact Time SRC

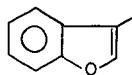
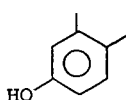
Figure 3: Fraction SESC-4 Monterey Coal Short
Contact Time SRC



% Aromatic C = 59

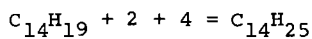
% Aromatic H = 43

Aromatic Part $\text{C}_{20}\text{H}_{14}$

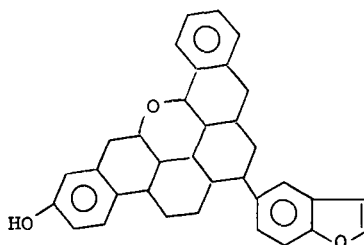


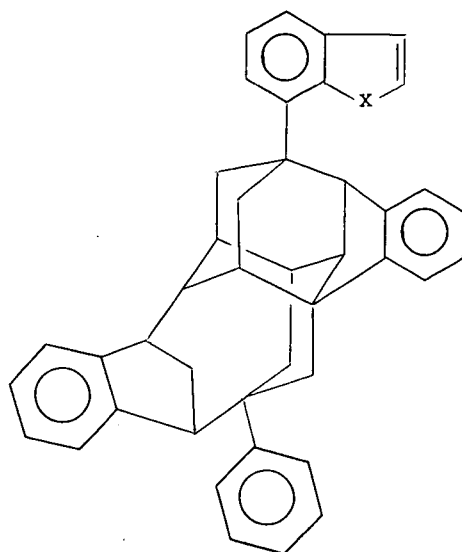
Aliphatic Part $\text{C}_{14}\text{H}_{19}$

1 Aliphatic Ether + 4 Substitutents



$\text{C}_{14}\text{H}_{26}$ -- 3 Condensed Aliphatic Rings





Calculated Based on Experimental Data:

$C_{43}H_{36}NO_2$

Av. MW = 600

Aromatic $C_{27}H_{18-19}$ (1H -NMR, ^{13}C -NMR)

In formula:

(62% Aromatic C, 52% Aromatic H)

$C_{26}H_{18}$

Benzylic (2-3 ppm)

H_{10}

H_3

Aliphatic

C_{16}

H_7

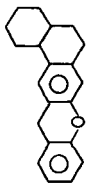
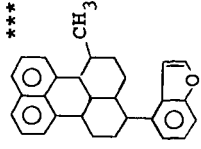
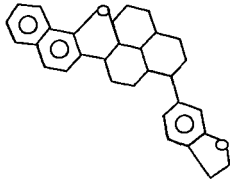
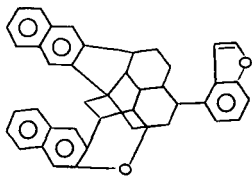
C_{16}

$H?$

H_{18}

Figure 4: Average Carbon Skeleton Formula for Wyodak SRC

Figure 5: Comparison of Structures and Hydrogen Consumption for Four Coals

Coal	Kentucky	Hiawatha	Monterey	Wyodak
Composition	$C_{100}H_{82}N_{1.7}O_{9.4}$	$C_{100}H_{84}N_{2.0}O_{9.5}$	$C_{100}H_{88}N_{1.6}O_{13.2}S_1$	$C_{100}H_{86}NO_{18}$
No. polycondensed saturated rings/100C	Coal 4 SESC-3 SCT*	6 4	10 5	
Structure				
g H consumed/ 100g coal during liquefaction (Normalized to 100% conversion)	SCT 0.43 LCT** 0.96	0.63 2.03	0.89 2.80	

*SCT = Short Contact Time <2 min.

**LCT = Long Contact Time >30 min.

***Ca. 30 min. contact time.

DEDUCTION OF THE STRUCTURE OF BROWN COAL BY REACTION WITH PHENOL

R.J. Hooper* and D.G. Evans[†]

* D.S.I.R. Industrial Processing Division, Private Bag, Petone, New Zealand

† Centre for Environmental Studies, University of Melbourne, Parkville, Victoria 3052, Australia.

INTRODUCTION

To make any real progress in the ability to predict and control the liquifaction of coal by hydrogenation it is necessary to know what chemical reactions are occurring. Modern preparative and analytical techniques such as elution chromatography, mass spectroscopy and proton nmr have made the task of characterizing the products of liquefaction reactions much easier than hitherto, but the task of characterizing the coal before reaction remains almost as intractable as ever, because these new methods depend on the analysis samples being in the liquid form (or in the case of mass spectroscopy, able to be completely vaporized).

This is not a new problem, of course. Over the years many solubilization techniques have been suggested as tools for deducing coal structure, e.g. oxidation, hydrogenation, alkaline hydrolysis, pyrolysis and extraction with powerful solvents (either alone or in conjunction with other methods such as thermal pre-treatment, use of ultrasonics, etc.). These suffer from one of two disadvantages: with the relatively mild physical methods insufficient coal is got into solution to be useful (less than 20% is typical); but with chemical methods, including pyrolysis, the treatment is so harsh that interpretation of the structure of the original coal in terms of that of the products is of dubious validity. In particular, use of elevated temperatures, as in pyrolysis or other thermal treatments, is to be avoided, as free radicals formed by cleaving fragments off the main body of the coal molecule may polymerize to form structures which were not present in the original coal.

If it is accepted that coal cannot be got into solution without altering its structure to some extent, we should look for methods in which these changes are not large enough to prohibit the drawing of adequate deductions about the structure of the original coal, while at the same time presenting the reacted coal in a form suitable for structural examination. This would require at least 80% of the coal to be solubilized, with the soluble material low enough in molecular weight to ensure that it in turn is soluble in mild organic solvents, as required for preparative techniques such as solvent fractionation or chromatography.

The methods we considered were Friedel-Crafts reactions of various kinds (alkylation and acylation) and depolymerization of the coal by using it to alkylate phenol, as first proposed by Heredy and co-workers (1), and extensively investigated by them (1-5) and by Ouchi and co-workers (6-11). From the recent review of these methods by Larsen and Kuemmerle (12) it appears that molecular weights of the coal fragments produced are higher for alkylation and acylation methods (typically several thousand, even after allowing for the added acyl or alkyl groups) than for the material depolymerized in phenol (less than a thousand). The only disadvantage of phenol depolymerization, compared with the other methods, was its relatively weak action on very high rank coals (< 90% C, daf). This did not concern us, as we were interested in examining brown coals from the Latrobe Valley, Victoria, Australia, with very low rank (65-70% C, daf). We therefore chose this method, which had already been shown by Ouchi and Brooks (9) to be very effective for this type of coal. We perhaps underestimated the difficulties that chemically combined phenol would cause us, as will be discussed later.

In our plan of attack we first depolymerized the coal using conditions suggested by Imuta and Ouchi (11), then divided it into five fractions of progressively increasing polarity, using solvent fractionation, then analysed these fractions separately by elemental and functional group analysis, and further characterized the fractions by running infrared and proton nmr spectra on them. After allowing for the effects of combined phenol these data were put together to build up a composite picture of the structure of the original coal. Heredy et al. (5) have carried out a similar investigation on a series of coals of different ranks. The present work differs from theirs in that it used a more powerful catalyst for the phenolation, a more decisive solvent fractionation scheme, and infrared as well as nmr analysis for characterizing the fractions. Also our coal was lower in rank than any of those they tested.

EXPERIMENTAL

Coal used

The coal tested was Morwell brown coal from Victoria, Australia. Its composition on a dry basis is shown in Table 1. This coal contains over 60% moisture as mined. It was ground wet to 80% < 25 mesh, and used in the wet state (60% moisture).

Phenolation reaction

179 g of wet ground coal, 75 g of p-toluenesulfonic acid catalyst and 1300 g of laboratory grade phenol were heated under nitrogen, and the water was removed from the coal by boiling at 183°C (the boiling point of phenol is 181.8°C). The remaining mixture was refluxed at 183°C for 4h, after which the phenol was removed by steam distillation, leaving a solid, black, tarry material of low melting point, which was separated by decantation, and extracted by refluxing for 2h with 1200 ml of ethanol/benzene azeotrope (65% benzene, 35% ethanol). The insoluble material was filtered off and dried in a vacuum oven for 12h at 50°C and 16kPa pressure (these conditions were later used to remove excess solvent from all the fractions - see Figure 1 below).

Solvent fractionation

To facilitate later structural analysis the coal was separated into structural types using the solvent fractionation scheme shown in Figure 1.

Analysis

The original coal and the various fractions were analysed for carbon, hydrogen and oxygen by the C.S.I.R.O. Microanalytical service. Ash contents were determined in a standard ashing furnace (13). Phenolic, carboxylic and carbonyl oxygen contents were determined by the State Electricity Commission of Victoria, using methods developed by them for brown coals (14).

Infrared spectra of the original coal and the fractions were measured on a Perkin Elmer 457 Grating Infrared Spectrophotometer. Liquid samples (fractions A and B) were analysed as a thin film or smear. Solid samples (C, D and original coal) were analysed in KBr discs containing 0.3% by mass of sample. These were prepared by grinding the KBr mixture for 2 minutes in a tungsten carbide TEMA grinding barrel, drying for 24h in a vacuum desiccator over phosphorus pentoxide, then pressing into discs at 10 tons force, at room temperature but under vacuum. Because fraction A was dominated by phenol a sample of it was further separated by elution chromatography in an attempt to separate from it material less dominated by phenol. Elution was carried out in a silica column, using elutants in the following order:

hexane, chloroform, methanol.

Proton nmr spectra were recorded on a Varian HA 100 nmr spectrometer at room temperature, with tetramethylsilane (TMS) as internal standard, with a sweep width of 0 to 1000 Hz from TMS. For fraction A a solution of deuterated chloroform was used; fractions B and C were not soluble in CDCl_3 and pyridene- d_5 had to be used; fractions D and the whole coal were barely soluble even in pyridene- d_5 , but enough dissolved to get spectra. These will not, of course, be representative of the whole material.

RESULTS

Yields and compositions

Table 1 shows the yields of the five fractions per 100 g of original dry coal and their compositions, including a breakdown of the oxygen into carboxylic, phenolic and other oxygen. Note that part of the ash-forming material has been removed by the solubilizing process (much of the non-organic material in Morwell coal is ion-exchangeable, and would have been replaced by hydrogen ions from the p-toluene-sulfonic acid; this was confirmed by ash analysis: e.g. ash from the original coal contained 50% SiO_2 and 10% MgO , whereas fraction D ash contained 80% SiO_2 and only 1% MgO). As the total yield of fractions was 202 g/100 g of original coal 102 g must have been added. This consists of combined phenol and unseparated solvents, as will be discussed later. This dilution results in the fractions having higher carbon contents and lower oxygen contents than the original coal. The hydrogen content decreases from A to D as the fractions become less aliphatic and more aromatic and polar.

Infrared spectra

The infrared spectra of the fractions and the original coal are shown in Figure 2. The spectra of the eluted sub-fractions of fraction A are not given here.

As already mentioned fraction A is dominated by phenol; nevertheless strong aliphatic absorptions can be seen at 2920, 2850, 1460 and 1380 cm^{-1} . The spectra of subfractions A1 (eluted by hexane, a very small part of A) and A2 (eluted by chloroform, about a quarter of A) showed these aliphatic absorptions very strongly. The spectrum for A1 showed little else, and this sub-fraction is probably virtually pure paraffins. The spectrum for A2 resembled the spectra for phenol ether and phenetole ($\text{C}_6\text{H}_5\text{OC}_2\text{H}_5$). Absorption due to hydrogen-bonded hydrogen is negligible, showing that all the phenol in this sub-fraction has been converted to ethers. The spectrum for subfraction A3 (which constitutes about three quarters of A) was dominated by phenol, but some aliphatic absorptions still showed, and this sub-fraction may well consist of phenol bonded to small coal fragments by methylene bridges. The absorptions for A, A2 and A3 at 1250 cm^{-1} are probably due to ether oxygen.

Fraction B is in many ways similar to fraction A, but with much weaker aliphatic absorption. It has a strong absorption due to hydrogen-bonded hydrogen at 3400 cm^{-1} , a weak aromatic absorption at 3030 cm^{-1} and many other absorptions characteristic of phenol. It also shows weak aliphatic absorptions at 2920, 1460 and 1380 cm^{-1} , and ether oxygen absorption at 1250 cm^{-1} .

Fractions C, D and E have spectra similar to those of the original coal. Phenol no longer dominates, although the hydrogen bonded -OH absorption at 3400 cm^{-1} is still strong. Aliphatic absorption is weak in C and E and negligible in D. The shoulder at 1700 cm^{-1} due to carboxylic oxygen, which was quite strong for the whole coal, is also quite pronounced for fractions C and D. (It was absent from fractions A and

B). This checks well with the data in Table 1 obtained by chemical analysis. The broad absorption from $1200-1000\text{ cm}^{-1}$ present in the whole coal is also present in fractions C and D although absent from A, B and E. Doubtless oxygen groups contribute to this, but we believe it is mainly due to silica, which is a major constituent of the ash. It could be virtually removed by deashing the coal with strong acids or by float/sink separations.

Nmr spectra

Figure 3 shows nmr spectra for fractions A, B, C and E.

Table 2 shows the forms the protons are present in, as determined from these spectra. The data for fraction D and the whole coal are shown in brackets, as these samples were virtually insoluble in pyridine, and the spectra represent only the small soluble portions. This table demonstrates the difficulties the coal chemist faces in trying to use proton nmr on physical solutions of coal: e.g. the soluble part of the whole coal shows no hydrogen-bonded protons despite the evidence of table 1; it shows no triaromatic or methylene bridge protons, despite the presence of appreciable amounts of these in the fractions; on the other hand it shows far more methylene α and methyl β than do the fractions.

The nmr data confirm and amplify the infrared data: hydrogen bonded protons are present from phenolic and carboxylic groups in the coal and phenol groups added into the chemically combined phenol. The monoaromatic content (of fractions A and B especially) is high, also because of added phenol, but di-ring aromatic material is also present in all fractions (even triaromatic in C), which must have come from the original coal. The aliphatic material observed in the infrared spectra of A, B and C is now seen to consist principally of methylene bridges and short, branched aliphatic chains (α and β - methyl predominate).

DISCUSSION

Combined phenol

The total combined phenol was estimated as follows:

Using the yield and composition data of Table 1 elemental balances were drawn up, as in Table 3. The third last line gives the masses of the various constituents of the added material. The second last line gives the amount of phenol this would account for, assuming all the added oxygen was from phenol (none from ethanol or methanol). The last line gives the remainder, which is close in composition to benzene (which could be present as a contaminant in fractions B and C). In the fractionation scheme shown in Figure 1 ethanol contamination of any fraction is unlikely, but pentane contamination of fraction A and methanol contamination of D and E are possible. We rejected these because pentane was not picked up from fraction A by hexane elutriation while preparing subfraction A1 (this was negligible in mass), and D was too deficient in hydrogen and oxygen to contain any appreciable amount of methanol. Methanol could have been present in E, but the mass of this fraction was so small that any such effect would be negligible.

Distribution of hydrogen on a phenol - and solvent-free basis

We can now determine the distribution of hydrogen in the original coal, but first we have to estimate the hydrogen distribution in fraction D, which could not be determined by nmr analysis. In another paper presented to this Congress (15) we reported results of the hydrogenation of fractions A to D in tetralin. Fraction D yielded a low-hydrogen residue, which still could not be analysed by nmr, and a high-hydrogen

liquid product separated by boiling off excess tetralin. From its nmr analysis and the known amount of functional group hydrogen in the original fraction (0.05 g/100 g original coal) we concluded that the aliphatic hydrogen in the original fraction was about 0.3 g/100 g, and the remaining 0.8 g of hydrogen/100 g was aromatic hydrogen of various kinds.

In Table 4 the results of the nmr analyses (Table 2), the estimates of combined phenol and contaminant benzene (Table 3), and the above estimates of the distribution of hydrogen in fraction D are manipulated to give a composite estimate of hydrogen in various forms in the original coal (the aromatic hydrogen in fraction D is assumed to follow the same pattern as in A, B and C, and the aliphatic hydrogen is also assumed to be distributed as in A, B and C). From this we can calculate by difference the hydrogen present in various forms in the original coal (second last line of Table 4).

Distribution of structural types

The distribution of hydrogen calculated above, together with the distribution of functional group oxygen (Table 1), between them define a statistically probable structure for Morwell brown coal. Rather than attempt to draw a structure we give in Table 5 estimates of the numbers of carbon atoms associated with each type of hydrogen atom that not only predict approximately the correct mass of carbon per 100 g of coal but also allow for approximately the required number of substituents in the aromatic groups, and for the bridges connecting the groups. There may, of course, also be some carbon not associated with hydrogen, such as acyl bridges and tertiary carbons in side chains (see later). We note in passing that the greatest difficulty in meeting the above requirements is in accommodating the oxygen not accounted for in functional groups.

We will conclude with a brief discussion of the forms taken by the three main structural groups: oxygen groups, aromatic groups and aliphatic groups.

Oxygen groups: As seen from Table 1, 25% of the dry coal was oxygen, 5% in the form of phenolic groups, 5% carboxylic, and 3% carbonyl. The present work throws little light on the remaining 12%. Some ethers are thought to be present, but we cannot confirm this: ethers noted in fractions A and B could have come from the phenolation reaction. There was some indication of the presence of benzofuran groups from the infrared spectra of residues left after the reaction of fractions C and D with tetralin (15). No doubt other heterocyclic oxygen is present also.

Aromatics: The presence of relatively large proportions of higher aromatic structures (diphenyl, naphthalene and polynuclear) is noteworthy, and unexpected from previous studies on brown coal (16, 17). The total aromatic content may have been overestimated slightly by the procedure used to estimate the hydrogen distribution of fraction D, but this would make little difference to the contents of the higher aromatics.

Aliphatics: The most surprising result of this work is the high methylene bridge content (more than 25% of all hydrogen), which again was not expected from earlier models (16). However it should be noted that in the study by Heredy et al. (5) similar to the present one 12% of the hydrogen in a lignite was found to be in the form of methylene bridges. It seems unlikely that these bridges were formed by the phenolation reaction (indeed Heredy's favored mechanism requires the prior presence of such bridges, and the large content found in this work appears to confirm his mechanism as being the most important one in the phenolation reaction). If the quantities in Table 5 are calculated out in terms of the numbers of structures rather than their masses, we get 0.45 mole of aromatic groups per 100 g of coal and 0.65 mole of methylene bridges per 100 g. This means that there is more than one bridge per aromatic group, i.e. a high degree of crosslinking must be present, probably in

a three-dimensional network. Possibly dihydroanthracene structures may also be present.

Another surprising result is the high number of β -methyl and β -methylene groups (0.23 mole/100 g coal) without corresponding α -methylenes (only 0.02 mole/100 g). This could be explained only by the presence of tertiary butyl groups (note that Swann et al. (18) recovered 2,6-di-*t*-butyl-4-methylphenol from a similar brown coal by evacuation at 35°C). The material reported here as β -methyl occurred at $\delta = 1.2$ (Figure 3), which Heredy et al. (5) interpret as β -methylene groups in naphthenic rings. If they are right this would put quite a different complexion on this finding; however their interpretation differs from those of other authorities (e.g. Ref. (19)), and would require a simultaneous occurrence of α -methylene groups, which is not borne out by our Figure 3.

REFERENCES

- (1) Heredy, L.A. and Neuworth, M.B. Fuel 1962, 41, 221.
- (2) Heredy, L.A., Kostyo, A.E. and Neuworth, M.B. Fuel 1963, 42, 182.
- (3) Heredy, L.A., Kostyo, A.E. and Neuworth, M.B. Fuel 1964, 43, 414.
- (4) Heredy, L.A., Kostyo, A.E. and Neuworth, M.B. Fuel 1965, 44, 125.
- (5) Heredy, L.A., Kostyo, A.E. and Neuworth, M.B. Adv. Chem. 1966, 55, 493.
- (6) Ouchi, K., Imuta, K. and Yamashita, Y. Fuel 1965, 44, 29.
- (7) Ouchi, K., Imuta, K. and Yamashita, Y. Fuel 1965, 44, 205.
- (8) Ouchi, K. Fuel 1967, 46, 319.
- (9) Ouchi, K., and Brooks, J.D. Fuel 1967, 46, 367.
- (10) Ouchi, K., Imuta, K. and Yamashita, Y. Fuel 1973, 52, 156.
- (11) Imuta, K. and Ouchi, K. Fuel 1973, 52, 174.
- (12) Larsen, J.W. and Kuemerrle, E.W. Fuel 1976, 55, 162.
- (13) BS1076 Part 3 1973.
- (14) McPhail, I. and Murray, J.B. Victorian State Electricity Commission, Sci. Div. Rep. MR-155, 1969.
- (15) Hooper, R.J. and Evans, D.G. Paper to Coal Liquifaction Fundamentals Symposium, ACS/CSJ Congress, Honolulu, 1979.
- (16) Anon. Coal Research in C.S.I.R.O. No. 6, March 1959, p12.
- (17) van Krevelen, D.W. "Coal", Elsevier, Amsterdam, 1961.
- (18) Swann, P.D., Harris, J.A., Siemon, S.R. and Evans, D.G. Fuel 1973, 52, 154.
- (19) Bartle, K.D. and Smith, J.A.S. Fuel 1965, 44, 109.

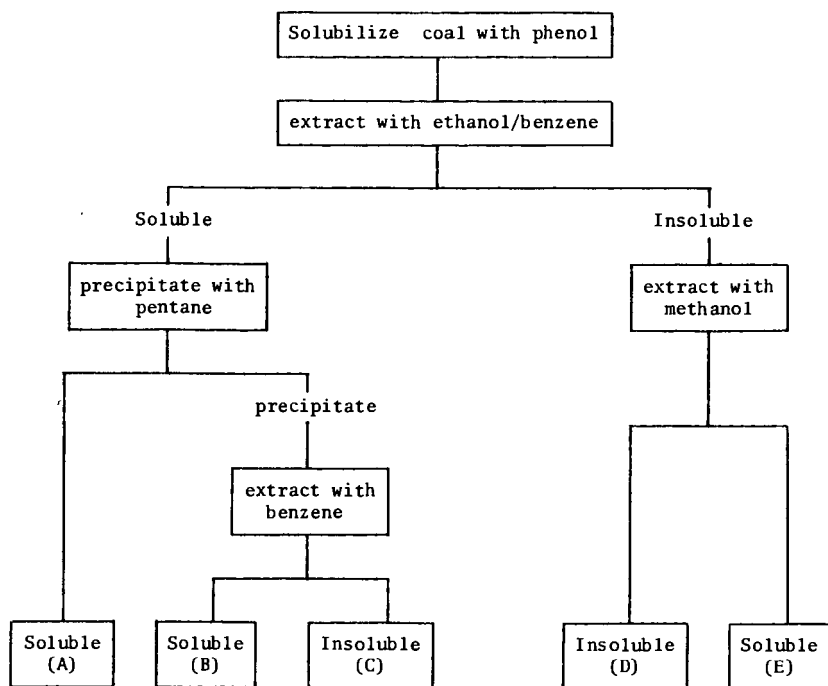


Figure 1: The fractionation scheme used to separate coal into four soluble fractions and an insoluble residue.

	fraction						Whole Coal
	A	B	C	D	E	Composite	
yield, g/100g original coal	28	66	78	28	2	202	100
composition, mass %							
C	76	74	69	71	56	72	63
H	7	6	5	4	6	5	5
O phenolic	4	4	3	6	ND	(4)	5
O carboxylic	0	1	3	2	ND	(2)	5
O carbonyl	ND	ND	ND	ND	ND	ND	3
O total	17	16	21	18	24	18	25
ash	ND	ND	2	3	ND	(1)	4
unaccounted	1	4	3	4	14	4	3

Table 1: Yields and compositions of the fractions. ND means not determined. Ash contents were not determined on fractions A, B and E, which were liquids. Functional group oxygen was not determined on fraction E because insufficient of it was available. The figures in brackets for the composition of the composite should be little affected.

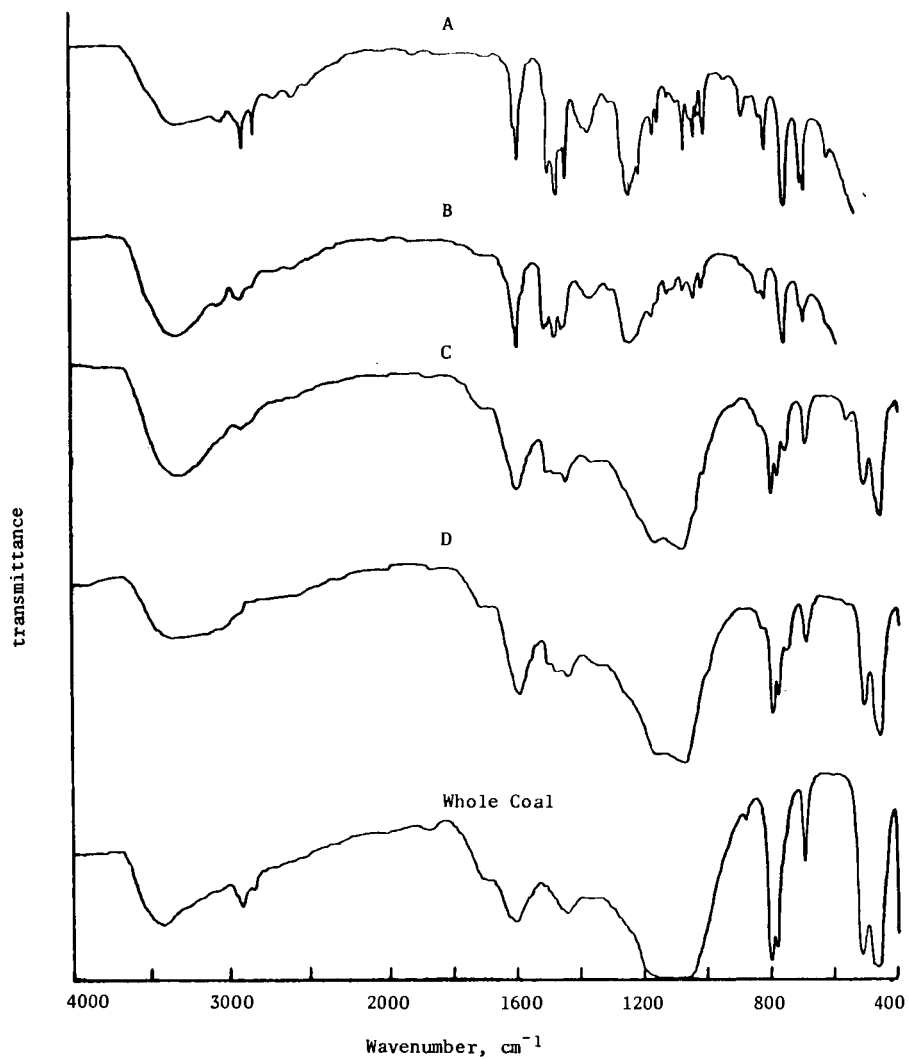


Figure 2: Infrared spectra for the original coal and the fractions A to D separated by the fractionation scheme shown in Figure 1. Fractions A and B, thin film; C, D and whole coal, KBr disc.



Figure 3: Nmr spectra for fractions A, B, C and E.
A is dissolved in CDCl_3 ; B, C and E in pyridene- d_5 .

δ ppm	proton type	fraction						Whole Coal
		A	B	C	D	E	Composite	
> 8.0	hydrogen bonded	7	17	19	(0)	27	(15)	(0)
8.7-8.0	triaromatic (5)	0	0	6	(10)	0	(3)	(0)
8.0-7.2	two-ring aromatic (5)	6	10	8	(48)	13	(63)	(46)
7.2-6.2	monoaromatic	63	58	44	(35)	37		
5.8-4.3	olefinic	1	0	0	(0)	0	(0)	(0)
4.3-3.4	methylene bridge	4	9	17	(trace)	9	(10)	(0)
3.4-3.2	acetylinic	0	0	0	(0)	trace	(0)	(0)
3.2-2.4	methin, methylene α	3	0	0	(0)	0	(3)	(11)
2.4-2.0	methyl α	1	4	(4)		15		
2.0-1.4	methylene β	3	1	0	(0)	0	(1)	(4)
1.4-1.0	methyl β	13	4	1	(4)	0	(5)	(39)
1.0-0.6	aliphatic γ	0	0	0	(0)	0	(0)	(3)

Table 2: Distribution of protons by type in the various fractions as measured from nmr spectra. Figures are % of the total protons in the particular fraction. Allowance has been made for residual protons in the deuterated solvents (CDCl_3 for A, pyridene- d_5 for others). The figures for fraction D and the whole coal are put in brackets to indicate that these samples were barely soluble and the spectra do not represent the whole material, only the small soluble part. α , β , γ refer to the positions of these protons with respect to aromatic rings.

fraction	C	H	O	ash	un- accounted	total
A	21	2	5	0	0	28
B	49	4	11	0	2	66
C	54	4	16	1	3	78
D	20	1	5	1	1	28
E	1	0	0	0	1	2
total	145	11	37	2	7	202
original coal	63	5	25	4	3	100
added material	82	6	12	-2	4	102
added phenol	54	4	12	0	0	70
remainder	28	2	0	-2	4	32

Table 3: Materials balances on material added to the coal by phenolation and fractionation. All figures are g/100 g of original dry coal.

	hydrogen bonded	aromatic			meth. bridge	aliphatic				total
		tri	di	mono		α CH ₂	α CH ₃	β CH ₂	β CH ₃	
A	0.14	0.00	0.12	1.23	0.08	(0.02	0.04)	0.06	0.25	1.94
B	0.67	0.00	0.40	2.30	0.36	0.00	0.04	0.04	0.16	3.97
C	0.74	0.23	0.31	1.72	0.66	0.00	0.16	0.00	0.04	3.86
D	(0.05)	(0.03	0.10	0.65)	(0.16	0.00	0.04	0.02	0.07)	1.12
E	0.03	0.00	0.02	0.04	0.01	0.00	0.02	0.00	0.00	0.12
total	1.63	0.26	0.95	5.94	1.27	0.02	0.30	0.12	0.52	11.01
phenol	0.74	-	-	3.01	-	-	-	-	-	3.75
benzene	-	-	-	2.46	-	-	-	-	-	2.46
coal	0.89	0.26	0.95	0.47	1.27	0.02	0.30	0.12	0.52	4.80
total	1.63	0.26	0.95	5.94	1.27	0.02	0.30	0.12	0.52	11.01

Table 4: Hydrogen present in various forms in fractions, original coal, combined phenol and benzene contaminant, g/100 g original dry coal (figures in brackets have involved making some assumptions about the distribution.

hydrogen type	atomic C/H	mass C/H	H (Table 4) g/100 g coal	C g/100 g coal
monoaromatic	6/2	36	0.47	17
two ring aromatic	10/4	30	0.95	28
triaromatic	14/4	39	0.26	10
α methylene	1/2	6	0.02	0
β methylene	1/2	6	0.12	1
methylene bridge	1/2	6	1.27	8
α methyl	1/3	4	0.30	1
β methyl	1/3	4	0.52	2
carboxyl	1/1	12		2
total				69

Table 5: Calculation of carbon in various structural forms, g/100 g dry coal.

THE CHEMISTRY OF ACID-CATALYZED COAL DEPOLYMERIZATION

Laszlo A. Heredy
Rockwell International, Energy Systems Group
8900 De Soto Avenue, Canoga Park, California 91304

Since its introduction in the early 1960's, acid-catalyzed depolymerization has become a widely used method to convert coal into soluble products for structural investigations. It was first shown by Heredy and Neuworth⁽¹⁾ that coal could be depolymerized by reacting it with phenol-BF₃ at temperatures as low as 100°C. The method was based on the assumption that coal contains aromatic structures linked by aliphatic bridges, such as methylene bridges, which are sufficiently reactive to participate in an acid-catalyzed transarylation reaction. This general type of structure was proposed by Neuworth, et al.,⁽²⁾ to explain the chemistry of low-temperature pyrolysis of coal. The overall reaction of this proposed structure with phenol-BF₃ is illustrated in Figure 1. One of the final products of the depolymerization is dihydroxy-diphenylmethane.

The depolymerization reaction was modified by Ouchi, Imuta, and Yamashita⁽³⁾ who substituted p-toluenesulfonic acid (PTSA) for BF₃ as the catalyst and increased the reaction temperature to 180-185°C. A very high degree of depolymerization, with pyridine soluble product yields over 90%, was achieved under these conditions. Darlage and Bailey⁽⁴⁾ investigated the effects of reaction temperature, various solvents and coal preoxidation on depolymerization product yields using a number of acid catalysts. They found that meta-substituted phenols were more effective aromatic substrates for the depolymerization reaction than phenol. The preoxidation of coal, particularly of some sulfur-rich bituminous coals, with dilute aqueous nitric acid considerably increased the yield of depolymerization products.⁽⁵⁾

A general review of the acid-catalyzed coal depolymerization method has been published recently by Larsen and Kuemmerle.⁽⁶⁾ The objective of this paper is to discuss some specific aspects of the chemistry of coal depolymerization.

I. THE RELATIVE REACTIVITIES OF VARIOUS BRIDGE STRUCTURES TOWARD PHENOL-BF₃

Although no systematic studies have yet been reported regarding the relative reactivities of aliphatic bridge structures, or more generally, aliphatic-aromatic carbon-carbon bonds, which may be present in various coals, toward phenol-BF₃, some important trends have been established in model compound experiments.^(1,7) The results of these experiments are summarized in Tables 1 and 2 and in Figure 2.

The data on isopropyl group transfer in Table 1 show that the secondary aliphatic-aromatic carbon-carbon bond is much more reactive when it is located on either a phenolic ring or on a phenanthrene ring than on a nonactivated benzene ring. The relative reactivities of the secondary carbon bond in the first two structures could not be evaluated because the isopropyl group transfer went to completion both in the case of ortho-isopropylphenol and of retene. The data on n-propyl group transfer in Table 2 show, as expected, that a bond between a primary aliphatic carbon and an aromatic carbon is less reactive than a secondary carbon-aromatic carbon bond under otherwise similar conditions.

Figure 2 shows the comparison of the relative reactivities of four aromatic-aliphatic carbon-carbon linkages. A comparison of the reactivities of the two linkages a' and b', which involve primary aliphatic carbon atoms, clearly show enhanced reactivity at bond a' due to the activating effect of the phenolic hydroxyl group. A comparison of the reactivity of linkage a' with that of the corresponding bond in para-n-propylphenol (Table 2) indicates that the reactivities of (-CH₂-CH₂-) substituted aromatics are similar whether the substitution is in a bridge or in a chain structure. The relative reactivities found with model

compound B indicate that $-CH_2-$ bridges can play a special role in coal depolymerization because in this case bonds on both sides of the bridge structure are activated (compare the reactivities of bonds b and b' , respectively).

It is probable that cleavage of aliphatic ether bonds contributes to coal depolymerization, particularly in the case of lignites and subbituminous coals. Although the reactivity of various ethers with phenol- BF_3 has not been investigated, several studies on the BF_3 -catalyzed cleavage of various aliphatic ether linkages have been reported.^(8,9) It was shown that the reaction of ethers with benzene gives alkylbenzenes. The relative ease of reaction varied considerably with different ethers. Diisopropyl ether and dibenzyl ether reacted vigorously with benzene upon saturation with BF_3 . Isopropyl, phenyl, and benzyl ethyl ethers reacted violently. On the other hand, ethyl, isoamyl, and n-amyl ethers reacted only at higher temperatures and elevated pressures (150°C and 10-20 atm).

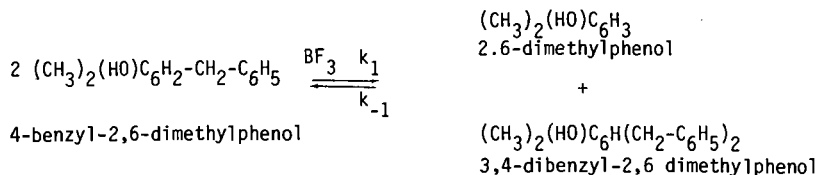
II. INVESTIGATION OF THE KINETICS OF BF_3 -CATALYZED BENZYL GROUP TRANSFER

Kinetic investigations of BF_3 -catalyzed benzyl group transfer in benzylphenol systems were reported by Heredy.⁽¹⁰⁾ These systems were chosen for investigation because of the particular interest in the role that $-CH_2-$ bridges may play in coal depolymerization.

One of the investigations was made with para-benzylphenol. Experiments were made first with the para-benzylphenol/phenol (1-14C)/ BF_3 system to study the rate of benzyl group transfer from benzylphenol to phenol (1-14C). It was found, however, that the rate of benzyl group transfer to para-benzylphenol was much faster than to phenol (1-14C), and therefore, no meaningful kinetic measurements could be made on the latter system. In another experiment, the kinetics of benzyl group transfer was studied in the para-benzylphenol- BF_3 system. The kinetic measurements were made in sealed glass tubes at 100°C using a para-benzylphenol to BF_3 mole ratio of 6.25/1.0. The two principal reactions which take place in this system are shown in Figure 3. In agreement with the reaction scheme shown in Figure 3, the rate of disappearance of the sum of para- and ortho-cresols followed a second order rate equation. The ratio of the initial reaction rates of reaction 1a to 1b was found to be approximately 4.0. In addition to phenol and benzene, significant amounts of diphenylmethane and some para-cresol were formed during the latter part of the reaction. Also, isomerization to ortho-benzylphenol took place as a result of the reverse reactions of 1a and 1b.

A more detailed kinetic study of benzyl group transfer was made using the 4-benzyl-2,6-dimethylphenol/ BF_3 system. This system was selected for investigation for the following reasons: (a) In the benzylphenol/ BF_3 system two parallel major reactions have taken place giving dibenzylphenol and phenol in one reaction, and hydroxybenzylphenols and benzene in the other. It was expected that the additional activating effect of the two methyl groups on the phenolic ring will sufficiently enhance the reactivity of the methylene-aromatic carbon-carbon bond on the side of the phenolic ring to make the cleavage of that bond the predominant reaction; (b) The chemical shifts of the benzyl protons and of the 2-methyl protons of the starting material and of the main products were sufficiently different to permit the quantitative analysis of the reaction mixture by proton NMR spectrometry. The chemical shifts of the benzyl $-CH_2-$ groups and of the methyl groups in the starting material and in the products are shown in Table 3.

The reaction which was studied is shown in the following equation:



The kinetic measurements were made in CS₂ solution at 70°C using sealed NMR sample tubes as the reactors. After the completion of the prescribed reaction period each sample tube was quickly cooled to room temperature and transferred to the NMR spectrometer for recording the spectra. When a solution of 4-benzyl-2,6-dimethylphenol and BF₃ (mole ratio 4.5 to 1.0) was used, the absorption under the methylene peak (3) and the methyl peak (2) increased from an initial value of zero as the reaction advanced, showing the formation of 3,4-dibenzyl-2,6-dimethylphenol. Independent gas chromatographic analysis showed the formation of an equivalent amount of 2,6-dimethylphenol. Reaction rate constants were determined for both the forward (k₁) and the reverse (k₋₁) reactions for three different BF₃ concentrations. The following correlations were determined:

$$\text{Rate (forward reaction)} = k_1 [\text{BF}_3] [(\text{CH}_3)_2(\text{HO})\text{C}_6\text{H}_2\text{-CH}_2\text{-C}_6\text{H}_5]^2$$

$$\text{Rate (reverse reaction)} = k_{-1} [\text{BF}_3] [(\text{CH}_3)_2(\text{HO})\text{C}_6\text{H}(\text{CH}_2\text{-C}_6\text{H}_5)_2] [(\text{CH}_3)_2(\text{HO})\text{C}_6\text{H}_3]$$

At 70°C and at a concentration of BF₃ = 1.0 moles per litre, k₁ = 2.6 ± 0.3 × 10⁻⁴ min⁻¹ lit. moles⁻¹ and k₋₁ = 16.0 ± 1.8 × 10⁻⁴ min⁻¹ lit. moles⁻¹. The benzyl group transfer in this system is clearly a bimolecular substitution reaction where the rate determining step involves a reaction between a protonated benzyl compound (benzenium ion) and a phenolic compound or its BF₃- complex. There is no indication of the formation of the benzyl cation in this particular system. It should be noted here that the data obtained on the transfer of n-propyl groups (Table 2) indicate that, similarly, the main reaction in that transfer does not involve the formation of the 1-propenium cation. If that were the case, isomerization to the 2-propenium cation would take place with the predominant formation of iso-propylphenols. On the other hand, the formation of diaryl-methenium cations was indicated in model compound studies reported by Franz et al.,⁽¹¹⁾ who studied the behavior of triaryl-methanes under depolymerization conditions using both PTSA and phenol-BF₃ as the catalyst.

III. COMMENTS ON THE CHEMISTRY OF COAL DEPOLYMERIZATION

After reviewing the information on the reactivities of various bridge structures which may be present in coal, it will be instructive to summarize available data on coal depolymerization yields as a function of coal rank. One can attempt then to correlate the product yields obtained by depolymerization with various structural features of coals over the coalification range which has been investigated.

Depolymerization yields determined with phenol-BF₃ at 100°C are summarized in Table 4,⁽¹²⁾ and the yields obtained with phenol-PTSA depolymerization at 185°C are shown in Figure 4.⁽³⁾ In the case of the phenol-BF₃ catalyst, the phenol-soluble product yield was the highest (75%) for the lignite. It gradually decreased to about 10% for the low-volatile bituminous coal, although the low product yield obtained with subbituminous coal does not fit this correlation. In the case of depolymerization with phenol-PTSA, the pyridine-soluble product yield was over 90% for coals of 70-84% C content; for coals with higher C content, the yield dropped sharply and it reached about 10% for a coal with 93% C. Benzene-ethanol was a more selective solvent than pyridine for fractionating the depolymerization products obtained with PTSA catalyst: a linear relationship between the yield of the soluble extract and the carbon content of the starting coal was observed.

The following comments can be made with regard to a correlation of the coal depolymerization product yields with the relative reactivities of aliphatic carbon and oxygen bridge structures in coal:

- (1) In low-rank coals, particularly in lignites, the cleavage of aliphatic ether and benzyl ether oxygen bonds may contribute significantly to depolymerization. Many of the aliphatic bridges, which participate in depolymerization, may be linked to single phenolic rings. The reactivity of an aliphatic structure linked to a

phenolic ring is sufficient to permit its participation in the depolymerization reaction. On the other hand, spectrometric studies indicate⁽¹³⁾ that these coals do not contain significant amounts of sufficiently reactive condensed aromatic structures which could participate in depolymerization.

- (2) In high-volatile bituminous coals ($C = 80-84\%$), the breaking of aliphatic bridges is seen as the major means of depolymerization. Many of these bridges may be linked to phenolic rings, others to condensed aromatic rings such as phenanthrene. Ether oxygen bonds play a less important role because most of these bonds are in aromatic ethers which do not react with BF_3 .
- (3) In higher rank bituminous coals ($C > 84\%$), the depolymerization product yield decreases sharply with increasing rank. It is probable that this decrease is related to the nature of the aliphatic bridge structures. It is postulated that in lower rank coals a sufficient number of the bridge structures are short aliphatic chains ($N_c = 1$ to 4). On the other hand, in higher rank coals, nearly all of the bridge structures are condensed hydroaromatic rings; with structures of this type, several bonds must be broken between two aromatic groups to effect depolymerization.
- (4) Among the aliphatic bridge structures, $-CH_2-$ bridges may play a particularly important role in coal depolymerization. Even if the number of such bridges is relatively small, the probability of their cleavage is high because, in general, both carbon-carbon bonds of the bridge are activated under the reaction conditions used in coal depolymerization. This view is supported by experimental data obtained in depolymerization studies made with phenol- BF_3 where the yield of soluble depolymerized products was proportional to the amount of $-CH_2-$ bridge structures found in the soluble products.⁽¹²⁾

REFERENCES

1. L. A. Heredy and M. B. Neuworth, *Fuel*, **41**, 221 (1962)
2. E. A. Depp, C. M. Stevens, and M. B. Neuworth, *Fuel*, **35**, 437 (1956)
3. K. Ouchi, K. Imuta, and Y. Yamashita, *Fuel*, **44**, 29 (1965)
4. L. J. Darlage and M. E. Bailey, *Fuel*, **55**, 205 (1976)
5. L. J. Darlage, J. P. Weidner, and S. S. Block, *Fuel*, **53**, 54 (1974)
6. J. W. Larsen and E. W. Kuemmerle, *Fuel*, **55**, 162 (1976)
7. L. A. Heredy, A. E. Kostyo, and M. B. Neuworth, *Fuel*, **42**, 182 (1963)
8. J. J. O'Connor and F. J. Sowa, *JACS*, **60**, 175 (1935)
9. W. J. Monacelli and G. F. Hennion, *JACS*, **63**, 1722 (1941)
10. L. A. Heredy, *Studies on the Chemistry and Mechanism of Transbenzylation*, Doctoral Dissertation, Carnegie Institute of Technology, Pittsburgh (1962)
11. J. A. Franz, J. P. Morrey, G. L. Tingey, W. E. Skiens, R. J. Pugmire, and D. M. Grant, *Fuel*, **56**, 366 (1977)
12. L. A. Heredy, A. E. Kostyo and M. B. Neuworth, *Fuel* **44**, 125 (1965); *Coal Science, Advances in Chemistry Series*, **55**, 493 (1966)
13. H. L. Retcofsky, *Applied Spectroscopy*, **31**, 116 (1977)

TABLE 1
BF₃-CATALYZED ISO-PROPYL GROUP TRANSFER TO PHENOL (1-¹⁴C)

Starting Compound*	Conversion (%)	Product Distribution (wt %)		
		para-isopropyl-phenol (1- ¹⁴ C)	ortho-isopropyl-phenol (1- ¹⁴ C)	Residue
Cumene	8.0 ⁺	3.5	0.8	3.7
ortho-isopropylphenol	100.0	74.5	14.5	11.0
Retene (1-methyl-7-isopropylphenanthrene)	100.0 ⁺⁺	61.5	10.2	28.3

*Starting compound to labelled phenol molar ratio: 1 to 20. Reactions performed at 100°C for four hours. Mixture saturated with BF₃

+Benzene, in an amount equivalent to the isopropylphenols, was also recovered

++A methylphenanthrene fraction, in an amount equivalent to isopropylphenols, was also recovered

TABLE 2
BF₃-CATALYZED REACTION OF PARA-N-PROPYLPHENOL WITH PHENOL (1-¹⁴C)

Reaction Conditions:
 Ratio of para-n-propylphenol to phenol (1-¹⁴C): 1 to 20
 Mixture saturated with BF₃ at reaction temperature
 Temperature: 100°C
 Reaction Period: 4 hours

<u>Product Distribution (wt %):</u>	
para-n-Propylphenol (unreacted)	: 18.0
para-n-Propylphenol (1- ¹⁴ C)	: 43.0
ortho-n-Propylphenol (1- ¹⁴ C)	: 14.5
para-iso-Propylphenol (1- ¹⁴ C)	: 5.3
ortho-iso-Propylphenol (1- ¹⁴ C)	: 1.2
Residue	: 18.0
Total	: 100.0

TABLE 3
CHEMICAL SHIFT VALUES OF METHYLENE AND METHYL
PROTONS OF BENZYL DERIVATIVES OF 2,6-DIMETHYLPHENOL

COMPOUND	CHEMICAL SHIFT (ppm)*			
	METHYLENE		METHYL	
	(3)	(4)	(2)	(6)
2,6-DIMETHYLPHENOL	---	---	2.08	2.08
4-BENZYL- 2,6-DIMETHYLPHENOL	---	3.70	2.03	2.03
3,4-DIBENZYL- 2,6-DIMETHYLPHENOL	3.80	3.70	1.95	2.10

*TETRAMETHYLSILANE = 0.00 ppm

TABLE 4
DEPOLYMERIZATION OF COALS OF DIFFERENT RANKS WITH PHENOL-BF₃ AT 100°C

Coal Type	C, % dmmf	Total Soluble ^(a) Yield, %	Combined Phenol Content of Soluble Fraction, %
Lignite	70.6	75.2	41.2
SubB	76.7	23.4	32.8
hvab	82.4	47.4	16.3
hvab	85.1	28.8	12.4
hvab	85.8	25.0	13.0
lvb	90.7	9.8	15.5

^(a) Coal-derived part of phenol soluble material

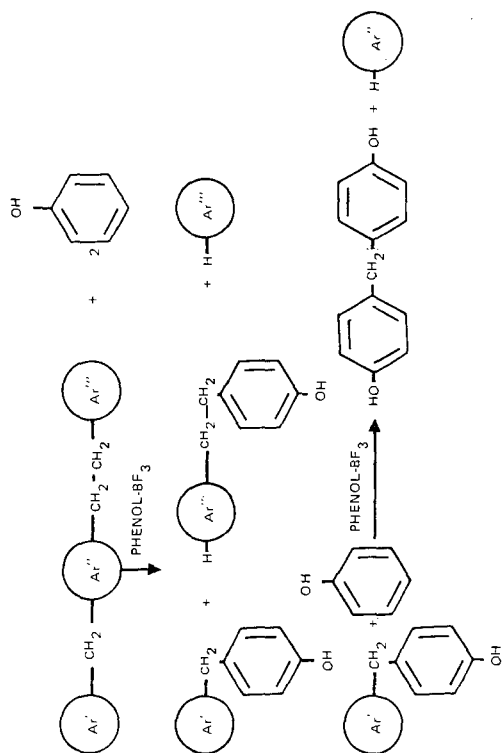
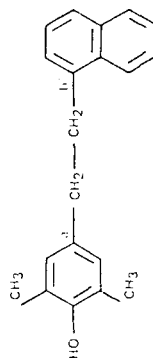


Figure 1. Coal Depolymerization via Transalkylation with Phenol-BF₃

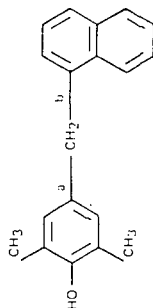
FIGURE 2
RELATIVE REACTIVITIES OF MODEL COMPOUNDS WITH PHENOL-BF₃

Model Compound	Reacting Bond	Relative Reactivity
A	a'	77
A	b'	2
B	a	70
B	b	41

Model Compound A:



Model Compound B:

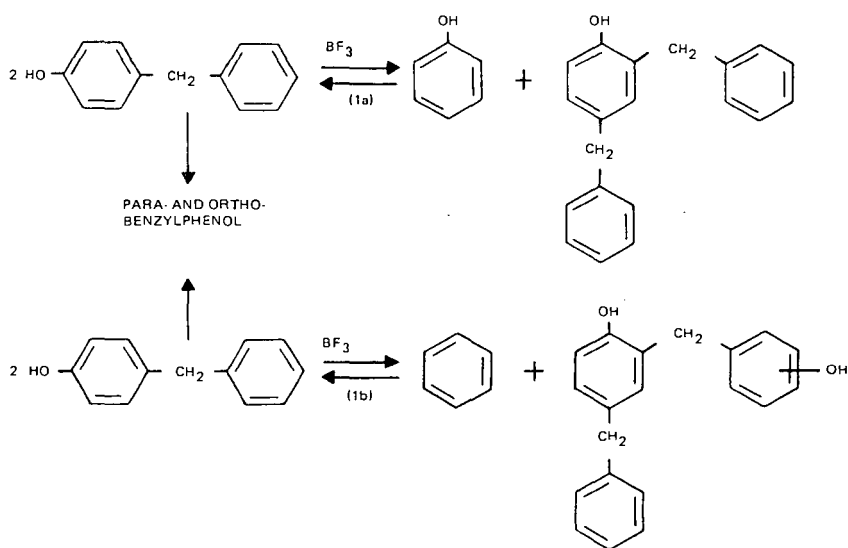


Reaction Conditions:

Ratio of Model Compounds to Phenol: 1 to 10
Mixture Saturated with BF₃ at Reaction Temperature
Temperature: 100°C
Reaction Period: 4 hours

FIGURE 3.

BF_3 -CATALYZED BENZYL GROUP TRANSFER IN BENZYLPHENOLS



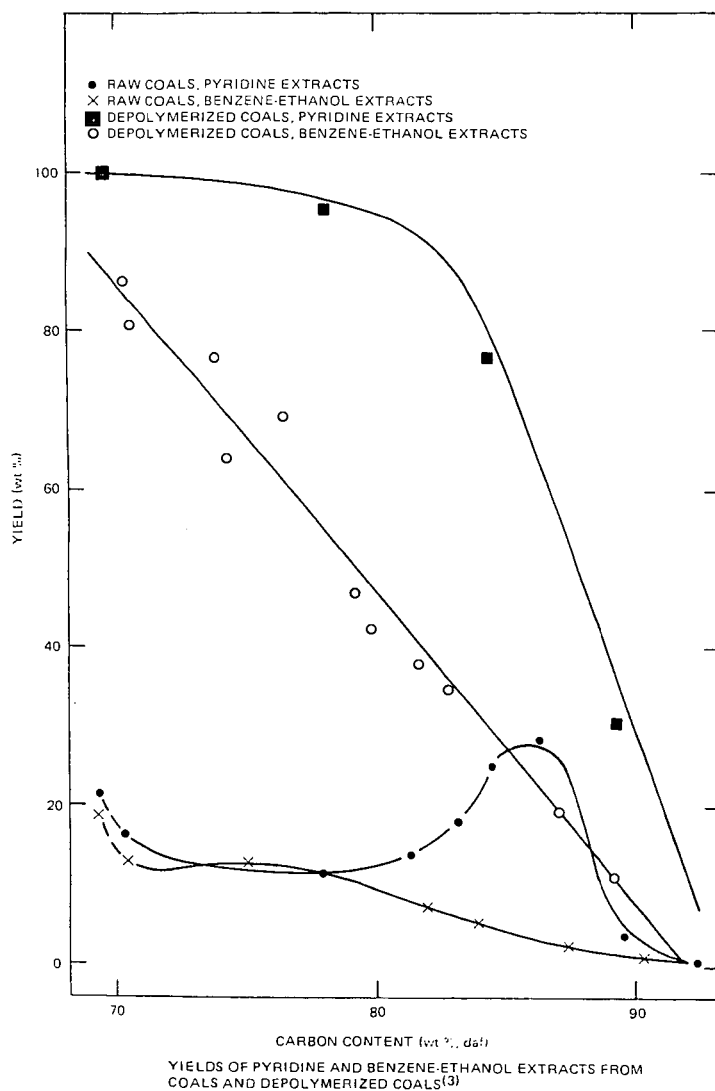


FIGURE 4. -

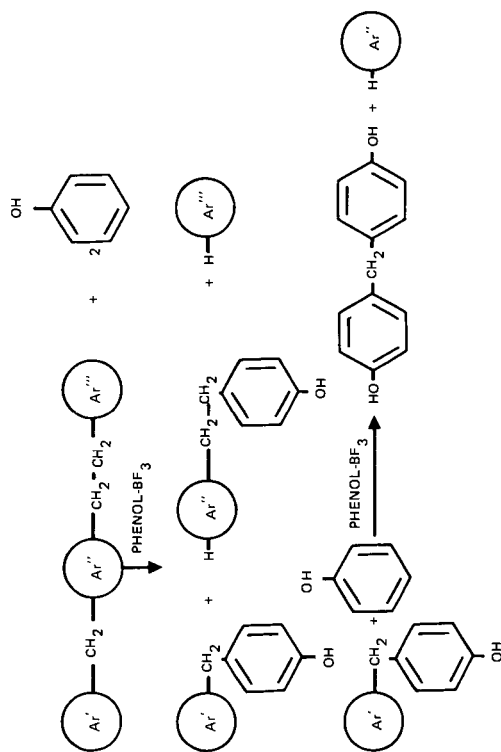
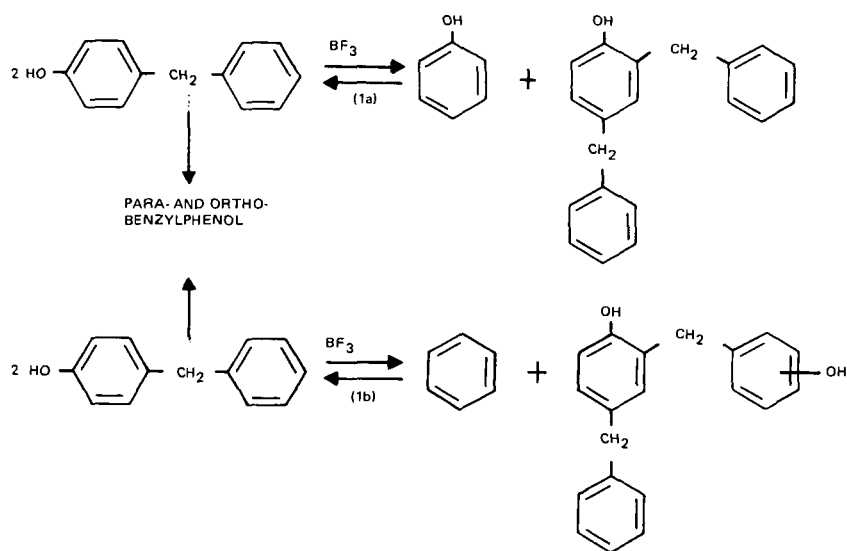
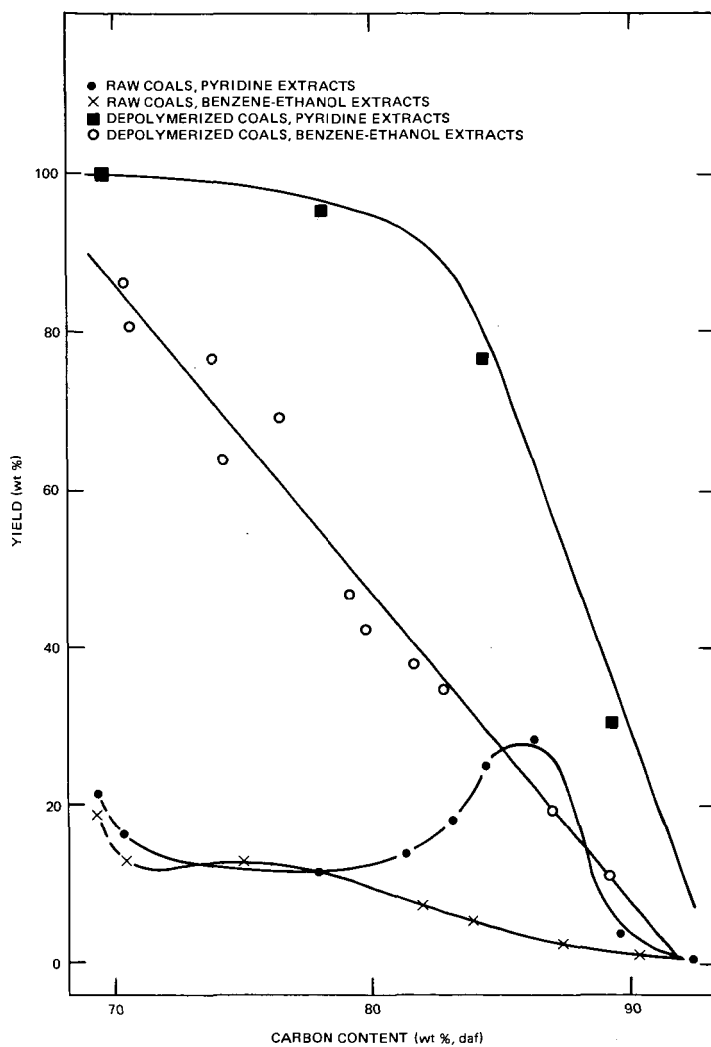


Figure 1. Coal Depolymerization via Transalkylation with Phenol-BF₃

FIGURE 3.

BF₃-CATALYZED BENZYL GROUP TRANSFER IN BENZYLPHENOLS





YIELDS OF PYRIDINE AND BENZENE-ETHANOL EXTRACTS FROM
 COALS AND DEPOLYMERIZED COALS⁽³⁾

FIGURE 4.

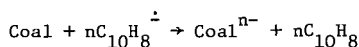
COAL ALKYLATION REACTION. THE CHARACTERISTICS OF THE ALKYLATION REACTIONS AND PRODUCTS

Lawrence B. Alemany, C. Indhira Handy and
Leon M. Stock

Department of Chemistry
The University of Chicago
Chicago, Illinois 60637

INTRODUCTION

Sternberg and his associates found that the treatment of many coals with alkali metals in the presence of electron transfer agents formed polyanions which could be alkylated to form compounds which were soluble in common organic solvents including heptane and benzene (1). More recently, we discussed the proton and carbon nmr spectra of typical gpc fractions of polybutylated Illinois No. 6 coal (2). This work revealed that there were significant differences in these fractions with variations in the degree of aromaticity, the ratio of C-butylation to O-butylation, the extent of butylation on aliphatic and aromatic carbon atoms, and the amount of carbonyl and vinyl derivatives. In addition, the low molecular weight fractions contained paraffinic hydrocarbons which presumably were liberated as the coal matrix collapsed. The results obtained in this work are compatible with the essential features of the reaction process proposed by Sternberg and his associates (1,2). He suggested that the electron transfer agent, naphthalene, transfers electrons from the metal to molecular fragments in the coal. Under these conditions,



the aromatic molecules of the coal are reduced, and the basic anions produced under the experimental conditions react with acidic hydrogen atoms to yield aryloxides and stable carbanions. Ether cleavage and elimination reactions also occur under these experimental conditions. In addition, carbon-carbon bond cleavage reactions take place. Also, carbonyl compounds are reduced to semiquinones or ketyls. In the presence of sufficient concentrations of soluble electron transfer reagents, an equilibrium mixture of soluble and insoluble polyanions containing carbanions, aryloxides, mercaptides, ketyls, nitrobenzene bases and so forth is generated. Because few rearrangement reactions occur under basic conditions the structures of the anionic products are quite closely related to the structures of the molecular fragments in coal. These anionic compounds are readily alkylated by primary iodides. However, the alkylation reaction is complicated by competitive electron transfer reactions which yield butyl radicals. Thus, the coal alkylation reactions occur by the reactions of the nucleophilic anionic compounds with the alkyl iodide and by the reactions of the aromatic hydrocarbon compounds with the butyl radical.

The rich chemistry of the coal polyanion and the presumably close relationship between the structures of the coal polyanion and the initial coal molecules prompted us to study the reaction conditions and the reaction products carefully and then to examine the reaction of the coal polyanion with 90%-enriched butyl iodide-1-C-13.

EXPERIMENTAL PART

Materials.--Successful alkylations require the use of thoroughly purified reagents in an air and moisture-free environment. The reagents used in this work were all carefully purified by distillation or recrystallization shortly before use. The Illinois No. 6 coal samples (Anal.: C, 70.19; H, 5.18; N, 0.62; Cl, 0.14; S(pyritic), 0.82; S(sulfate), 0; S(organic), 2.71; O(by diff.) 11.43; Ash, 8.19) were dried at 100° in vacuo for 16 hrs. Tetrahydrofuran was refluxed in a nitrogen atmosphere over lithium aluminum hydride for 4 hrs prior to distillation from the hydride. The distillate was stored under argon. Tetrahydrofuran could not be purified as readily by distillation from potassium. We found that the resonances of vinyl, carboxyl and other unidentified groups were present in the nmr spectra of concentrated samples of the distillate when potassium was used as the purification reagent.

Preliminary Experiments.--Initial work centered on the study of the reaction of potassium with tetrahydrofuran and with naphthalene in tetrahydrofuran.

Potassium (20 mmol) was added to tetrahydrofuran (50 ml) under argon. Aliquots free of potassium were withdrawn periodically. These aliquots were hydrolyzed and titrated to determine the extent of the reduction of the solvent. This reaction was negligible even after 5 days, Figure 1A.

In the next experiment, potassium (20.1 mmol) was added to a stirred solution of naphthalene (3.10 mmol) in tetrahydrofuran (50 ml) under argon. The characteristic dark green solution of naphthalene radical anion and dianion formed within 4 min. Aliquots free of potassium were withdrawn from the reaction mixture. These aliquots were hydrolyzed and titrated to determine the extent of conversion of naphthalene to the radical anion and dianion. After about 4.5 hrs, the titrimetric procedure revealed that the naphthalene was converted to a mixture equal in reducing power to 80% dianions. The reaction was followed for 5 days. The results are shown in Figure 1B.

In the third experiment of this series, potassium (20.1 mmol) and naphthalene (3.10 mmol) in tetrahydrofuran (50 ml) were allowed to react for 4.5 hrs. Coal (0.860g) was then added. The reaction mixture immediately became brown. During the next several days the reaction mixture changed color as the reactions proceeded. Aliquots free of potassium but containing solid coal particles were withdrawn from this mixture and titrated to determine the extent of conversion of the coal to the coal polyanion. In certain instances, aliquots free of potassium and solid coal particles were withdrawn from the reaction mixture and titrated to determine the extent of conversion of the solid coal to soluble anionic substances. The reaction was allowed to proceed for 5 days at ambient temperature under argon. An aliquot of the mixture was then withdrawn to establish the extent of the reaction. The results are shown in Figure 1C.

The results obtained in several experiments revealed that 21 ± 1 negative charges per 100 carbon atoms were introduced into the coal.

Coal Alkylation with Butyl Iodide-1-C-13.--Potassium (26.1 mmol) was added to a stirred solution of naphthalene (3.14 mmole) in tetrahydrofuran (45 ml) under argon. After 45 min, -325 mesh coal (1.00g) and an additional wash quantity of tetrahydrofuran (10 ml) were added. The mixture was stirred for 5 days. The excess potassium (2.98 mmol) was removed. A small quantity of insoluble coal (0.041g) was unavoidably lost in the removal of the metal. A solution of 90%-enriched butyl iodide-1-C-13 (6.88g) in tetrahydrofuran (10 ml) was added to the stirred solution in 15 min. This quantity corresponds to a 2-fold excess of the amount of reagent needed for the alkylation of a coal polyanion with 21 negative charges per 100 carbon atoms and naphthalene dianion. Potassium iodide began to precipitate from the reaction mixture almost immediately. The alkylation reaction was allowed to proceed for 2 days. Potassium iodide rapidly settled from the reaction mixture when stirring was interrupted.

The reaction mixture was then exposed to the atmosphere and the coal product was isolated. The mixture was centrifuged and the very dark brown, tetrahydrofuran-soluble material was removed by pipet. Fresh solvent was added to the residue and the mixture was stirred. The mixture was then centrifuged and the soluble material was removed by pipet. This procedure was repeated several times. The final extracts were clear, pale yellow solutions. The combined extracts were filtered through a 1.4μ frit. The filtrate was concentrated in vacuo at 50°C to yield a freely flowing, dark brown material (2.252g). Residual volatile materials were removed in several stages in vacuo. The amounts of material present after 2 hrs were 1.956g; after 16 hrs, 1.678g; after 41 hrs, 1.581g; and after 68 hrs, 1.521g. This product is dark brown and does not flow.

Water was added to dissolve the potassium iodide present in the tetrahydrofuran-insoluble material. The mixture was then stirred and subsequently centrifuged to yield a clear, yellow supernatant solution and a small residue. This residue was treated in the same way several times to extract all the water soluble materials. The final extracts were colorless and did not yield a precipitate when treated with sodium tetraphenylborate. The residue obtained in this way was dried in a stream of dry nitrogen to constant weight (0.686g).

The water-soluble material was filtered through a 1.4μ frit. An aliquot of the solution was treated with excess sodium tetraphenylborate. The potassium tetraphenylborate which precipitated was collected and dried. This analysis indicates that 18.1 meq of potassium ion were formed in the reaction.

The tetrahydrofuran-soluble portion of the butylated, carbon-13 labelled Illinois No. 6 coal (1.5208g) was chromatographed on silica gel (Baker, 60-200 mesh, 24g) to remove materials such as the electron transfer agent and the related reduction and alkylation products. These materials were eluted with pure hexane (about 250 ml) and 5:95 tetrahydrofuran: hexane (about 250 ml). The dried eluent weighed 0.9967g. The coal products were then eluted with pure tetrahydrofuran (about 250 ml) followed by 50:50 tetrahydrofuran: methanol (about 250 ml) and pure methanol (about 250 ml). The dried eluent weighed 0.5350g. The recovery was virtually quantitative.

A portion of the coal product (168.1 mg) was dissolved in pure tetrahydrofuran (2 ml) and chromatographed on Styragel(R) gpc columns (Waters Associates). Columns with a molecular weight exclusion limit of 10,000 (2 x 61 cm.) and 2,000

(2 x 61 cm.) were connected in series. Tetrahydrofuran was used as the mobile phase (0.36 ± 0.01 ml min⁻¹). About 30 fractions (3.7 to 3.8 ml) were collected in each experiment. The tetrahydrofuran was removed in vacuo and a stream of filtered, dry nitrogen was used to remove the final traces of the solvent. The coal product obtained with C-13 labelled butyl iodide was partitioned into 17 fractions (total weight 178.4 mg). Samples to be used for nmr spectroscopy were dried thoroughly at 25° at about 5 torr for 40-45 hrs to remove the remaining traces of tetrahydrofuran.

The spectroscopic methods used in this study have been described previously (2).

Other Alkylation Experiments.--In other experiments, lithium and sodium were used in place of potassium. 1,2-Dimethoxyethane was used in place of tetrahydrofuran. Butyl chloride, butyl bromide, butyl mesylate, butyl triflate, and methyl iodide were used in place of butyl iodide. The conditions used in these experiments were very similar to the conditions used in the procedures described in the previous paragraphs. The isolation procedure was modified in those cases where the ionic salt, e.g. sodium iodide, was soluble in tetrahydrofuran. In these instances, the tetrahydrofuran-soluble product was washed with water to remove the salt prior to further study.

Repetitive Alkylation Reaction.--The tetrahydrofuran-insoluble materials were, in certain instances, subjected to a second alkylation reaction. In these cases, there were three notable differences in the experimental results. First, the green color of the naphthalene dianion persisted for a significantly longer time following the addition of the coal residue. Second, gas evolution, presumably butene-1, was detectable during the addition of butyl iodide or butyl mesylate but, significantly, not during the addition of methyl iodide. Third, the rate of formation of potassium iodide was much more rapid such that the rate difference between butyl iodide and methyl iodide was not evident.

The reaction products were separated into tetrahydrofuran-soluble and tetrahydrofuran-insoluble fractions as already described. The chromatographic separations and spectroscopic investigations were also performed as described.

RESULTS AND DISCUSSION

The rates of reduction of tetrahydrofuran (A), naphthalene (B), and Illinois No. 6 coal (C) are shown in Figure 1. These preliminary experiments established that potassium reacted only very slowly with tetrahydrofuran under the experimental conditions used for the formation of the coal polyanion. Naphthalene was rapidly converted to a mixture of anion radicals and dianions under the same conditions. The initial reaction between the electron transfer reagent and the Illinois No. 6 coal was quite rapid. However, the reaction slowed to nearly constant rate after about 12 hours. During the last four days of reaction the coal molecules acquired about 0.1 negative charges per 100 carbon atoms per hour.

The titrimetric data indicated that the coal polyanions derived from this coal quite reproducibly had 21 ± 1 negative charges per 100 carbon atoms when potassium was used as the reducing agent. The evidence obtained in the magnetic resonance work on the reaction products suggests that these negative charges reside largely on the oxygen atoms of the phenoxide and alkoxide residues and on the carbon skeletons of the aromatic fragments of the coal structure.

Potassium is a much more effective reducing agent than either sodium or lithium. This feature of the reaction is illustrated by the extent of reduction (measured by the number of negative charges per 100 carbon atoms) and the extent of alkylation (measured by the number of alkyl groups introduced and the weight of the reaction products). The results are summarized in Table I.

TABLE I
THE REDUCTION AND ALKYLATION OF ILLINOIS NO. 6 COAL WITH
LITHIUM, SODIUM, AND POTASSIUM

Reagent Pair	Reduction ^a	Alkylation ^b
Lithium, Butyl iodide	12.0	12.2 (0.78g)
Sodium, Butyl iodide	12.9	13.2 (1.17g)
Potassium, Butyl iodide	19.3	20.1 (1.52g)

^aNegative charges acquired per 100 carbon atoms.

^bButyl groups introduced per 100 carbon atoms. The weight of tetrahydrofuran-soluble product obtained from 1.00g of coal.

The reactions of the coal polyanion with methyl iodide and butyl iodide were compared in tetrahydrofuran. The reaction could be monitored quite readily by the rate at which potassium iodide precipitated from solution. We estimate that methyl iodide is about 10-fold more reactive than butyl iodide under these conditions. This result, of course, suggests that the SN₂ reactions of the coal polyanion are more significant than the electron transfer reactions. Although there is a clear distinction in the reaction rate, the extent of the alkylation reaction is the same for methylation and butylation with about 21 alkyl groups introduced per 100 carbon atoms. The amount of tetrahydrofuran-soluble alkylation product is also similar for methylation and butylation under comparable conditions.

The observations concerning the butyl halides and sulfonates are summarized in Table II.

TABLE II
ALKYLATION REACTIONS WITH BUTYL DERIVATIVES

Reagent, equivalents ^a	First Reaction		Second Reaction		Total %
	Solubility, ^b %	Residue, ^c g	Solubility, ^b %	Residue, ^c g	
BuCl, 2.0	23	1.00	--	--	--
BuBr, 2.0	51	0.64	--	--	--
BuI, 2.0	62	0.49	74	0.18	79
BuOSO ₂ CH ₃ , 2.0	64	0.51	polymer	--	--
BuOSO ₂ CF ₃ , 2.0	polymer	--	--	--	--

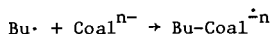
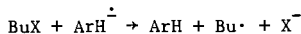
^aBased on the number of negative charges acquired by the coal.

^bThe percentage of the original coal which has been converted to soluble product. The values reported here have been corrected for the extent of the alkylation reaction.

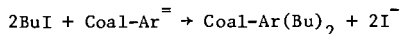
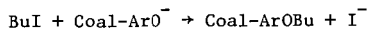
^cThe weight of the tetrahydrofuran-insoluble residue. No correction has been applied for either alkylation or mineral matter.

The reactions of the potassium coal polyanion with the butylation reagents differed markedly. Both the percentage of soluble product and the weight of residue indicate that the reactions of the chloride and the bromide are distinctly less effective than the reactions of the iodide. The butyl sulfonate esters were much more reactive. In one case, the mere addition of freshly distilled butyl triflate to tetrahydrofuran at room temperature caused the polymerization of the solvent. In the other case, the addition of butyl mesylate to the reaction mixture was effective for the production of soluble products in 64% conversion. However, when the reaction was repeated with the residue, a polymerization reaction ensued and a gas, 1-butene, was evolved from the reaction mixture.

These observations indicate that butyl iodide is adequately reactive for the alkylation of the polyanion. This reagent effectively converts more than 90% of the original carbonaceous matter in the coal to soluble alkylation products. The fact that the reactions of butyl chloride and butyl bromide do not give similar results suggests very strongly that SN2 reactions rather than electron transfer reactions are primarily responsible for the production of soluble materials. This interpretation is based on the fact that the reactivities of nucleophiles with butyl iodide, bromide, and chloride are in the approximate order 100:60:1 and that these substitution reactions are all slow relative to the electron transfer reactions of the butyl halides with anion radicals. To illustrate, the rate constants for the reactions of primary alkyl iodides with anion radicals of the kind formed under the conditions of these experiments are about 10^7 l/mole sec (3). The rate constants for the reactions of primary alkyl iodides with nucleophiles are much smaller, only about 10 l/mole sec in the fastest processes (4). Thus, we infer that the butyl halides all undergo rapid electron transfer reactions to produce butyl radicals during the initial stages of the alkylation process. We also infer that this process is less important



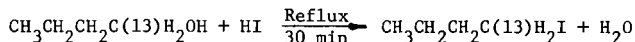
for the formation of soluble products than the alkylation reactions



which proceed much more slowly. Indeed, we observed that the precipitation of potassium iodide from the reaction of butyl iodide with the coal polyanion appeared to be complete only after about 24 hrs. Thus, the much slower reactions of the polyanion with the other halides would not be complete in 48 hrs.

In another experiment, we tested the utility of 1,2-dimethoxyethane as a solvent for the reaction. The results obtained in this experiment revealed that the coal polyanion was formed to the same extent as in tetrahydrofuran. In addition, the alkylation of the polyanion with butyl mesylate proceeded to give 65% soluble product. This datum is comparable with the result for butylation in tetrahydrofuran, 64%. Hence both solvents are equally useful for the alkylation reaction.

When we were satisfied that the alkylation reaction could be accomplished both effectively and reproducibly, we undertook the synthesis of C-13-enriched butyl iodide. Conventional procedures were used to produce the desired compound in 90% isolated yield using concentrated hydroiodic acid.



The coal alkylation reaction was carried out using the enriched compound and the products were separated using the procedures described in the Experimental Part. The proton and carbon nmr spectra of one fraction (comparable to fraction 9 in the previous report (2)) are presented in Figures 2 and 3.

The proton nmr spectra of the coal products obtained in this work are quite similar to the spectra of the products obtained by Sun and Burk and discussed previously (2). No additional comments on this aspect of the work are necessary.

The carbon nmr spectra, on the other hand, provide much new information concerning the alkylation reaction. To illustrate, the resonances at $\delta 67.7$, 72.9 , and 64.2 indicate that O-butylation has occurred dominantly on aryloxides with concomitant butylation on alkoxide and possibly carboxylate fragments. The broad band of resonances at $\delta 35$ indicate that C-butylation is also important and that butyl groups are bonded to quaternary and tertiary sp^3 carbon atoms and possibly to aromatic carbon atoms. These results and the other spectroscopic data for other fractions enriched in carbon-13 will be discussed.

ACKNOWLEDGEMENT

This research was supported by the Department of Energy under contract EF-77-S-02-4227.

REFERENCES AND NOTES

1. (a) H.W. Sternberg, C.L. DelleDonne, P. Pantages, E.C. Moroni, and R.E. Markby, Fuel, **50**, 432 (1971). (b) H.W. Sternberg and C.L. DelleDonne, ibid., **53**, 172 (1974).
2. L.B. Alemany, S.R. King, and L.M. Stock, ibid., **57**, 000 (1978).
3. B. Bockrath and L.M. Dorfman, J. Phys. Chem., **77**, 2618 (1973).
4. S. Bank and D.A. Juckett, J. Amer. Chem. Soc., **97**, 567 (1975).

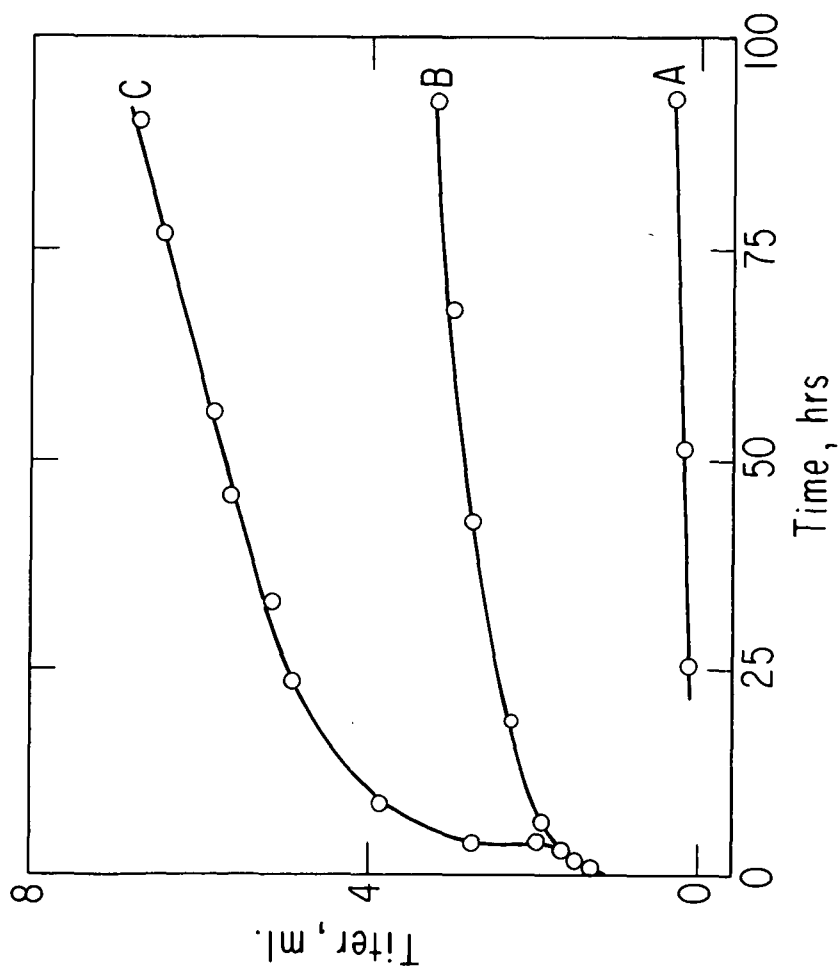


Figure 1.—The rates of reduction of tetrahydrofuran (A), naphthalene (B), and Illinois No. 6 coal (C) are presented by a comparison of the titer required for aliquots of separate reaction mixtures over 100 hrs.

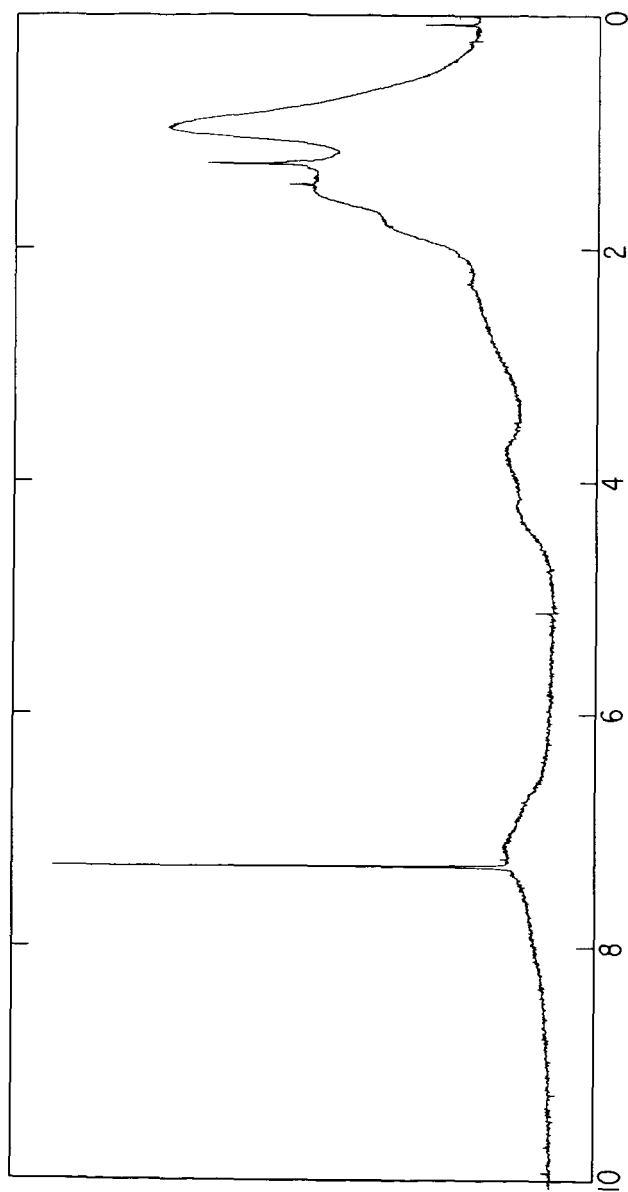


Figure 2.--The proton nmr spectrum of a representative fraction of coal butylated with the C-13 enriched reagent. The intense signal at $\delta 7.3$ results from residual chloroform.

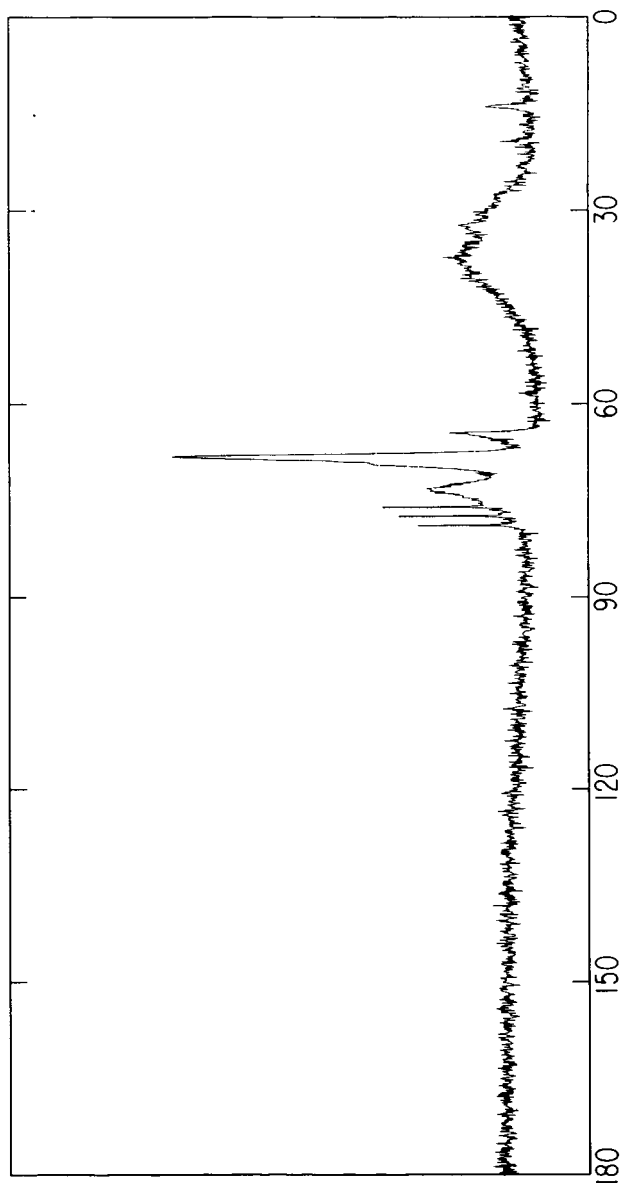


Figure 3.--The carbon nmr spectrum of a representative fraction of coal butylated with the C-13 enriched reagent. The three sharp signals at about $\delta 77$ result from chloroform.

DATA ON THE DISTRIBUTION OF ORGANIC SULFUR FUNCTIONAL GROUPS IN COAL

By: Amir Attar and Francois Dupuis

Department of Chemical Engineering, University of Houston, Houston, Texas 77004

1.0 Introduction

Coals contain inorganic sulfur compounds, like iron pyrite and gypsum and organic sulfur, which is bound to the organic matrix. Detailed reviews of sulfur functional groups in coal were recently published by Attar (1977)(1) and Attar and Corcoran (1977)(2). The chemistry, the kinetics and the thermodynamics of reactions of the sulfur were described by Attar (1978) and therefore will not be reviewed here in detail.

This work had two objectives:

1. to identify and quantify the organic sulfur group functionalities in different coals, and
2. to examine the implications of these functionalities on potential desulfurization processes.

The main results are:

1. The majority of the organic sulfur in high ranked coals, i.e., LVB is thiophenic while in low ranked coals, i.e. lignites, most of the organic sulfur is thiolic or sulfidic.
2. 18-25% of the organic sulfur is in the form of aliphatic sulfides in all coals.
3. Part of the organic thiols are present in the form of ionic thiolates, presumably of calcium.
4. Coals containing mainly thiolic groups can be easily desulfurized.

2.0 Principle of the Method of Analysis

Detailed description of the principle of the method of analysis was published by Attar and Dupuis (1978)(4). Therefore only the main points will be described here.

1. All the organic sulfur functional groups can be reduced to H_2S if a sufficiently strong reducing agent is used.
2. Each sulfur group is reduced at a rate which can be characterized by a unique activation energy and a frequency constant.
3. If a sample which contains many sulfur groups is reduced and the temperature is gradually increased, each sulfur group will release H_2S at a different temperature given by:

$$\frac{A_i RT_{mi}^2}{\alpha E_i} = c \frac{E_i}{RT_{mi}} \quad (1)$$

where T_{mi} is the temperature of the maximum E_i and A_i are the activation energy and the frequency factor, and α is the linear rate of temperature increase. The rate of evolution of H_2S from the reduction of the i -th group can be described by:

$$\frac{d[H_2S]_i}{dt} = \frac{A_i}{\alpha} [H_2S]_{i0} \exp\left[-\frac{E_i}{RT} - \frac{A_i RT}{E_i} c - \frac{E_i}{RT}\right] \quad (2)$$

where $[H_2S]_{i0}$ is the total amount of H_2S that reduction of the i -th group would release. The detailed derivation of the previous equations was done by Jüntgen (1964)(5), and Jüntgen and Van Heek (1968)(6).

4. The value of T_{mi} is a characteristic unique to the sulfur functionality reduced and the area of each peak is proportional to the quantity of sulfur present in the form of the group reduced.

The implication of these discussions is that the area of the peak whose maximum is at T_{mi} is proportional to the concentration of sulfur present in the sample in the form of the i -th group. Therefore, quantitative determinations of the i -th sulfur group can be accomplished by determining the area of each peak.

3.0 Experimental

The experimental system consists of six parts:

1. a reduction cell,
2. a gas feed and monitoring system,
3. a hydrogen sulfide detector,
4. a recorder,
5. an integrator, and
6. a temperature programmer.

Figure 1 is a schematic diagram of the experimental system. The coal sample is placed in the reduction cell with a mixture of solvents catalyst and a reducing agent. The gas flow rate is then adjusted and the temperature is programmed up. The rate of evolution of H_2S is recorded vs. the cell temperature and the signal of each peak is integrated using the integrator. A more detailed description of this system was recently published by Attar and Dupuis (1978)(4).

The data described in this paper were derived using an improved version of the same experimental system. The following modifications were made:

1. stronger reducing conditions were used in order to obtain more complete reductions of the organic sulfur,
2. the sensitivity of the detector was improved, and
3. the cell design was changed and now it is possible to obtain detailed analysis on a routine basis.

Figure 2 shows a typical kinetogram.

4.0 Results and Discussion

The distributions of sulfur functional groups (USFG) in four types of solids are described:

1. sulfur containing polymers with well characterized sulfur functional groups,
2. raw coals,
3. treated coals, and
4. iron pyrite.

The analysis of the DSFG consists of two parts:

1. the qualitative assignment of a peak of a kinetogram to a given chemical structure, and
2. the determination of the quantity of each sulfur group in the (coal) sample.

4.1 Qualitative Identification of the Sulfur Groups

Tests of polymers with a known structure were used to identify the temperature at which each sulfur group releases its sulfur. Four polymers were tested:

1. polyphenylene sulfide (7) as a representative of aromatic sulfides,
2. polythiophene as a representative of thiophenic sulfur,
3. a copolymer produced from cyclohexene and 1,2 ethylene dithiol (7), as a representative of aliphatic and alicyclic sulfides, and
4. vulcanized natural rubber as a representative of aliphatic sulfides and disulfides.

All the polymers contained some thiolic sulfur.

The use of sulfur containing polymers can be used to identify the temperature region where each sulfur group is reduced only if two conditions are fulfilled:

1. the rate of the chemical reaction controls the rate of release of H_2S when both coal samples and polymer samples are examined,
2. the rate of the reduction of each sulfur functional group depends only on the hydrocarbon structure in its immediate vicinity.

Table 1 shows the results of tests of the various polymers and the maximum temperature for each group.

4.2 Quantitative Analysis of the Concentrations of Sulfur Groups

4.2.1 Recovery of Organic Sulfur

Quantitative analysis can be accomplished provided that all the sulfur present in the form of each group is reduced to H_2S . It is also assumed that the distribution does not change during the analysis and that all the H_2S released is detected and determined.

Each mole of sulfur, when reduced, produces one mole of H_2S . Therefore, the number of moles of H_2S formed during the reduction of each group is proportional or equal to the number of moles sulfur present in the sample in that form.

The recovery of sulfur from model compounds containing aliphatic thiols, thiophenes and aryl sulfides was 94-99%.

Table 2 shows the results of the quantitation of the kinetogram of three samples of Illinois #6 coal with different particle sizes. The two most important conclusions from these tests are that the recovery of thiophenes and aromatic sulfides depends on the coal particle size used and that to a first order approximation, the recovery of other groups is independent of the coal particle size. 17

is conceivable that during the analysis, in the interior of large coal particles, the sulfur groups can condense and form (graphitized) compounds which are less amenable to reduction. The strong reducing agent used can penetrate into smaller coal particles and inhibit the rate of condensation. While aliphatic thiols and sulfides are reduced at low temperature, before condensation commences, the reduction of thiophenes occur simultaneously with the condensation and therefore in a large particle thiophenic group could form condensed thiophenes which are less amenable to reduction.

4.2.2 Recovery of Pyritic Sulfur

Table 3 shows that a very small fraction of the pyritic sulfur is recoverable when pure crystalline iron pyrite is tested. In all the cases tested, the recovery never exceeded 1-2%. Somewhat larger recovery is obtained when slow heating rates or reducing agents with smaller reducing potential are used. When strong reducing agents are used, a layer of metallic iron is believed to be formed on the surface of the iron sulfide which prevents diffusion of the reducing species.

Small iron pyrite particles, of the order of 1-10 microns are often reduced more effectively than larger particles because they are less crystalline and often contain more impurities than larger particles.

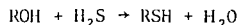
4.3 Resolution

The evolution of H_2S from aliphatic sulfides and from iron pyrites coincides to the extent that it is almost impossible to resolve the two peaks. However, since iron pyrite can be determined independently using ASTM D3131, it was possible to estimate the relative contribution of pyritic sulfur and sulfidic sulfur to the unresolved peaks. Somewhat better resolution was obtainable at slow rates of heating, however in these cases the overall recovery and the signal to noise ratio were reduced.

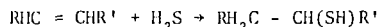
4.4 The Sulfur Distribution in Raw Coals

Table 4 shows the distribution of the various classes of sulfur in five coals and table 5 shows the distribution of the organic sulfur groups in the same five coals. The results shows that the content of thiols is substantially larger in lignites and HVB coals than in LVB coals. The fraction of aliphatic sulfides is approximately the same in coals with different ranks and vary around 20% of the organic sulfur. If it is accepted that all the unrecovered organic sulfur is due to thiophenes (and aromatic sulfides), then the data indicate clearly that larger fractions of the organic sulfur is present as thiophenic sulfur in higher ranked coals than in lower ranked coals. The accepted theory on the hydrocarbon structure of coal is that higher ranked coals are more condensed than lower ranked coals. It should not, therefore, be surprising that the sulfur groups are also more condensed, more thiophenic, in higher ranked coals than in lower ranked coals.

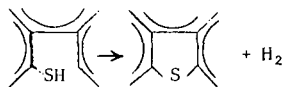
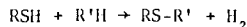
The data on the relative amounts of $-SH$, $R-S-R$ and thiophenic sulfur can be explained as follows: suppose that most of the organic sulfur is initially trapped by the organic matrix in the form of thiolic sulfur. Typical "trapping reactions" are:



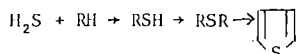
and



During the coalification, thiols can condense to form sulfides and eventually aromatic sulfides and thiophenes:



The sequence of the condensation reactions is therefore:



In other words, the sulfides are an intermediate form which the sulfur may have before it is converted to the thiophenic form. Thus, it should not be surprising that the fractions of sulfidic sulfur is approximately constant since during the coalification, sulfidic groups are formed from thiolic groups and are consumed to produce thiophenes. These processes are condensation processes which are believed to occur in the structure of coal during coalification.

4.5 The Sulfur Distribution in Treated Coals

Various treatments are known to be selective to specific sulfur groups. It was therefore interesting to examine the kinetogram of treated coals. Three treatments are described:

1. oxidation with H_2O or HNO_3 ,
2. removal of the alkaline minerals with HCl , and
3. methylation of the coal with methyl iodide.

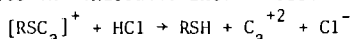
4.5.1 Oxidation

Mild oxidation of coal with acidic solutions of hydrogen peroxide or nitric acid dissolves the iron pyrite and converts the thiols to sulfonic acids. Some organic functional groups oxidize to the corresponding sulfides and sulfones (8). However, in general, the latter process requires strong oxidizing conditions. From the analytical point of view one might think that it is not important whether the organic sulfur groups are oxidized or not, since the reducing agent used converts them back very rapidly to the non-oxidized form. Therefore, the results of the analysis will not differentiate between the reduced and the oxidized form of a sulfur group. In other words, oxidation could have been used to remove the interference from pyrite without much effect on the determination of the other sulfur groups. However, oxidation appears to increase the resistance to mass transport and thus to reduce the resolution. Figure 3 shows the kinetograms of two coal samples analyzed for the U.S. Department of Energy. The first is the original coal, the second is an oxidized sample. The results show that the oxidation did

not remove any organic sulfur although the pyritic sulfur was removed. The signals are however much less resolved in the oxidized sample than in the raw coal. Since the oxidation was conducted in an acidic inorganic solution, and because it is known that sulfonic acids can be hydrolyzed to hydrocarbons and sulfuric acid, some of the thiols seem to disappear as a result of the oxidation.

4.5.2 HCl Treatment

Dilute HCl dissolves the organic and carbonate salts of calcium, magnesium and iron. Since some H_2S can react with basic calcium and iron salts, it was desired to examine the effect of HCl treatment on the kinetogram. Figure 4 shows the kinetograms of raw coal and HCl extracted coal. The most important difference between the kinetograms is that the second peak due to thiophenols disappeared and the thiols peak is increased. It is plausible that some of the sulfur which is determined as thiophenolic is indeed thiolic. Thiols can react with calcium to form calcium thiolates, reduction of which may require larger activation energy than thiols. HCl treatment replaces the calcium with hydrogen and converts the thiolates into thiols:



4.5.3 Treatment with Methyl Iodide

Samples of Illinois #6 were treated with methyl iodide, CH_3I , and the products were analyzed using two methods: The method of Postovski and Harlampovich (9) for thiols and aliphatic sulfides, and using our thermokinetic method. The results of the analysis are described in table 6. The results show that only a very small fraction of the organic sulfur is indeed accounted for by the CH_3I method and therefore the value of this method as an analytical tool is questionable.

The kinetograms of an untreated but demineralized sample and that of a demineralized sample treated with CH_3I are shown in figure 5. The data show that the methyl iodide treatment results in lower recovery of organic sulfur and in a change in its distribution. In particular, some of the sulfur which is originally detected as aromatic thiol is apparently alkylated and becomes aromatic sulfide. However, the alkylation must also reduce the rate of mass transport since the thiophenes and aromatic sulfides are not visible in the kinetogram of the treated coal.

5.0 Implications to Coal Desulfurization

It is widely recognized today that coal desulfurization efficiency depends on the distribution of sulfur in the original coal to pyritic and organic sulfur. Pyritic sulfur can be removed relatively easily while it is more difficult to remove organic sulfur.

Preliminary data show that part of the organic sulfur can be easily desulfurized. In particular, it seems that the thiolic sulfur and part of the sulfidic sulfur can be easily removed. Therefore, the authors suggest coals may be classified into two groups: coals which can be easily desulfurized, (most

of their organic sulfur is thiolic) and coals which can not be easily desulfurized (most sulfur is non-thiolic). Thus, thermokinetic tests can be used to screen coals and to infer which are best used as feeds for precombustion desulfurization.

References

1. Attar, A., "The Fundamental Interactions of Sulfur and Modelling of the Sulfur Distribution in the Products of Coal Pyrolysis." A paper submitted in the 83rd National Meeting of the AIChE held in Houston, TX., March 20-24 (1977). In print in Vol. IV, "Coal Processing Technology," CEP Technical Manual (1978).
2. Attar, A. and Corcoran, W. H., Ind. Eng. Chem., Proc. Res. and Dev., 16 (2), 168 (1977).
3. Attar, A., Fuel, 57, 201 (1978).
4. Attar, A., and Dupuis, F., Prep. Div. Fuel Chem., ACS, 23 (2), 44 (1978). The paper is present in the preprints but is not listed in the table of contents.
5. Jüntgen, H., Erdöl and Kohle, 17, 180 (1964).
6. Jüntgen, H., and Van Heek, K. H., Fuel, 47, 103 (1968).
7. Supplied by Phillips Petroleum whom the authors wish to thank.
8. Attar, A., and Corcoran, W. H., Ind. Eng. Chem., Prod. Res. and Dev., 17 (2) 102 (1978).
9. Postovski, J. J. and Harlampovich, A. B., Fuel, 15, 229 (1936).

Table 1: Qualitative Identification of Sulfur Groups

Model Compound	Weight %	α °C/mm	$T_{max}^{\circ}C$	Group-SH (Account mg/g sample)	λ	T_{max}	Group-S-S- (Account mg/g sample)	λ	T_{max}	Group-S-S- (Account mg/g sample)	λ	T_{max}	Derivatives or Account mg/g sample	λ	Total Account
Benzyl Sulfide	1	16				350									10.11
Benzyl Sulfide	133	4				190-270	10.11								12.49
Rubber (chunk)	101	4.5				220-280	12.49								7.27
Rubber (ground)	61	4	170	1.29									500	5.96	8.50
Polythiophene	58	4.5	185	1.85									510	6.94	
Polyphenylene Sulfide crosslinked	12	4.5	170			230						430			33.6
Polyphenylene Sulfide LMW	4.3	10	160	94.98								450	221.12		129.2
Polyphenylene Sulfide HMW	4.2	10	190	50.67								460	117.9		55.23
Polymer Ethane	10.5	9.5	190-230	28.20								390	52.05		
Polymer Ethane	12.5	9.5	180	14								330	5.29	7.76	23.75
Thiathrene								18.95							

The total sulfur content of rubber and polyphenylene sulfide (HMW and LMW) was determined with LECO equipment.

Sulfur content of rubber - 1.35%

Sulfur content of polyphenylene sulfide LMW 38%

HMW 34%

Table 2: The Effect of Particle Size on the Analysis of Sulfur Functional Groups


Run #	Coal	Mesh Size	Sample weight mg	-SH mg g coal	ϕ -SH mg g coal	R-S-R FeS ₂ mg/g coal	ϕ -S- ϕ mg g coal	 mg g coal	Total mg g coal	Recovery %
S-111	Illinois #6	-100+120	32.7	1.33	1.44	4.15	1.17	*	8.07	19
S-112	"	-200+270	32.3	1.11	1.58	3.48	*	*	6.16	14.7
S-113	"	-325	32.2	1.69	1.80	3.11	*	67	7.26	17.1
* Not detected										

Table 3: The Effect of Pyrite Particle Size on the Recovery of Sulfur

Particle Size		% Recovered
mesh	microns	
-60+100	149-250	0.9
-100+120	125-149	1.9
-120+170	88-125	1.6
-170+200	77-88	1.5
-200+270	53-74	1.5
-270+325	44-53	0.9
-325	< 44	2.1

* The estimated error is $\pm 0.4\%$.

Table 4: Sulfur Class Distribution in Five Coals

Coal	Denote	Total s (wt.%)	Pyritic s (wt.%)	Sulfatic s (wt.%)	Organic s (wt.%)
Illinois	A	4.5	1.23	0.06	3.2
Kentucky	B	6.6	5.05	0.135	1.43
Martinka	C	2.20	1.48	0.12	0.60
Westland	D	2.60	1.05	0.07	1.48
Texas lignite E		1.20	0.4	—	0.80


Table 5: Distribution of Organic Sulfur Groups in Five Coals

Coal	% Organic s Accounted	Thiolic	Thiophenolic	Alip Sulfide	Aryl Sulfide	Thiophenes*
A	44	7	15	18	2	58
B	46.5	18	6	17	4	55
C	81	10	25	25	8.5	21.5
D	97.5	30	30	25.5	—	14.5
E	99.7	6.5	21	17	24	31.5

* Corrected for "unaccounted for" sulfur

* C and E are calculated on total sulfur content

Table 6: Analysis of Illinois #6 Coal by the CH_3I Method by Thermokinetics

	LECO % mg/gm		ASTM % mg/gm		DSFG % mg/gm		CH ₃ I method % mg/gm		DSG on CH ₃ I treated coal (S-103) % mg/gm	
Total Sulfur	4.5	45								
Sulfate Sulfur			0.04	0.4						
Pyritic Sulfur			1.23	12.3	4.81	0.6				
Organic Sulfur { -SH φ-SH R-S.R. A-S.A. 					6.1		1.36		8.6	
					8.5				3.45	
					8.6		0.96		8.0	
					4.3					
Total Organic Recovered			3.23	32.3	85.1	27.5	7.2	2.32	62.1	20.05

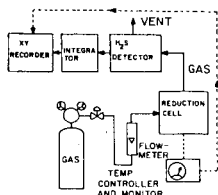


FIGURE 1 SCHEMATIC DIAGRAM OF EXPERIMENTAL SYSTEM

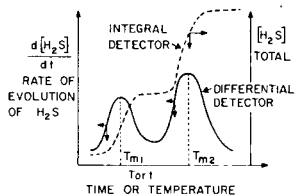


FIGURE 2 ANALYSIS OF A MIXTURE CONTAINING TWO GROUPS USING A DIFFERENTIAL AND AN INTEGRAL DETECTORS

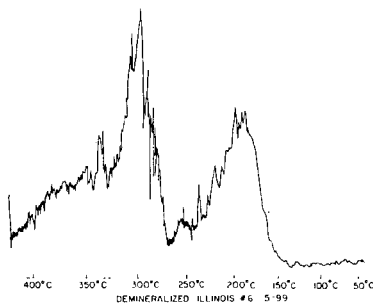
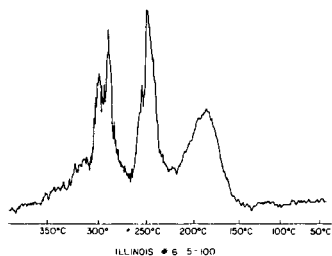


Figure 3

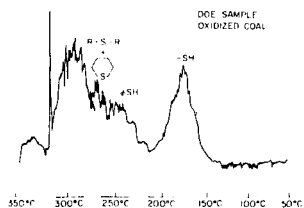
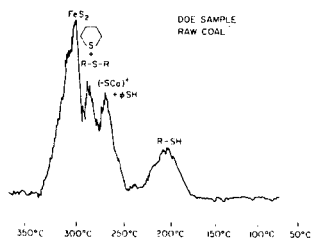


Figure 4

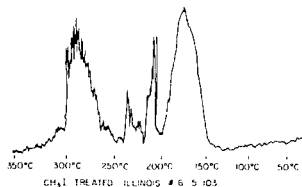
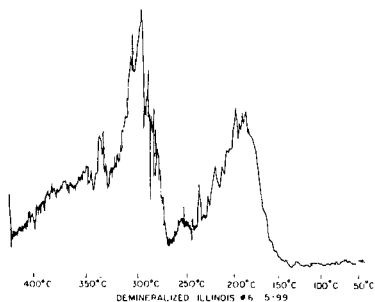


Figure 5

Chemical Structure of Heavy Oils Derived from Coal Hydrogenation by Mass Spectroscopy

S. Yokoyama, N. Tsuzuki, T. Katoh, Y. Sanada,
D. M. Bodily* and W. H. Wiser*

Coal Research Institute, Faculty of Engineering,
Hokkaido University, Sapporo, 060, Japan

*Department of Mining, Fuels Engineering, University of Utah,
Salt Lake City, Utah 84112, U. S. A.

Introduction

Coal hydrogenation heavy oil consists of numerous complicated hydrocarbons and nonhydrocarbon compounds, consequently the elucidation of the chemical structure is extremely complicated and time consuming. Thus, the chemical structure of coal liquids have been investigated mainly to the present by means of ^1H - and ^{13}C -NMR techniques or a combination thereof. In other words the technique of mass spectrometry for structural analyses is advantageous to gain information of the individual compounds regarding molecular weight and compound types [1,2]. A combination of dual-packed adsorption liquid chromatography (LC) and gel permeation chromatography (GPC) developed by the Bureau of Mines API project 60 [3] for separation into compound types and further into their molecular size are appropriate to the sample preparation procedure for mass analyses, because molecular coefficient were assumed to be approximately the same for LC-GPC sub-fraction inasmuch as they have characteristic compound types and narrow molecular weight distribution. On the other hand, results of GPC technique which is a very useful method to clarify complicated mixtures of heavy oil derived from coal, was compared to the mass results. It can be concluded that both results from mass and GPC analyses should be used independently to elucidate the chemical structure of coal liquids.

Experimental

Sample preparation of heavy oil

Hydrogenation reaction of Hiawatha, Utah coal (C: 72.0, H: 5.6, N: 1.7, S: 0.90, O: 19.8, d.a.f.%) was performed with the condition of 950°F of reaction temperature and 1800 psi of hydrogen pressure with ZnCl_2 impregnated to coal as catalyst by an entrained-flow tubular coil reactor of the University of Utah process [4]. The reaction products were trapped in three reservoirs connected to the reactor in series and was separated according to their condensability. Heavy oil products collected in the first reservoir nearest to the reactor was subjected to investigation in this work. Separation procedures to characteristic materials prior to gaining acid-base-less neutral compounds were described in our previous reports [5] and also shown in Fig. 1. Neutral heavy oil obtained was separated subsequently into compound types of saturated hydrocarbons (Fr-P), mono-aromatic (Fr-M), diaromatic (Fr-D), three and more large aromatic rings (Fr-T) and polyaromatic-polar compounds by means of dual-packed silica alumina adsorption liquid chromatography modified partially the Bureau of Mines API-60 method, with an additional solvent of 70% benzene-30% cyclohexane system to obtain separately a narrow cut of concentrate of 3 and 4 aromatic ring compounds. Elution curve of liquid chromatography are shown in Fig. 2. Respective type compounds Fr-M, D and T were separated further by GPC packed Bio-beads S-X4 and 8 according to their respective molecular size into 7 fractions. In Fig. 3, GPC elution curves for Fr-M, D and T were shown.

Mass spectra were measured by Hitachi M-52 GC-MS spectrometer. Mass spectra of each series of GPC subfraction for Fr-M, D and T were analyzed with the low resolution and low ionization voltage method by GC-MS technique for Fr-M-3 to 7 and Fr-D-3 to 7 and by direct insert technique for high molecular fraction of

Fr-M-1, 2, Fr-D-1, 2 and Fr-T-1 to 7, respectively.

Mass spectrometry was scanned repeatedly with 6 or 10 sec. interval times during the period of elution from GC column or volatilization of samples introduced into the ionization chamber and multiple mass spectra of about 50 to 800 for respective LC-GPC subfraction were measured to obtain the representative gross mass spectral data for complicated mixtures. Numerous mass spectra were treated by computer (Hitachi, HITAC 10 II) for the summing up of these spectra to calculate them as an integrated mass spectra.

Results and Discussion

Each series of LC-GPC subfractions were investigated previously for chemical characterization by ^1H - and ^{13}C -NMR method [6,7] and were elucidated to have approximately mono-, di- and tri- and/or tetraaromatic derivatives for Fr-M, D and T, respectively, as the average structural unit. It was also confirmed that values of aromaticity for GPC subfractions of individual compound types increase gradually with the increasing GPC fraction number from 1 to 7 and have also the largest fa values for Fr-T and the smallest one for Fr-M at the same elution volume of GPC. From the results described above, the separation effects of LC and GPC according to compound types and molecular size were assumed to be excellent. Considering these characteristics for chemical structure, LC-GPC subfraction are found to be suitable as samples for mass analyses because the molecular ion coefficient is not so large in difference among respective compounds in the same fraction.

Integral mass spectra of LC-GPC subfraction

On the measurement of mass spectra by means of the low energy ionization method, species of ion peaks observed were mostly parent ion and isotopic ion ($\text{P}+1$) and were minor for fragment peaks like ($\text{P}-1$), indicating that the cleavage of molecules are minor. Although, Fr-D-1 and Fr-T-1 which are the highest molecular weight in that they have large aliphatic substitution, were observed in the predominant fragment peak of odd mass number at lower mass range, therefore the data of these fractions were not included in this report. On the integral mass spectra of series of LC-GPC subfraction, the average number molecular weight were calculated from the mass to charge ratios (M/e) for respective parent peaks and those intensities, and are shown in Fig. 4. By increasing the fraction numbers of GPC for each compound type series, the molecular weight diminishes progressively from about 400 or 500 to 200 in proving the satisfactory fractionation of GPC. In Fig. 4, molecular weight results derived from vapor pressure osmometry were compared with the results of mass analyses to ensure the accuracy of conventional methods. The correlation between both are excellent except for a slight deviation from the theoretical line with the increase in molecular weight.

Compound types of LC-GPC subfraction

Deficiency of hydrogen number for M/e of parent peak can be predicted the type of compound by assigning the value of z number. Assuming that molecular ion coefficients are approximately similar, the contents of respective type compound for GPC fraction 1 or 2 to 7 of Fr-M, D and T were estimated semiquantitatively. Consequently, hydrocarbon types for Fr-M-1 to 7 were assigned mainly to alkylbenzenes ($Z=-6$), alkylmononaphthenobenzenes ($Z=-8$) and alkylindanaphthenobenzenes ($Z=-10$) and for Fr-D-2 to 7 to alkyl-naphthalenes ($Z=-12$), alkylmononaphthenonaphthalenes ($Z=-14$) and alkylindanaphthenonaphthalenes ($Z=-16$) and for Fr-T-2 to 7 to alkylphenanthrene or alkylanthracene ($Z=-18$), alkylpyrene ($Z=-22$), alkylcrysene ($Z=-24$) and these naphthenologs ($Z=-20$, -26). Distribution of various compound types for Fr-M, D and T in summing the contents of respective GPC subfraction 1 to 7 were shown in Fig. 5.

Alkyl carbon distribution

The same Z values in the integrated mass spectra for individual LC-GPC subfraction were selected to obtain the distribution of alkyl carbon in respective hydrocarbon types. In Fig. 6, the content distribution of molecular weight or alkyl carbon number on the same Z values were plotted for Fr-M, D and T series.

These ranges of alkyl carbon numbers move progressively from low to higher ones with 5 to 10 carbon extents in proceeding to GPC fraction 7 to 1 for respective hydrocarbon types. Therefore, separability of GPC for various hydrocarbon types was confirmed further by mass analyses as to be divided satisfactorily according to molecular sized especially by alkyl carbon number on these samples. It can be seen that Fr-M consists of larger alkyl carbon substitution which reaches 35 carbons for Z=-6 series, indicating a lower aromaticity and decreasing of Z values which indicates an increase of naphthene ring, distribution of alkyl carbon decrease. On the other hand, alkyl carbon number of Fr-T have a range of 0 to 10 indicating a lower aromaticity which is in agreement with the results from $^1\text{H-NMR}$ structural analyses.

GPC correlation for molecular weight vs elution volume

To predict the molecular weight distribution and chemical structure from the GPC elution curve, the GPC correlation curve between molecular weight and elution volume for corresponding structural compounds are necessary. However, it was very difficult to gain information of these relations because the supply of reference sample were limited. If the coal liquid itself can be used as a reference compound for calibration, useful GPC correlation of various compound type can be obtained. Molecular weight at maximum distribution by difference of alkyl carbon number for each GPC fraction on respective Z series shown in Fig. 6 were compared with elution volume for corresponding fraction. The correlation between the two were shown in Fig. 7. The relationship between the two for respective Z values on Fr-M, D and T are in fair as GPC correlations.

Molecular weight distribution for whole samples of Fr-M, D and T were constructed by summation of peak intensities for parent peak belonging to the same Z series corresponding to all GPC fractions, and were shown with the solid lines in Fig. 8. On the other hand, GPC elution curves for Fr-M, D and T were cited again in the same figure for comparison. The results from mass analyses for Fr-D and T do not include the data of Fr-D-1 and Fr-T-1 because of uncertain results of mass analyses for these as described previously, therefore a slight discrepancy were recognized in the vicinity of high molecular range. Although, considerable agreement between both derived from different methods are satisfactory.

References

- [1] A. G. Sharkey, Jr., J. L. Shultz, T. Kessler and R. A. Friedel, "Spectrometry of Fuels", Plenum Press, p. 1 (1970)
- [2] H. J. Coleman, J. E. Dookey, D. E. Hirsch and C. J. Thompson, *Anal. Chem.*, **45**, No. 9, 1724 (1973)
- [3] D. F. Hirsch, R. L. Hopkins, H. J. Coleman, F. O. Cotton and C. J. Thompson, *Anal. Chem.*, **44**, 915 (1972)
- [4] R. E. Wood and W. H. Wiser, *Ind. Engng. Chem. -Process Design Dev.*, **15**, 144 (1976)
- [5] S. Yokoyama, D. M. Bodily and W. H. Wiser, 172nd ACS National Meeting, San Francisco, Sep. 1976
- [6] S. Yokoyama, D. M. Bodily and W. H. Wiser, The 36th Annual Meeting of Chem. Soc. Japan, April, 1977
- [7] S. Yokoyama, D. M. Bodily and W. H. Wiser, The 37th Annual Meeting of Chem. Soc. Japan, April, 1978

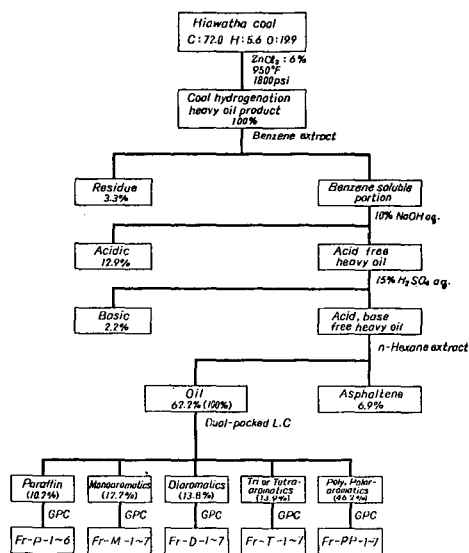


Fig. 1 Separation scheme

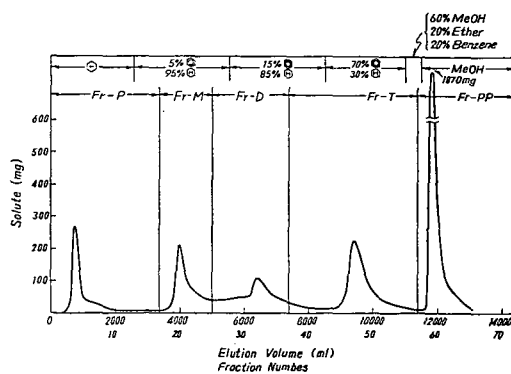


Fig. 2 Elution curve of dual-packed liquid chromatography

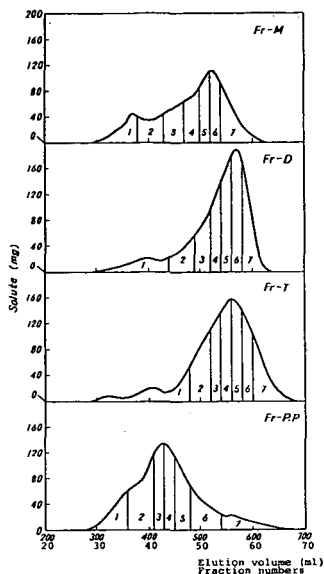


Fig. 3 GPC chromatogram of Fr-M, Fr-D, Fr-T and Fr-PP

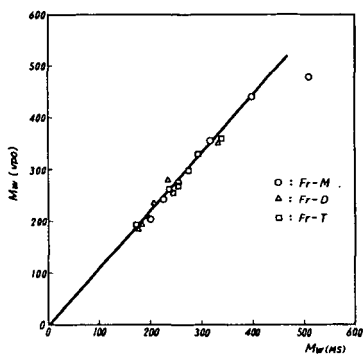


Fig. 4 Molecular weight results from VPO and Mass spectrometry

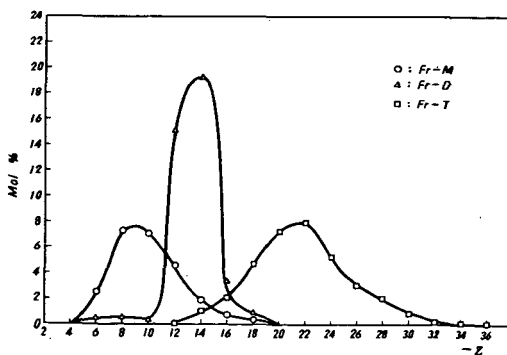


Fig. 5 Distribution of hydrocarbon type compounds for LC-GPC subfractions

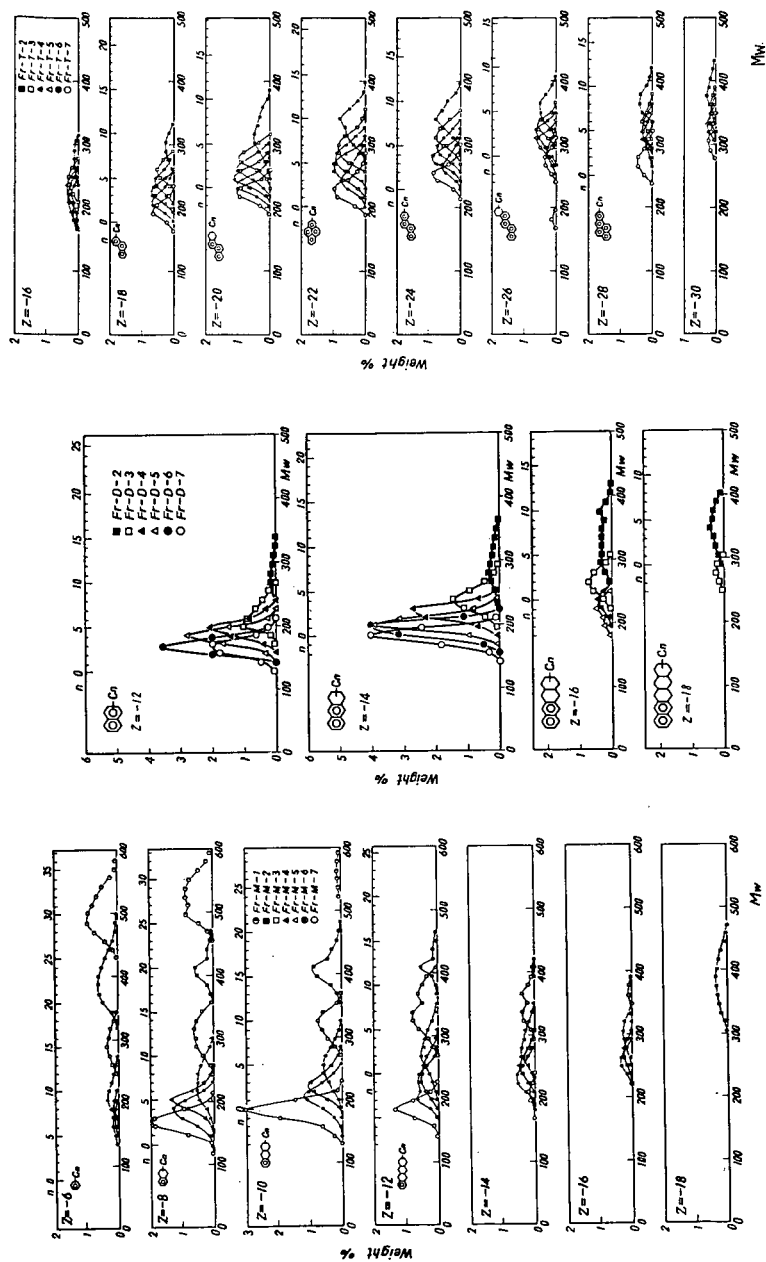


Fig. 6 Distribution of hydrocarbon compound types for Fr-M, Fr-D and Fr-T

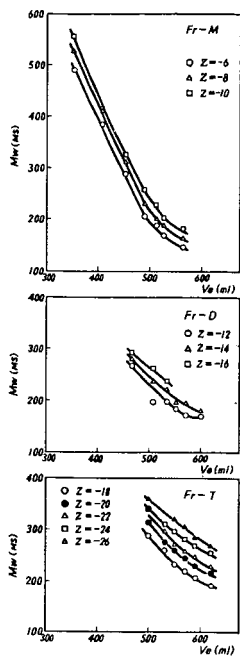


Fig. 7 Relationship between molecular weight and elution volume for various type of compound

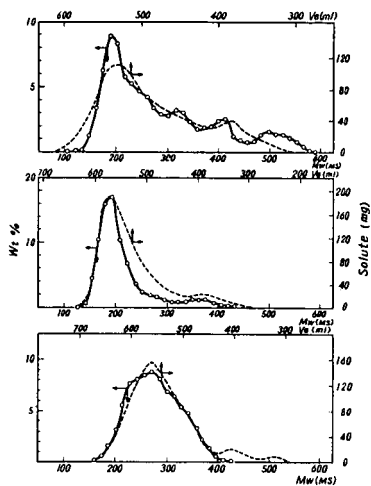


Fig. 8 Comparison with molecular weight distribution and GPC elution curves

STRUCTURAL ANALYSIS OF QUINOLINE EXTRACTS AND HYDROLYSIS PRODUCTS OF COALS

Koji Ouchi, Kazuyuki Iwata, Masataka Makabe, Hironori Itoh

Faculty of Engineering, Hokkaido University, Kita 13, Nishi 8, Sapporo, Japn.060.

The mean structure of coals has been extensively investigated by X-ray, magnetic susceptibility, gases evolved during carbonization, IR spectra etc., and the structural analysis was first developed by van Krevelen(1) using density and refractive index. Among these the method which gives the most precise image appears to be NMR method. However this method is limited in that it can be applied only to soluble material by special solvents. Usually coals can be dissolved only in part, therefore the results do not represent the whole coal.

Thus in the present work we tried to increase the solubility of coals using chemical reaction or strong solvent(quinoline), which would have the smallest change in the unit structure(cluster unit). The results of structural analysis of the products with these two methods are in good agreement, although both methods and their yield are quite different. This means that the structural image obtained here represents the true mean structure of coals.

Experiments

1) Coal sample. Vitrinites of 12 coal samples were concentrated using the sink and float method. Their analytical values are shown in Table 1.

2) Quinoline extraction. 5g of crushed coal under 100 Tyler mesh and 100g of purified quinoline were placed in a 500ml autoclave with a magnetic stirrer and after replacing the atmosphere by nitrogen this was heated at 350~380°C for 1~4 hours. After cooling the products were centrifuged and filtered. The residue was washed with fresh quinoline and methanol. The filtrate was concentrated under vacuum and poured into 500ml of 2N HCl, filtered, washed with hot and cold water and dried.

3) NaOH-alcohol reaction(2). 5g of coal, 5g of sodium hydroxide and 50g of ethyl alcohol were placed in an autoclave of 230ml with a magnetic stirrer and, after replacing the atmosphere by nitrogen, this was heated at 300°C or 350°C for 1 hour. After neutralizing with HCl the precipitate was centrifuged, filtered and dried. The product was then extracted with pyridine by shaking for 10 hours at room temperature.

4) ¹H-NMR. ¹H-NMR was recorded in d-quinoline for quinoline extracts and in d-pyridine for pyridine extracts of NaOH-alcohol reaction products, using TMS as an internal standard. The concentration was 5% for d-quinoline and 2% for d-pyridine.

Results and Discussion

First the extraction conditions were examined using Indian Ridge coal and Balmer coal. The results are shown in Table 2. The effect of temperature from 350 to 375°C, of time from 1 hour

to 6 hours and of nitrogen pressure from 0.1 MPa to 10 MPa were examined. The results were in an error range and we adopted a rather higher temperature for older coals.

The extraction or reaction condition, extraction yield, ultimate analysis of extracts and their molecular weight are shown in Table 3. Quinoline extraction yield attains maxima in a range of 81~87 %C, but there is some scattering of results even with the same carbon percent. If we plot the extraction yield vs. H of raw coals a linear relationship was seen in a range of 91.5~81.2 %C (Fig 1). In younger coals it decreases linearly. Teshio coal has an extraction yield of 20.4%, but after hydrolysis with NaOH solution (5N) at 250°C for 6 hours, the extraction yield increases to 35.9%. Therefore the ether linkages appear to be a cause of the decrease of extraction yield in the younger coal range. In the hydrolysis reaction associated with partial hydrogenation using NaOH-alcohol the younger the coals are, the easier the products dissolve in alcohol. This also means that the younger coals have an abundance of ether linkages.

The carbon percent of extracts in the younger coal range increases in comparison with that of raw coals. The quinoline extraction of NaOH-alcohol reaction conditions are somewhat severe for the younger coals and some oxygen containing functional groups such as carboxyl or hydroxyl groups decompose at those temperatures, which results in a reduction of oxygen content. In the higher coal rank the analytical values of extracts are nearly the same as those of the raw coals, although the extraction yield is higher, which means that there is no change in their structure except for some splittings of ether linkages and a slight saturation of aromatic rings which took place in the reaction of NaOH-alcohol (3). In short, the unit structure (or structure of cluster unit) in the raw coals may be preserved without change in the quinoline extracts or in the pyridine extracts of NaOH-alcohol except for some changes of functional groups in the younger rank coals.

The results of the structural analysis are shown in Table 4. In bituminous coals in which the extraction yield of both methods is nearly 100%, the results show an amazing coincidence in both methods except for slightly higher values for f_a , σ_{al} , \mathcal{C}_{al} , although the methods are completely different. The higher values for these indices come from a slight hydrogenation in the NaOH-alcohol reaction. In the younger rank of coal the difference is somewhat higher, but in spite of this the coincidence is sufficient to discuss the rough unit structure, although the extraction yield and method are quite different. This small difference comes partly from the difference of extraction yield and partly from the slight hydrogenation of coal in NaOH-alcohol reaction. When we pursue the change of structural indices with time at 260°C for Taiheiyō coal in NaOH-alcohol reaction f_a changes from 0.7 at 1 hour to 0.5 at 22 hours. The extrapolated value of f_a for 0 hour almost corresponds to that of the quinoline extract. The extrapolated value of R_a is 1.4 which also coincides well with 1.5 of quinoline extract. All other indices show the same coincidence. We have shown these extrapolated values in Table 4.

The results show that the aromatic ring number of the younger coals is 1~2 with 0.5 naphthenic ring, that of 80~85°C coal 2~3 with 0.5 naphthene ring and that of 90°C coal 5 with 1 naphthene ring. The molecular weight per unit structure of younger coals is 160~180, that of 80~85°C coal 200~300 and that of 90°C coal 320~340. Oxygen content per unit structure decreases from younger coals

to the older coals, but as described before those values in younger coals do not represent the true ones. If we take the analytical values of raw coals, we can obtain the corrected oxygen number per unit structure, as shown in Table 4.

Referring to the fact that the ether linkages are rich in younger coals, we can say that the unit structures consisting of benzene or naphthalene rings with 0.5 naphthenic ring are linked mainly by the ether linkages and methylene bonds in younger coals. In bituminous coals the unit structure consisting of 2-5 aromatic rings and about 1 naphthene rings are linked with each other mostly by the methylene bonds. The youngest coal has 2.5-2.8 oxygen atoms per unit structure. The bituminous coals have about 1 oxygen atom per unit structure and the highest rank of coal has 0.3.

Appendix

Structural analysis. Hydrogen was divided into the following four types. Aromatic hydrogen H_a : 6-9ppm, hydrogen attaching α carbon H_α : 2-5ppm, hydrogen attaching over β carbon except for terminal methyl H_β : 1.1-2ppm, hydrogen in terminal methyl H_r : 0.3-1.1ppm. First 60% oxygen is assumed to be the hydroxyl group and the hydrogen in this hydroxyl group was subtracted from the total hydrogen. The residual hydrogen was distributed in the above four types.

The structural indices was calculated from the following equations when the molecular weight was not known.

$$\text{aromaticity, fa} = \frac{C/H - 1/2 \cdot (H_\alpha + H_\beta) / H - 1/3 \cdot (H_r / H)}{C/H} \quad (1)^4$$

H/C ratio in hypothetical unsubstituted aromatics,

$$H_{\text{aus}}/C_{\text{aus}} = \frac{H_a/H + 1/2 \cdot (H_\alpha/H) + 0.6O/H + 2 \cdot (0.4O + N)/H}{C/H - 1/2 \cdot (H_\alpha + H_\beta) / H - 1/3 \cdot (H_r / H)} \quad (2)^4$$

$$\text{degree of substitution, } \sigma = \frac{1/2 \cdot (H_\alpha/H) + 0.6O/H + 2 \cdot (0.4O + N)/H}{H_a/H + 1/2 \cdot (H_\alpha/H) + 0.6O/H + 2 \cdot (0.4O + N)/H} \quad (3)^4$$

degree of aliphatic substitution,

$$\sigma_{\text{al}} = \frac{1/2 \cdot (H_\alpha/H)}{H_a/H + 1/2 \cdot (H_\alpha/H) + 0.6O/H + 2 \cdot (0.4O + N)/H} \quad (4)^5$$

$$\text{number of aromatic carbon per unit structure, } C_{\text{aus}} = \frac{3}{(H_{\text{aus}}/C_{\text{aus}}) - 1/2} \quad (5)^6$$

$$\text{number of total carbon per unit structure } C_{\text{us}} = C_{\text{aus}}/\text{fa} \quad (6)$$

$$\text{number of aliphatic carbon per unit structure, } C_{\text{alus}} = C_{\text{us}} - C_{\text{aus}} \quad (7)$$

$$\text{number of hydrogen per unit structure, } H_{\text{us}} = 12C_{\text{us}} \cdot H\% / C\% \quad (8)$$

$$\text{total ring number per unit structure, } R_{\text{tus}} = C_{\text{us}} - H_{\text{us}}/2 - C_{\text{aus}}/2 \quad (9)$$

$$\text{aromatic ring number per unit structure, } R_{\text{aus}} = 1/2 \cdot (C_{\text{aus}} - H_{\text{aus}}) + 1, \quad (H_{\text{aus}} = (H_{\text{aus}}/C_{\text{aus}}) \cdot C_{\text{aus}}) \quad (10)^7$$

naphthenic ring number per unit structure, $R_{nus} = R_{tus} - R_{aus}$ (11)

molecular weight per unit structure, $Mol.Wt.us = 12C_{us}/C\%$ (12)

(5) is only valid for cata condensed aromatic nuclei. (9) is approximately valid when the degree of polymerization is large.

The absolute values of the number of each type of atoms were used when the molecular weight was known. In this case (9) was calculated as follows.

degree of polymerization $n = C/C_{us}$ (C is the total number of carbon per molecule) (13)

total number of aromatic carbon per molecule, $C_a = C_{aus} \cdot n$ (14)

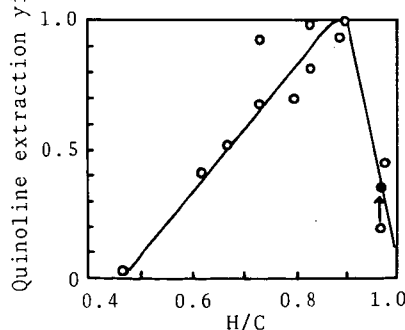
total ring number per molecule, $R_t = (C - H)/2 + 1 - C_a/2$, (H is total number of hydrogen per molecule) (15)¹⁾

total ring number per unit structure, $R_{tus} = R_t/n$. (16)

(Reference)

- 1) J. Schuyer, D.W. van Krevelen, "Coal Science", Elsevier Pub. Co., Amsterdam (1957)
- 2) M. Makabe, Y. Hirano, K. Ouchi, Fuel, 57, 289 (1978)
- 3) M. Makabe, K. Ouchi, Fuel Proc. Tech., in press.
- 4) Modification of equation of J.K. Brown, W.R. Ladner, Fuel, 39, 87 (1960)
- 5) Modification of equation of Y. Maekawa, K. Shimokawa, T. Ishii, G. Takeya, Nenryo Kyokaiishi (J. Fuel Soc. Japan), 46, 927 (1967)
- 6) S. Yokoyama, N. Onishi, G. Takeya, J. Chem. Soc. Jpn., Chem. and Ind. Chem. 10, 1963 (1975)
- 7) D.R. Clutter, L. Petrakis, R.L. Stenger, R.K. Jensen, Anal. Chem. 44, 1395 (1972).

Fig 1. Relation of quinoline extraction yield vs. H/C of raw coals.



● Hydrolysis product

Table 1. Analysis of sample coals.

*S+O

No	Name	Ash %	ultimate analysis(daf) %				Odiff
			C	H	N	S	
1	Teshio	7.0	71.5	5.8	1.8	-	20.9*
2	Taiheiyo	5.3	77.9	6.3	1.1	0.2	14.5
3	Akabira	3.9	81.2	6.0	1.7	-	11.1*
4	Basewater	2.8	83.6	5.6	1.7	0.7	8.4
5	Miike	8.9	83.9	6.3	1.2	2.1	6.5
6	Daiyon	2.4	84.0	5.8	2.0	0.8	7.4
7	New Yubari	2.5	86.7	6.2	1.1	-	6.0*
8	Indian Ridge	1.5	87.4	5.3	0.9	-	6.4*
9	Goonyella	1.5	87.9	5.4	1.9	0.6	4.2
10	Balmer	2.5	89.4	5.0	1.4	0.4	3.9
11	Beatrice	0.8	91.5	4.7	1.3	0.6	1.9
12	Hongei	1.0	93.4	3.7	1.1	0.3	1.5

Table 2. Examination of quinoline extraction yield.

Coal	Indian Ridge				Balmer	
Temperature °C	350	360	370	375	380	380
Time hrs	4	6	1	1	4	4
Pressure MPa	5	0.1	10	0.1	1	10
Extraction yield %	63.0	64.0	61.5	68.0	51.9	50.0

Table 3. Extraction or reaction condition, yield, ultimate analysis and molecular weight of extracts.

No	Reaction ¹⁾	Temperature °C	Time hr	Yield %	ultimate analysis %				molecular weight
					C	H	N	Odiff	
1	Q	350	4	35.9 ²⁾	83.0	6.2	3.6	7.2	-
	N	300	1	97.8 ³⁾	78.4	7.8	1.6	12.2	755
2	Q	350	4	44.9	82.9	7.0	2.1	8.0	-
	N	300	1	98.1 ³⁾	80.8	8.1	1.3	9.8	870
3	Q	350	1	93.8	81.8	5.7	2.4	10.1	-
	N	300	1	96.9 ³⁾	82.6	7.2	1.9	8.3	890
4	Q	350	4	69.0	83.6	5.5	2.2	8.7	-
5	Q	350	4	100.0	84.5	6.2	1.4	7.9	-
6	Q	350	4	81.0	82.7	5.8	2.9	8.6	-
7	Q	350	4	97.8	85.8	5.7	1.4	7.1	-
	N	350	1	91.1 ³⁾	86.8	6.4	1.7	5.1	1160
8	Q	375	1	68.0	87.2	5.2	1.4	6.2	-
	N	350	1	52.4 ³⁾	86.9	6.5	1.3	5.3	905
9	Q	350	4	93.0	86.7	5.2	3.8	4.3	-
10	Q	380	4	51.9	88.1	5.0	2.4	4.5	-
11	Q	370	4	41.6	88.8	4.9	1.7	4.6	-
12	Q	350	4	1.3	-	-	-	-	-

1) Q:quinoline extraction, N:NaOH-alcohol reaction,pyridine extracts.

2)Hydrolysis product with NaOH solution at 200°C,6hrs.

3)Pyridine extraction yield of NaOH-alcohol reaction products.

Table 4. Results of structural analysis.

No	1		2			3		4	5
Reaction ¹⁾	Q	N	Q	N	N ⁵⁾	Q	N	Q	Q
Ha%	0.38	0.11	0.37	0.13	-	0.43	0.22	0.51	0.37
Hx%	0.28	0.36	0.25	0.35	-	0.34	0.39	0.29	0.32
H ₃ %	0.27	0.41	0.32	0.41	-	0.16	0.29	0.16	0.25
H ₂ %	0.06	0.12	0.06	0.10	-	0.08	0.10	0.05	0.06
fa	0.75	0.53	0.71	0.52	0.70	0.79	0.63	0.82	0.75
Haus/Caus	0.82	1.00	0.88	0.97	0.90	0.81	0.89	0.78	0.75
σ	0.47	0.77	0.43	0.65	0.45	0.48	0.54	0.41	0.46
σ-al	0.20	0.39	0.20	0.40	0.17	0.20	0.34	0.17	0.23
Cus	12.5	11.5	11.1	12.3	11.5	12.3	12.4	13.1	16.0
Caus	9.4	6.0	7.9	6.4	8.0	9.7	7.7	10.7	12.0
Calus	3.1	5.5	3.2	5.9	3.4	2.6	4.6	2.4	4.0
Rtus	2.3	1.9	1.6	1.9	1.8	2.3	2.3	2.5	3.1
Raus	1.8	1.1	1.5	1.1	1.4	1.9	1.4	2.2	2.5
Rnus	0.5	0.9	0.1	0.8	0.4	0.4	0.8	0.4	0.6
Mol.Wtus ²⁾	181	176	161	183	181	180	180	188	227
Ous ³⁾	0.8	1.4	0.8	1.1	2.0	1.1	0.9	1.0	1.1
Ous ⁴⁾	2.8	2.5	1.6	1.7	-	-	-	-	-

No	6	7		8		9	10	11
Reaction ¹⁾	Q	Q	N	Q	N	Q	Q	Q
Ha%	0.39	0.39	0.26	0.52	0.28	0.48	0.55	0.63
Hx%	0.29	0.28	0.29	0.26	0.36	0.31	0.27	0.24
H ₃ %	0.25	0.25	0.27	0.16	0.27	0.15	0.15	0.09
H ₂ %	0.06	0.08	0.11	0.05	0.09	0.06	0.02	0.04
fa	0.77	0.80	0.70	0.84	0.70	0.83	0.86	0.89
Haus/Caus	0.76	0.66	0.67	0.65	0.69	0.68	0.64	0.64
σ	0.48	0.43	0.53	0.35	0.45	0.42	0.35	0.29
σ-al	0.20	0.20	0.33	0.16	0.32	0.19	0.16	0.14
Cus	15.0	23.4	25.7	23.8	22.2	20.1	24.9	24.1
Caus	11.5	18.8	17.6	20.0	15.8	16.7	21.4	21.4
Calus	3.5	4.6	7.7	3.8	6.6	3.4	3.5	2.7
Rtus	3.0	4.8	5.7	5.3	4.9	4.6	5.9	5.4
Raus	2.4	4.2	4.0	4.5	3.4	3.7	4.9	4.9
Rnus	0.6	0.6	1.8	0.8	1.5	0.9	1.0	0.5
Mol.Wtus ²⁾	218	328	356	328	307	279	340	326
Ous ³⁾	1.2	1.5	1.1	1.3	1.0	0.1	0.4	0.3
Ous ⁴⁾	-	-	-	-	-	-	-	-

1)Q:quinoline extraction

N:NaOH-alcohol reaction

2)Molecular weight per unit structure

3)Number of (oxygen atom)diff. per unit structure

4)Corrected number of (oxygen atom)diff. per unit structure

5)Extrapolated values to 0 hour in the time variation reaction at 260°C.

Chemical Structures and Reactivities of Coal

as an Organic Natural Product

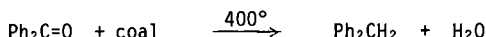
Clair J. Collins, Hans-Peter Hombach, Ben M. Benjamin

W. H. Roark, Brian Maxwell, and Vernon F. Raaen (1)

Contribution from the Chemistry Division
Oak Ridge National Laboratory, Oak Ridge, Tennessee 37830

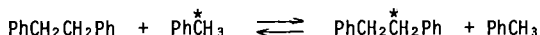
A. The Role of Tetralin in the Pott-Broche Process

It has recently been demonstrated (2) that several bituminous coals and lignites are better hydrogen donors than tetralin, a donor which has been employed, since its use in the Pott-Broche process (3), as the coal chemists' "standard." The better hydrogen-donating abilities of these various coals were tested toward several reactions (4), but that used as the model was the reduction, in a closed tube at 400°, of benzophenone to diphenylmethane:

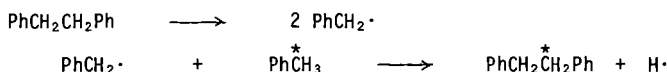


These results naturally raise the question of the role of tetralin, or of the recycle oil used in its place, during many of the solvent-refined coal processes — particularly since the solid product of such processes often contains no more hydrogen than the original coal (5). Neavel (6) examined the liquefaction of coal in tetralin and other solvents, using kinetic techniques, and found that donor and nondonor solvents appear to be equally capable in dispersing the coal after 5 minutes at temperatures of 400-570°C. Upon prolonged heating in nondonor solvents, the free radicals which form in the coal are thought to polymerize to higher molecular weight materials, whereas in the presence of tetralin, these radicals can be trapped by transfer of hydrogen.

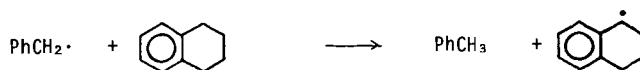
In order to test some of these concepts we carried out several experiments with carbon-14-labeled compounds. In one of these bibenzyl and toluene-¹⁴C were heated at 400° for one hour. There was intermolecular transfer of hydrogen with formation of toluene and other products, but the reisolated bibenzyl had undergone (to a small extent) an exchange reaction with toluene as shown by the fact that the reisolated bibenzyl contained carbon-14:



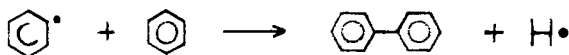
This exchange reaction must take place through a free-radical mechanism, possibly as follows:



When the two components — bibenzyl and toluene-¹⁴C — were heated in the presence of tetralin, however, there was no exchange between the two as shown by the fact that the reisolated bibenzyl was completely devoid of carbon-14. The reason must lie in the ready ability of tetralin to trap the benzyl radicals before they can react with toluene:



In several other reactions carried out with Illinois No. 6 coal and labeled substrate (e.g. α -naphthol- α - ^{14}C), the mixtures were heated for up to one hour in closed tubes at 400° , and benzene was used as a vehicle to ease material transfer. To our surprise, significant quantities of unlabeled biphenyl were discernible upon subsequent work-up. Although the yields were not determined, sufficient biphenyl was formed in one case to allow its isolation and identification by nmr. Through some as yet unexplained mechanism, a phenyl radical must have been produced, which then reacted with another benzene molecule to form biphenyl:



The presence of tetralin, however, inhibits biphenyl formation.

In an effort to determine whether tetralin does more than act as a radical scavenger during Pott-Broche-like processes, we prepared tetralin-1- ^{14}C (7) and heated it (1.933 g, 15.82 C/g , per mole) for one hour with 3.06 g of vitrain (from Illinois No. 6 coal). The product was extracted with pyridine, and the residue was treated with THF, plus a mixture of nonradioactive tetralin and naphthalene. The residue still contained carbon-14 which, on a tetralin basis represents 2.6-2.8% by weight of the residue. The pyridine soluble fraction also contained carbon-14 representing 1.6% by weight of that fraction (on a tetralin basis). Thus the tetralin- ^{14}C appears to have undergone a chemical reaction with the coal. We have previously reported (4) that tetralin and Illinois No. 6 coal when heated at 400° yield α - and β -methyl naphthalenes, in which the methyl groups undoubtedly have their origin in the coal.

The role of tetralin during coal conversion, therefore, is 1) to act as a dispersion vehicle; 2) to supply hydrogen radicals, when needed, to trap coal radicals, and 3) in a very minor way to undergo intermolecular reaction with the coal through making and breaking of C-C (and possibly other) bonds.

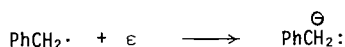
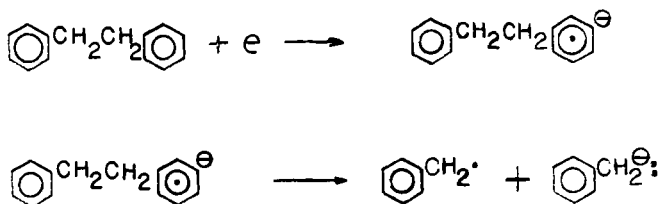
B. Reductions of Coal

Two chemical reactions for solubilizing coals have received much attention in recent years, these are 1) the Friedel Crafts reaction (8-19) and 2) reductions, either with lithium in suitable solvents (20-26), or electrolytically with lithium salts in ethylenediamine (27-32). Part of the interest in these reactions is undoubtedly due to the fact that they can be carried out at low temperatures.

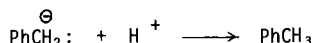
The chemical changes affected during coal reductions are usually considered to be breakage of ether and thioether linkages, as well as reduction of aromatic nuclei. Alkyl groups are not affected (33). The Birch-Hückel reaction (34) of aromatic rings to cyclic olefins is well known. It was recently reported (35) that the use of NaK in mixed ethers as a coal reductant cleaves the alkyl linking groups (e.g. $-\text{CH}_2-\text{CH}_2-$) between aromatic moieties, and results in an increase in the number of methyl groups in the reduced product. Oxidation studies (36, 37) have indicated a high frequency of ethylene connecting links in some bituminous coals, as shown by the isolation of large quantities of succinic acid. We therefore carried out the reduction of three model compounds under the conditions reported (37) by Hombach and Niemann, using glycol ethers as the solvent. The compounds chosen were diphenylmethane, bibenzyl, and 1,3-diphenylpropane. Of the three compounds, diphenylmethane exhibited some, and bibenzyl exhibited considerable C-C splitting in only 20 minutes, whereas 1,3-diphenylpropane was stable except for traces of toluene and ethylbenzene (when quenched with propanol-2). The results can be illustrated for bibenzyl, which was added to the solution (37) of "solvated electrons." The mixture was stirred for 20 minutes, then $^{14}\text{CH}_3\text{I}$ was added to the reaction mixture, followed by water and then pentane. The pentane solution was washed, dried, and subjected to g.c. analyses with an apparatus fitted with a carbon-14 radioactivity monitor (38). The

results are shown in Fig. 1. The products were separated on a preparative g.c. column (39) and identified through their nmr spectra.

Thus, to the methods previously employed for breaking bonds in coal molecules and thereby lowering their molecular weights, must now be added the use of "solvated-electrons" for breaking $-\text{CH}_2-\text{CH}_2-$ linkages. The mechanism for cleavage of bibenzyl must be approximately as follows



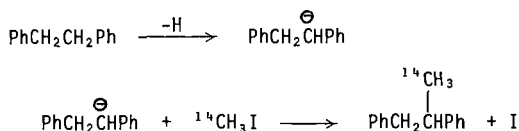
Toluene results by donation of a proton to a benzyl carbanion from the solvent:



The carbon-14-labeled ethylbenzene is formed by reaction of the benzyl carbanion with $^{14}\text{CH}_3\text{I}$:



The other product, 1,2-diphenylpropane is formed in the conventional manner:

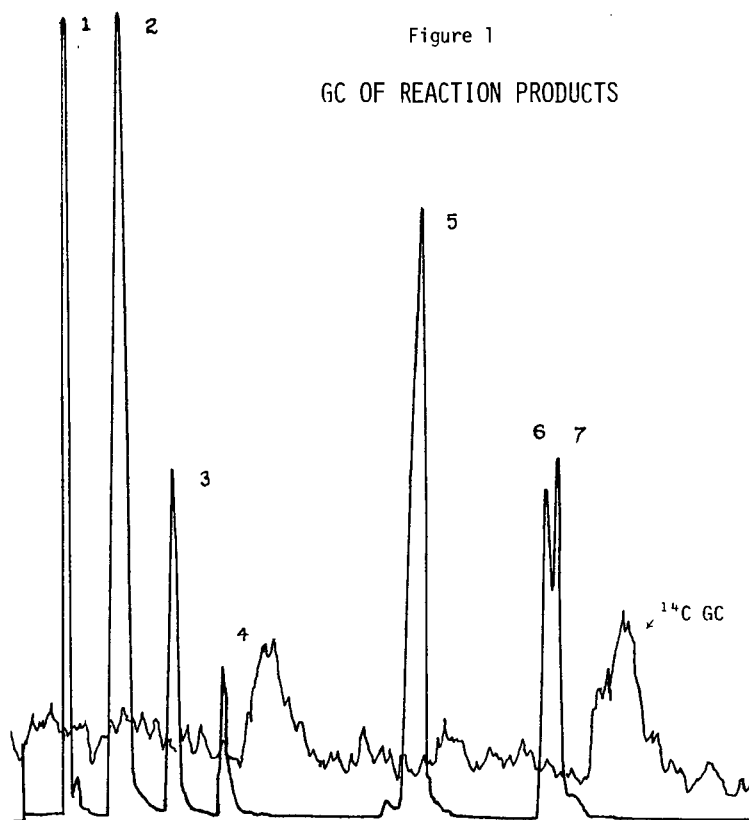


References

1. Research sponsored by the Division of Chemical Sciences, U. S. Department of Energy, under contract W-7405-eng-26 with the Union Carbide Corporation.
2. V. F. Raaen and W. H. Roark, *Fuel*, **57**, in press (1978).
3. See, for example, K. F. Schlupp and H. Wien, *Angew. Chem. Int. Ed. Engl.*, **15**, 341 (1976).
4. C. J. Collins, B. M. Benjamin, V. F. Raaen, P. H. Maupin and W. H. Roark, "Organic Chemistry of Coal," ACS Symposium Series No. 71, J. W. Larsen, Ed., Chapter 12, pp. 165-170 (1978).

5. D. D. Whitehurst, M. Farcasiu and T. O. Mitchell, "The Nature and Origin of Asphaltenes in Processed Coals," EPRI AF-252, pages (1) 2-17 (1976).
6. R. C. Neavel, Fuel, 55, 237 (1976).
7. C. J. Collins, J. Amer. Chem. Soc., 73, 1038 (1951).
8. C. Kröger, H. de Vries, Justus Liebigs Ann. Chem., 652, 35 (1962).
9. C. Kröger, H. G. Rabe, B. Rabe, Brennstoff Chem., 43, 179 (1962).
10. C. Kröger, H. G. Rabe, B. Rabe, Erdöl Kohle Erdgas Petrochem., 16, 21 (1963).
11. C. Kröger, Forschungsber. Nordrhein-Westfalen Nr., 1488 (1965).
12. W. Hodek, F. Meyer, G. Kölling, Amer. Chem. Soc. Symposium Ser., 55, 408 (1977).
13. W. Hodek, 7. Internat. Conf. on Coal Science, Prag 1968.
14. M. S. Iyengar, D. D. Banerjee, D. K. Banerjee, Nature (London), 186, 388 (1960).
15. F. Micheel, D. Laus, Brennstoff Chem., 47, 345 (1966).
16. F. Micheel, L. Rensmann, Makromolekulare Chem., 65, 26 (1963).
17. A. H. Haines, F. Micheel, Makromolekulare Chem., 80, 74 (1964).
18. F. Micheel, H. Licht, Makromolekulare Chem., 103, 91 (1967).
19. W. Hodek, G. Kölling, Fuel, 52, 220 (1973).
20. L. Reggel, R. A. Friedel, I. Wender, J. Org. Chem., 22, 891 (1957).
21. P. H. Given, V. Lupton, M. E. Peover, Nature (London), 181, 1059 (1958).
22. L. Reggel, R. Raymond, S. Friedman, R. A. Friedel, I. Wender, Fuel, 37, 126 (1958).
23. L. Reggel, W. A. Steiner, R. A. Friedel, I. Wender, Fuel, 40, 339 (1961).
24. H. W. Sternberg, C. L. Delle Donne, L. Reggel, I. Wender, Fuel, 43, 143 (1964).
25. L. Reggel, I. Wender, R. Raymond, Fuel, 43, 75 (1964).
26. L. Reggel et al., US Department of Interior, Bureau of Mines, Bulletin No. 615 (1965).
27. P. H. Given, M. E. Peover, Fuel, 39, 463 (1960).
28. R. E. Markby, H. W. Sternberg, I. Wender, Nature (London), 199, 997 (1963).
29. H. W. Sternberg, C. L. Delle Donne, R. E. Markby, I. Wender, Advan. Chem. Ser., 55, 516 (1966).
30. See also J. A. Franz and E. W. Skiens, Fuel, 57, 502 (1978).

31. H. W. Sternberg, R. E. Markby, I. Wender, J. Amer. Chem. Soc., 89, 186 (1967).
32. J. D. Brooks, R. A. Durie, H. Silberman, Australian J. Chem., 17, 55 (1964).
33. See, for example, A. J. Birch, G. Subba Rao, Advances in Organic Chemistry, 8, 1 (1972).
34. H. P. Hombach, K. Nieman, Ergänzungsband der Zeitschrift Erdöl und Kohle, Erdgas, Petrochemie, Compendium 1977/1978, p. 295-310.
35. V. F. Raaen, unpublished work (1975).
36. N. C. Deno, B. A. Greigger, S. G. Stroud, Preprints of Papers Presented at Anaheim Cal., March 12-17, 1978, Division of Fuel Chemistry of the American Chemical Society, 23, No. 2, Pages 54-57.
36. Klaus Niemann, Ph.D. Dissertation, "Reduktion von Kohle mit Hilfe solvatisierter Elektronen," Abteilung für Chemie an der Ruhr-Universität Bochum (1977).
37. A Barber-Coleman Series 5000 g.c. fitted with radioactivity monitor was employed.
38. Varian Aerograph Series 2800.



- 1 pentane
 2 1,2-dimethoxyethane
 3 toluene
 4 ethylbenzene
 5 2,5,8,11-tetra-oxadodecane
 6 1,2-diphenylethane
 7 1,2-diphenylpropane

The Effect of Reagent Access in Coal Reactivity

John W. Larsen^{1a,b}, P. Choudhury^{1a}, Tom Greene^{1a}
and E.W. Kuenmerle^{1a}

Department of Chemistry, University of Tennessee
Knoxville, Tennessee 37916
and Oak Ridge National Laboratory, P.O. Box X
Oak Ridge, Tennessee 37830

Hypothesis: The reactivity of bituminous coals under mild conditions is dominated by the accessibility of the reacting groups in the coal to reagents and not by the intrinsic reactivity of those groups. Evidence for this hypothesis will be presented. It is not conclusive evidence, but it is sufficient to warrant further exploration of this idea.

Bituminous coals contain cross linked, three dimensional macromolecular networks. Perhaps the best evidence for this comes from experiments in which the coal is swollen by solvents (1). The weight increase in several coals which have been exhaustively extracted with pyridine are shown in Table 1. These coals can be swollen to about twice their original volume by absorbing solvent. The solvent-coal interactions responsible for this inhibition are strong enough so that if the coal "molecules" were not covalently linked together, they would dissolve. The observed behavior is characteristic of a cross linked macromolecular network (2,3,4).

Coal is a highly porous, insoluble material. An attacking reagent has access to those parts of the surface of the coal which form the walls of the pores into which it can diffuse. Any solvent which expands the pore structure will enhance a coal's reactivity by increasing the surface area accessible to the reagents. One limitation on coal reactivity is the ability of reagents to penetrate the pore structure.

However, even ready penetration of the pores only gives access to the surface of the coal. For complete reaction, the reagent must diffuse into the coal network and penetrate to the bonds or groups with which it will react. It would seem that this diffusion process is likely to be very slow, and indeed may limit not only the rate of reaction but also the number of groups which ultimately react. Some examples of access limited reactions follow.

Analysis for Phenolic Hydroxyl. Maher and O'Shea (5) measured the phenolic hydroxyl content of Greta coal (DAF 82.4%C, 6.2%H, 1.7%N, 1.0%S) by titration in ethylenediamine solvent. They also extracted the coal with various solvents and measured the OH content of the extract and the residue. The data are shown in Table 2 and it is obvious that the results with the extracted coals are greater than that obtained with the whole coal. Precautions were taken to prevent oxidation and the generation of new phenolic OH groups by depolymerization seems unlikely. An increase in the accessibility of OH groups is the most reasonable explanation.

Friedel-Crafts Acylation. The Friedel-Crafts acylation of coals give products whose "solubility" increases with the size of the acyl group (6). These products are of very high (10^5 - 10^6) molecular weight (7). The proton nmr and ^{13}C nmr of octanoylated Bruceton coal are shown in Figs. 1 and 2. Peaks due to aromatic protons are absent from the proton nmr. The peaks due to the methylene α and β to the carbonyl group are broadened, while the methylene peaks at the terminal end of the chain show normal line widths. These data can be explained if acylation occurred at the coal surface and the resulting substance was solubilized, micelle like, by the interactions of the long chain with the solvent. The aromatic protons would still be in a solid environment, and their absorption would be too broad to detect. The motion of the portion of the acyl chain close to the coal surface would be hindered by close packing, giving rise to broad lines. The other end would have free motion and normal line widths as observed.

Heredy-Neuworth Depolymerization. Using currently accepted models for bituminous coal, it is clear that any reaction which cleaves the bonds between aromatic carbons and methylene groups should result in destruction of the coal and the products of low molecular weight products. The Heredy-Neuworth depolymerization is one such reaction (8,9). When applied to coal it gives mostly high molecular weight products, 80% greater than 3000. The colloidal material from a depolymerization can be further depolymerized if reacted again. The cleavage of these bonds in model compounds is not a slow reaction. These results can be explained by postulating limited access of the necessary reagents to the interior of the coal.

There are reactions which produce low molecular weight products from coals. Heat has ready access to the interior of coal, so pyrolysis would be expected to, and does, rapidly destroy the network and produce low molecular weight products. Vigorous reactions, such as oxidation, can chew their way into the coal by cutting small molecules off of the surface. This requires vigorous, unselective reactions. The attempts to use mild, selective reactions to solubilize coal lead to high molecular weight products.

If the hypothesis stated here is correct, its consequences for coal chemistry and processing will be enormous. Methods for gaining ready, rapid access to the interior of the coal network should be sought. The discovery of such methods will allow rapid, mild processing of coals. If rapid access cannot be obtained, pyrolysis may be the necessary first step of any process rapid enough to be commercially attracted.

Acknowledgement. We are grateful to the Department of Energy for support of this work and to EPRI for support of the acylation studies.

References

1. a) Department of Chemistry, University of Tennessee, b) Chemistry Division, ORNL.
2. This idea was first brought to our attention by Frank Mayo, and we acknowledge this with thanks.
3. P.J. Flory, "Principles of Polymer Chemistry", Cornell University Press, Ithaca, N.Y. 1953.
4. L.R.G. Treloar, "The Physics of Rubber Elasticity", Claredon Press, Oxford, 1975.
5. T.P. Maher and J.M. O'Shea, *Fuel*, 46, 286 (1967).
6. W. Hodek and G. Kolling, *Fuel*, 52, 220 (1973).
7. H.-P. Hombach, Ph.D. Thesis, Westfalischen Wilhelms-Universitat, Munster, 1972.
8. L.A. Heredy and M.B. Neuworth, *Fuel*, 41, 221 (1962).
9. For a review of the early chemistry of this reaction see J.W. Larsen and E.W. Kummerle, *Fuel*, 55, 162 (1976).

Table 1. Swelling^a of Four Pyridine Extracted Coals with A Series of Organic Solvents.

Coal	Toluene	Ethanol	Acetone	1,4 Dioxane	Pyridine
N.D. Lignite	1.20	1.35	1.44	1.49	1.82
Wyodak	1.33	1.43	1.54	1.71	2.16
Ill. No. 6	1.44	1.41	1.54	1.83	2.18
Bruceton	1.43	1.39	1.46	1.78	2.03

a) Ratio: weight of swollen coal at equilibrium: original weight of coal.

Table 2. Sum of phenolic groups in extracts and residues Basis: 100g of d.a.f. coal: 160 milliequivalents (from ref. 5).

Solvent	Extract		Residue		Total milli-equivalents
	Weight (g)	Total acidity (m.equiv./g)	Product (m.equiv.)	Weight (g)	
Iso-amyl alcohol	2.2	N.D.	N.D.	97.8	>195
Dimethyl formamide	22	3.21	71	78	176
Diethylamine	4.1	1.73*	7	95.9	185
Pyridine	16	2.51	40	84	178
Aniline	15	2.82	42	85	187
Ethylenediamine	23	2.88	66	77	172
Chloroform	4.7	0.92	4	95.3	161
Dichloromethane	2.0	0.30	1	98	293
				2.32	228

* Approximate figure only, obtained from stirred extractor experiment where yield was 3.5 per cent.

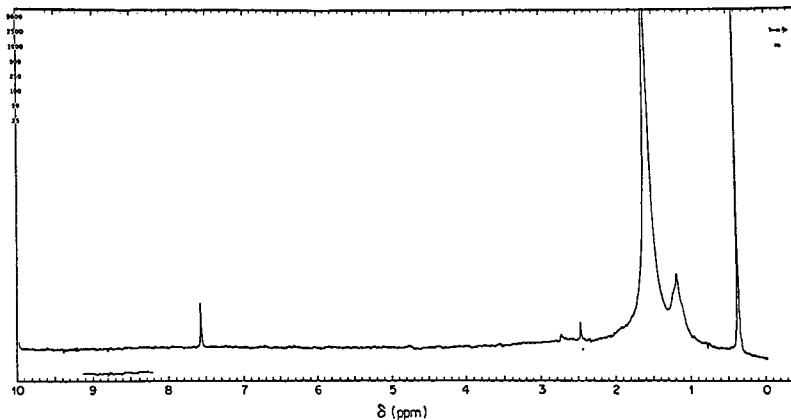


Fig. 1. Proton NMR Spectrum of Octanolyated Bruceton Coal in CDCl_3 .

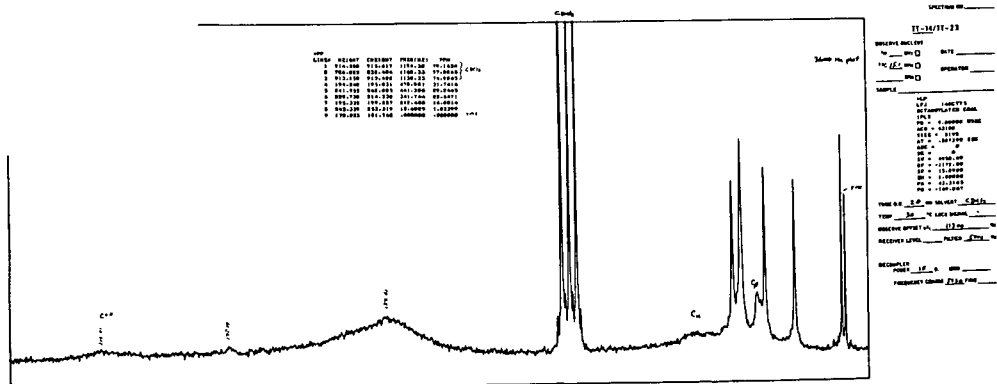
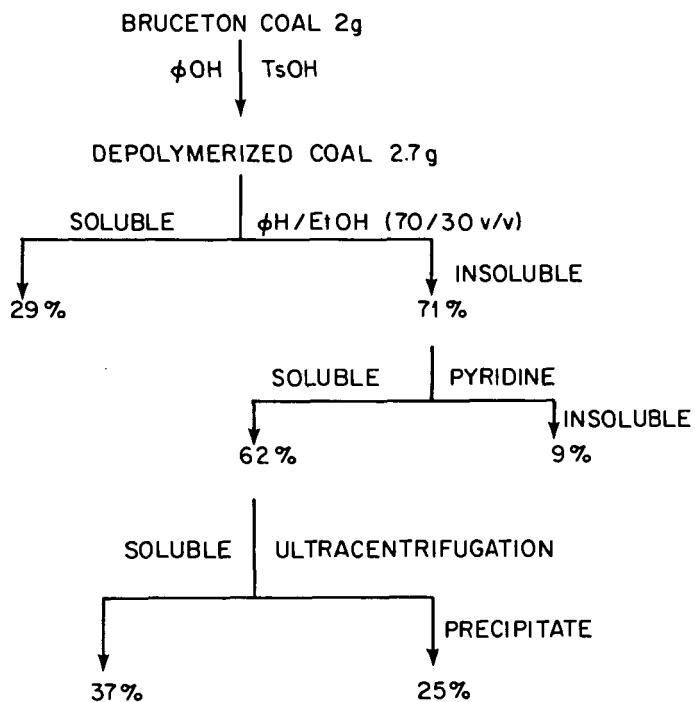
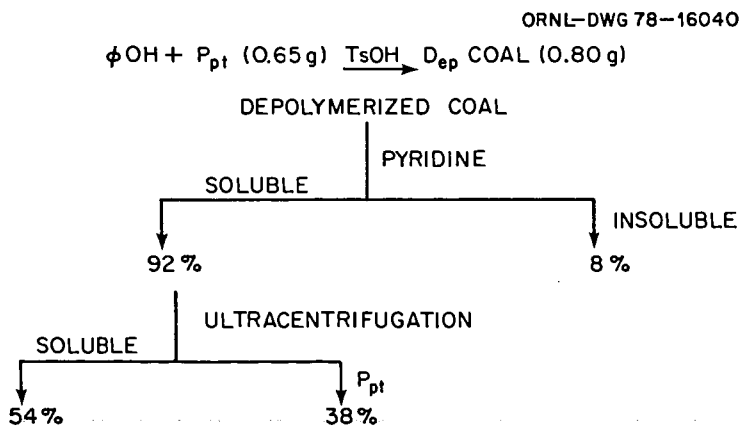
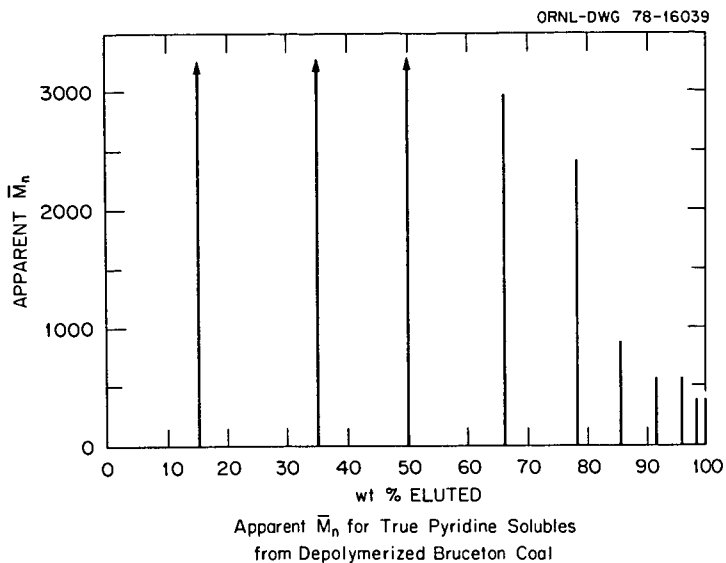


Figure 2. ^{13}C nmr Spectrum of Octanolyated Bruceton Coal (CDCl_3 solvent).





THE PHYSICAL STRUCTURE OF BROWN COAL

R.J. Camier, S.R. Siemon, H.A.J. Battaerd and B.R. Stanmore

Department of Chemical Engineering,
University of Melbourne,
Parkville, Vic. 3052.

Introduction

The behaviour of coal during processing is determined by its physicochemical composition and structure. The examination of the coal "molecule" has been hampered by the inability to find techniques which measure any meaningful properties of such large complex structures. Most attacks on the problem have been by means of breaking down the structure into smaller, more tractable pieces, examining these and inferring the original structure. With bituminous coals the severity of the treatment needed to rupture the molecules raises doubts as to the validity of the method. There is uncertainty even with brown coals which are geologically younger and bear more resemblance to the molecules of classical organic chemistry. This is reflected, for instance, in the diversity of models proposed for basic molecular arrangement (1-5).

Brown coals have the advantage that they can be broken down by the comparatively gentle treatment of alkali digestion (6) into fragments in the micron and submicron range. This results in a soluble fraction of humic acids and an insoluble residue, humins. With Victorian coals it has been found that maximum digestion occurs at pH 13 to give humic acid yields ranging from 15 to 40% of the dry coal mass (7).

This paper reports on a study of digested coal fractions which were subjected to particle size analysis using sedimentation techniques. For the humins fractions a gravitational sedimentation technique was adopted while the more finely divided humic acids required an ultracentrifuge to generate a sufficiently large force field. The nature of the fragments generated by this technique has resulted in a modified hypothesis of coal genesis.

Experimental

The coal examined was a sample of medium-light earthy coal from the Yallourn mine in the Latrobe Valley, Victoria. Its ultimate analysis on a d.a.f. basis was C 65.6%, H 5.18% and oxygen by difference 27.95%. A stock sample was prepared by wet ball milling, followed by further size reduction in a domestic food pulper and was then stored under water in a closed vessel.

For each test a 15 ml quantity of slurry was mixed with 500 ml quantity of 0.1 M NaOH solution to maintain pH at 13. After digesting overnight the slurry was wet-screened on a B.S. 350 mesh screen to remove +43 μ m oversize particles. The under-flow was then passed through a micropore filter of nominal pore size 1.2 μ m. The coal thus been fractionated by particle size into humins (the +43 μ m and the -43 μ m + 1.2 μ m fractions) and humic acids (-1.2 μ m fraction).

Some of each of the fractions was acid washed to remove sodium and reprecipitate the humic acids. A yellow supernatant liquid remained after precipitation of the humic acids, due to small quantities of fulvic acid. An elemental analysis was then carried out on the dried solids of each fraction.

Other samples of alkaline slurry were subjected to particle size analysis by sedimentation. With the -43 μ m + 1.2 μ m fraction this was done in a 50 mm diameter settling column with a tared pan at the base to continuously record the mass of sedimented solid. The data was analysed by the method of Odén (8) and the particle size distribution (Stokesian diameter) expressed on a mass % basis was calculated.

The humic acid fraction (-1.2 μ m) which was a dark brown suspension containing 4.7 mg/l of coal did not settle even after standing for six months. This slurry was

spun in a Beckmann ultracentrifuge with special long tubes to generate high g values. Alkali-resistant polyallomer tubes were used so that the solids which collected in the base could be removed in a special guillotine, then dried and weighed. The heights of suspension charged varied from 10 to 80 mm and rotational speeds up to 40 000 rpm were used. The data was again analysed by Odén's method, modified according to Brown (9).

Results

A typical output from the sedimentation balance for $-43\ \mu\text{m} + 1.2\ \mu\text{m}$ material so shown in Fig. 1. The occurrence of distinct peaks indicates that groups of closely-sized particles are present, the smallest being about $6\ \mu\text{m}$ in effective (Stokesian) diameter. The persistent appearance of the same size groups in all tests at different pH and with different coal types suggested that some fundamental unit was present. A microscopic examination of the material revealed that cylindrical rods about $0.9\ \mu\text{m}$ in diameter and $6\text{--}8\ \mu\text{m}$ long were common. When the drag coefficient for such particles was calculated from Lamb's formula for cylinders at low Reynolds' number (see Prandtl (10)), the terminal setting velocity was the same as for a spherical particle of about $6\ \mu\text{m}$ diameter.

The larger particle sizes could thus be accretions of these basic units and a number of such agglomerations were noted. The rods were arranged side by side, close packed in bundles. It appears that the alkali peels these rods from the coal mass and they subsequently agglomerate in solution, doubling in volume at each coalescence.

Elemental analyses of the fractions showed the 'rod' fraction ($-43\ \mu\text{m} + 1.2\ \mu\text{m}$) is rich in both hydrogen and carbon compared with the original coal, Fig. 2 although the effect is partly obscured by the oxidation which takes place in alkaline solution. The same trends appeared in all coal samples tested.

The particle size distribution for the humic acid fraction is depicted in Fig. 3. No material sedimented out until the most extreme conditions were applied (40 000 rpm for 24 h), when some lightening of colour at the top of the solution was observed. The sedimented particles had a Stokesian diameter of around $2\ \mu\text{m}$, which means that a particle size gap of three orders of magnitude exists between these and the next largest particles detected ($5\ \mu\text{m}$). Taking the density of coal substance to be $1.43\ \text{g/cm}^3$, a solid sphere of diameter $2\ \mu\text{m}$ would have a molecular mass of 4,000. If the molecules were rod-shaped, even smaller molecular masses would be predicted. Literature values of the molecular mass of regenerated humic acids range between 800 and 20 000 with the values clustering around 1,000 and 10,000 (11,12,13).

Since the humic acid fraction constitutes 30% of the dry coal mass, about one third of the coal is in the form of small macromolecules, and bound to the coal structure with bonds weak enough to be disrupted by dilute alkali.

It is of interest to note that the particle size gap supplies a rational basis to the traditional German classification scheme of defining humic acid and humins on the basis of a particle size separation (filtration).

Discussion

The presence of geometrically uniform rods and the absence of particles over such a wide particle size range have implications for our understanding of coal chemistry and genesis. The following discussion attempts to harmonise these observations.

Three explanations have been considered to explain the rods found during this work. These are that they are:-

- i) bacterial remains
 - ii) plant cell remains
 - iii) artifacts formed during phase separation in the coalification process.
- Since bacteria, including rod-like bacilli are active during the biological digestion

stage of coalification, remnants of their protoplasm may have been incorporated into the coal matrix. If this were so, their protein content should result in a high nitrogen content and the results are listed in Table 1.

TABLE 1.
Nitrogen content (d.a.f.) of Coal Size Fraction

Material	original coal	+43 μ m	-43 μ m+1.2 μ m	-1.2 μ m
Nitrogen content (% daf)	0.75	0.63	0.78	0.70

Although the nitrogen content of the rod fraction is higher than the others, it can only be significant if the rods constitute less than about 2% of the total mass of the -43 μ m + 1.2 μ m fraction. Since their concentration appears to be much greater than this, the hypothesis is unattractive.

The abundance of identifiable cell fragments observed under the microscope lends weight to the second hypothesis. Cell sizes vary with location in the plant and remains of coniferous tracheids or other cells would be of the correct size. The composition of the rod fraction is close to that of lignin and the rods have been observed peeling off larger woody fragments. The cell remains explanation must therefore be considered as a possibility in the absence of other information.

The third hypothesis is more speculative and far-reaching in its implications. It is generally accepted (14) that the first step in the genesis of coal is the destruction of cellulose and the degradation of lignin to monomer which either is a humic acid or polymerises to give humic acids. The polymerisation of these acids takes place by condensation as indicated by the decrease in acidity with increase in molecular mass. As the concentration of monomer decreases, a gel point is reached and a giant network is formed, swollen by the solvent water. As the polymerisation proceeds further, the network will become cross-linked, resulting in shrinkage and water exclusion.

Considering macromolecules in surface energy terms, the solubility parameter has been defined as

$$\delta = \left[\frac{E}{V} \right]^{\frac{1}{2}}$$

where E is the molar cohesive energy and V is the molar volume. For two polymers A and B, the materials are compatible if (15),

$$(\delta_A - \delta_B)^2 < 4.2 \text{ kJ/l}$$

If this inequality does not hold phase separation of polymers will occur. The solubility parameter of coal over a wide range of coal ranks has been measured (15,17,18) and is plotted in Fig. 4. The value of δ falls nearly linearly from 32 to 23 as the carbon content rises from 70 to 89% and rises slowly thereafter. At 89% carbon, polar groups are largely absent and aromatisation has commenced. By extrapolation back to the 65-70% carbon range occupied by brown coals, the line is steep enough such that a difference of only 1% in carbon content is sufficient to create incompatibility between coal molecules.

A large polymer molecule is able to exist with different parts of the chain in different phases and an increase in the concentration of the species will concentrate solvated parts together as well as concentrating the precipitated parts. With two different polymers e.g. polystyrene and polybutadiene blocks of one will form within a continuous phase of the other, with domain sizes between 10 and 100 nm usual. This segregation into phases will be enhanced by the swelling effect of the remaining polymer.

In the case of coal formation, woody residues intermingle with condensation polymers which are swollen by the water-soluble products from the degradation of

cellulose and lignin. The local changes in carbon content brought about by condensation polymerisation may be sufficiently large for phase separation to occur and the rods may be formed from local high-carbon regions, compare Fig. 2. Rod-shaped inclusions are known to form in materials like polyethylene oxide/polypropylene oxide copolymers within certain concentration limits as listed below.

high concentration of A	spheres of B dispersed in A
↓	rods " " " " "
	alternate layers of A and B
	rods of A dispersed in B
low concentration of A	spheres " " " "

In this view rods are precipitates formed from the humic acid groundmass and represent a further step in the coalification chain.

The revised model of coal structure which emerges from this study envisages a gel of humic acid molecules swollen by water and incorporating particulates. These include rods and detrital matter like pollen, cell remains, exinite material etc. which are held together by the humic acid "glue". The bonds linking this mass together must be of a homopolar non-regenerable type as rheological studies of Victorian coals have shown that the bonds are broken by shear action during mechanical working and do not remake on standing (19). This excludes the hydrogen bond commonly regarded as the major bond type for brown coal gels, as hydrogen bonds are known to remake after rupture. It appears that van der Waals type bonds may hold the structure together. On rupture the water which is liberated on shearing would be able to attach at the vacant sites and thus prevent the remaking of the original stronger bonds.

Conclusions

1. Particle size analysis of alkali-digested brown coal provides a useful insight into coal structure.
2. Victorian coals contain significant quantities of cylindrical rod-shaped particles, 1 μ m in diameter and 6-8 μ m long, which are high in carbon and hydrogen.
3. No particles exist in alkali-digested coal solutions between 6 μ m and 2nm Stokesian diameter.
4. Brown coal can be regarded as a gel of humic acids which incorporates larger particles bound by non-regenerable bonds.

References

1. AGROSKIN A.A., "Chemistry and Technology of Coal", English translation from Russian, Israel Program for Scientific Translations, Jerusalem (1966)
2. FUCHS W., "Die chemie der Kohle", Springer, Berlin (1931)
3. DURIE R., in "Chemistry of Brown Coals", Coal Research in C.S.I.R.O., 6, 12, (1959)
4. BREGER, I.A., "Chemical and Structural Relationship of Lignin to Humic Substances", Fuel, 9, 204 (1951)
5. DRAGUNOV, S.S., in "Soil Organic Matter", Ed. Konova, M.M., Pergamon, London (1961) p. 65
6. MUKHERJEE, P.N., BHOWMIK, J.N. and LAHIRI, A., Fuel, 36, 417 (1957)
7. CAMIER, R.J., Ph.D. Thesis, Uni. of Melbourne, (1977)
8. ODÉN, S., Soil Science, 19, 1 (1925)
9. BROWN, C., "Particle Size Distribution by Centrifugal Sedimentation", J. Phys. Chem, 48, 246 (1944)
10. PRANDTL, L., "The Essentials of Fluid Dynamics", Blackie, London (1960) p. 190

11. BROOKS, J.D., "Advances in Coal Chemistry 1950 - 1970, Coal Research in C.S.I.R.O. 45, 20 (1971)
12. SAMEC, M., and PIRKMAIER, B., Kolloid - Z., 51, 96 (1930)
13. FUCHS, W., Brennstoff - Chem., 9, 178 (1928)
14. FLAIG, W., "The use of Isotopes in Soil Organic Matter Studies", Pergamon, New York (1966)
15. BRANDRUP, J., and IMMERGUT, E.H., "Polymer Handbook", Wiley, New York (1966)
16. VAN KREVELEN, D.W., Fuel, 44, 229 (1965)
17. KIROV, N.Y., O'SHEA, J.M. and SERGEANT, G.D., Fuel, 46, 415 (1967)
18. SANADA, Y., and HONDA, H., Fuel 45, 451 (1966)
19. COVEY, G.H., and STANMORE, B.R., "The Rheological Behaviour of Victorian Brown Coal", to be published, Fuel.

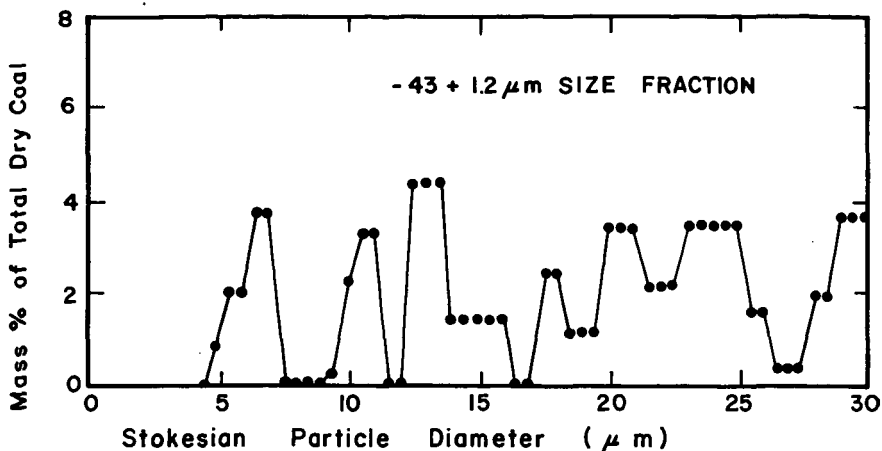


FIG. 1 PARTICLE SIZE DISTRIBUTION

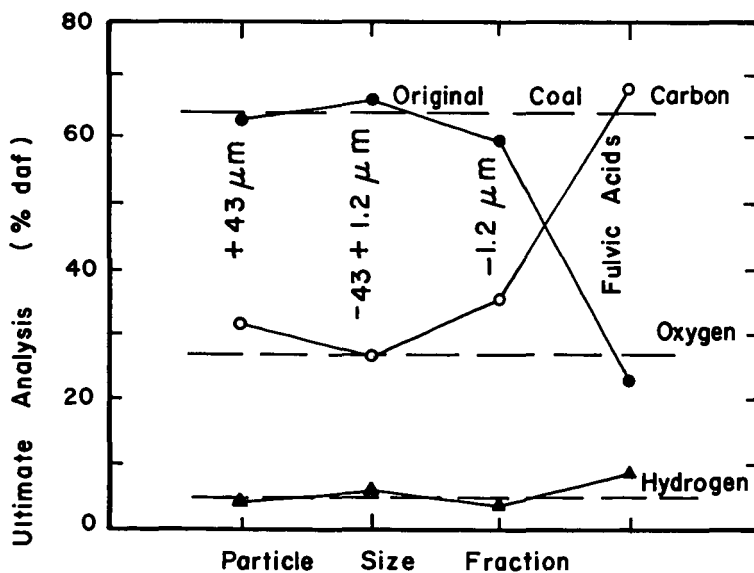


FIG. 2 ULTIMATE ANALYSIS OF FRACTIONS

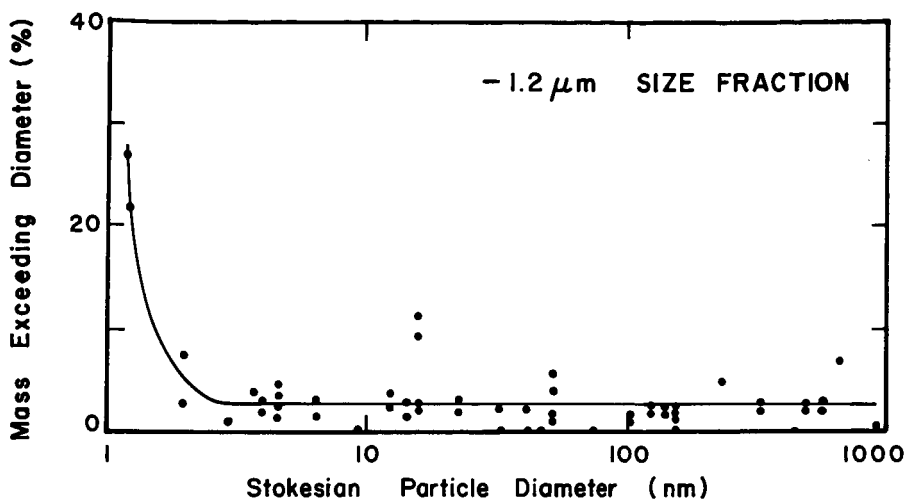


FIG. 3 PARTICLE SIZE DISTRIBUTION

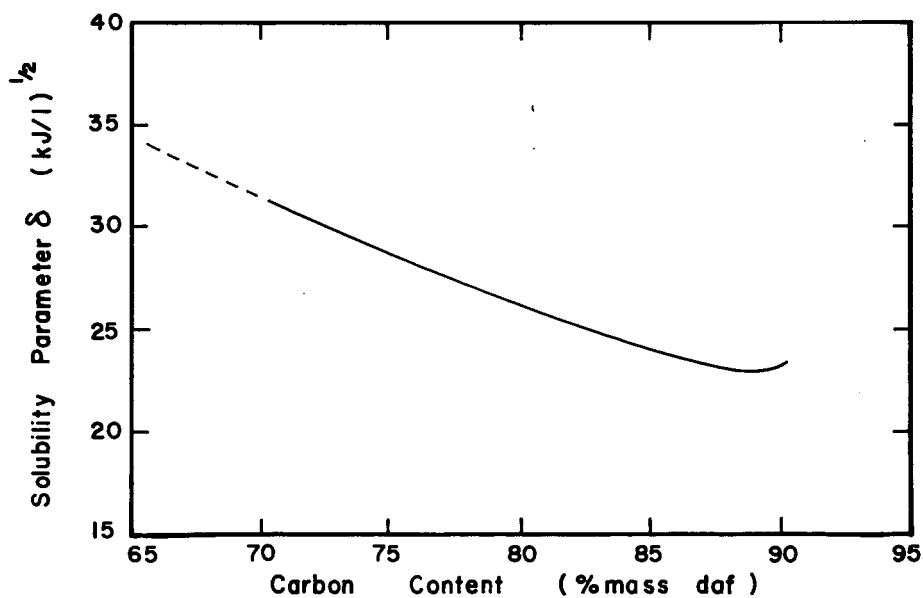


FIG. 4 SOLUBILITY PARAMETER vs % CARBON

THE ULTRAFINE STRUCTURE OF COAL DETERMINED BY ELECTRON MICROSCOPY

L. A. Harris and C. S. Yust

Metals and Ceramics Division
Oak Ridge National Laboratory
Oak Ridge, Tennessee 37830 USA

INTRODUCTION

The technological utilization of coal is dependent upon its physical characteristics as well as its chemistry. The size and spatial distribution of pores; and the size, distribution, and identity of the submicron size minerals are physical attributes of particular interest because of their influence in coal conversion processes such as liquefaction and gasification.

The present paper is one of a series in which electron microscope analyses including transmission, scanning transmission, and scanning reflection methods have been employed in examining bituminous coals (1, 2). These techniques have the advantage of revealing the microstructures of coal at magnifications substantially greater than that available with light microscopy. Consequently, a more detailed direct observation of the pores and submicron minerals within the coal may be obtained.

EXPERIMENTAL

Sample Selection and Preparation

Samples were selected from two high volatile bituminous coals, namely, Illinois No. 6 and Eastern Kentucky splint coal from Perry County. The selection of the above coals was based on the fact that both are of equal rank but of different lithotypes (i.e. maceral contents), microstructures, and geographically separated. Consequently some evaluation could be made of the variation in microscale features which could be significant in coal utilization or diagenesis.

Specimens were prepared from the above samples by slicing sections normal to the bedding and subsequently grinding them into optical thin sections approximately 10–15 μm thick. The optical sections were removed from the glass slide by acetone and thinned to electron transparency by ion bombardment (ion milled). The ion milling process was performed on fragments approximately 3 mm on edge using argon gas and a liquid nitrogen cold stage in order to ensure a sample free from thermal damage. The ion milled samples were fixed to electron microscope grids using silver conductive paint.

Analytical Methods

Both a high voltage transmission electron microscope (TEM) (1 Mv) and a scanning transmission electron microscope (STEM) (120 Kv) were used in this study. The STEM was fitted with an energy dispersion system utilizing a Si(Li) detector. Microchemical analyses of particles as small as 20 nm for elements of atomic number 11 or greater could be attained by use of the STEM and EDX.

* Research sponsored by the Division of Basic Energy Science, U.S. Department of Energy under contract W-7405-eng-26 with the Union Carbide Corporation.

RESULTS AND DISCUSSION

Figures 1 and 2 are TEM photomicrographs of specimens from the splint coal and the Illinois No. 6, respectively. The photomicrographs serve to illustrate the differences in microstructures between coals of the same rank. In general, the splint coal contains fragments of exinite, inertinite, and vitrinite closely compacted together, with the former two macerals making up over 70 volume percent of the total material. On the other hand, the Illinois No. 6 coal contains large bands of vitrinite interbedded with inertinite and exinite, where the latter two macerals combined comprise between 10 and 20 volume percent of the total macerals.

EASTERN KENTUCKY SPLINT COAL

Examination of the microstructure in Figure 1 reveals that the exinitic material (E) is essentially featureless in electron transmission. This material however, frequently contains relatively large and irregularly shaped pores (P). Immediately adjacent to the exinite is a region of vitrinite (V), containing a nearly uniform distribution of fine porosity. The boundary between the exinite and the vitrinite contains opaque fragments of mineral bearing inertinite as well as more finely divided inertinitic matter. The coarse porosity associated with the granular inertinite at the boundary is seen by detailed study to be continuous with the finer porosity that is observed in the vitrinite. This gradation of porosity from the inertinite to the vitrinite may be indicative of a transitional zone between the two macerals. The vitrinite bands observed in this field are relatively porous and as would be expected in a low density body, the porosity is highly interconnected.

The porosity associated with the exinitic maceral of the splint coal can be seen more clearly in Figure 3. The large, irregularly shaped pores often form distinct tubular channels which extend from the apparent center of the spore exinite to the boundary between the spore and the surrounding inertinite. Commonly, the channels contain spherical mineral particles, which appear to be associated with the formation of the channels. Other studies (3) on the interaction of fine metal particles on graphite surfaces have demonstrated that particulates can catalyze surface reaction and lead to generation of elongated pores of the type shown here. The particles in the exinite were identified by means of EDX analyses and selected area diffraction (see inserts in Figure 3) as the mineral aragonite (calcium carbonate) which presumably enters the exinite from the granular inertinite that typically surrounds the spore exines. Usually, the granular inertinite contains an appreciable amount of mineral matter, primarily as clays.

Previous porosity studies of coal by gas absorption methods (4) reveal a direct relationship between the fine porosity and the vitrinite content of a coal. These observations are confirmed by this study for both the splint and Illinois No. 6 coals in as much as all the vitrinite observed by TEM was found to contain large regions of fine porosity. In Figure 4, a TEM photomicrograph of a vitrinite fragment in the splint coal, the pore sizes range from approximately 2 nm, to greater than 20 nm. The smallest pores, some of which may even be less than 2 nm, appear to be related to connecting channels or irregularly shaped pores that cannot be described as spherical. Stereo pairs of these vitrinite fragments indicate a connecting network of pores suggesting high permeability.

ILLINOIS NO. 6 COAL

The granular constituent shown in the Illinois No. 6 microstructure (Fig. 2) contains a broad range of interconnecting pores (~40–50 nm in dia.) which may be classified as predominantly macropores (<50 μm). The exact identity of this constituent is not clear, however, it is thought to be a mixture of inertinite and exinite. The microstructure of this coal is dominated by large vitrinite bands

(V) which are separated by the highly porous regions. Areas of apparently interconnected fine porosity can be observed in both vitrinite bands (see arrows). Also noteworthy in this microstructure are the opaque (OP) fragments that have been found to contain minerals. The opacity of the mineral regions may be due to a greater thickness of the face caused by the greater resistance minerals have to ion milling.

Figure 5 is a TEM photomicrograph of a region of vitrinite in the Illinois No. 6 coal obtained at higher magnification (50K) in order to perform a more detailed analysis of the porosity associated with this maceral. Pore dimensions range from approximately 1 to 10 nm which classifies them as a mixture of micropores (<2 μm) and mesopores (2–50 μm). The detection of porosity in the 2 dimensional image becomes more difficult as the specimen thickens. However, when viewed in 3 dimensions via a stereo pair, the porosity in the thicker regions remains clear. Three dimensional viewing also reveals that the porosity is irregularly shaped, and is often present as volumes of highly interconnecting pores. In regions of locally high porosity as is observed in the center of Fig. 5, the degree of interconnectivity is relatively great whereas in the surrounding region the pore volumes are largely isolated.

Several vitrinite fragments were found to contain bands of minerals, aligned parallel to the bedding plane of the coal (Fig. 6). Many of the minerals exhibit well developed growth habits. A size analysis of the minerals (5) by direct measurement from the TEM photomicrographs reveals that the majority of minerals were under 30 nm in diameter with the average diameter being approximately 10 nm. Larger mineral fragments up to 300 nm on an edge were recorded but comprised only a small fraction of the total observable mineral matter. Subsequent analyses of small angle x-ray scattering (6) (SAXS) from a similar sample of Illinois No. 6 coal showed a multimodal size distribution (Fig. 7) which essentially confirms the TEM observations. For example, the peak at 3 nm relates to the fine pores observed in the vitrinite component whereas the peak at 10 nm fits the average mineral diameter, and finally the peak at 25 nm accounts for the larger mineral fragment plus the larger pores observed in the granular constituent.

In addition to the microstructural studies of these two bituminous coals an effort was also made to do EDX analyses via STEM on microareas of the macerals in order to obtain data related to the composition of the coal macromolecule. However, typically, the observation of detectable elements (i.e., of atomic number 11, Na or greater) always correlated with the presence of minerals, except for sulfur. These observations, though limited, do suggest that chemical analyses of coal which report the existence of heavy metals (>Na) in coal macerals as part of the organic constituent may be suspect. As witnessed in Fig. 6, the size range for minerals can be exceedingly small, e.g. less than 2 nm in diameter thus their detection by standard techniques very improbable.

CONCLUSIONS

The shape and size of pores in two high volatile bituminous coals of differing lithotypes have been directly observed by means of transmission electron microscope (TEM). The distribution of the porosity with respect to their maceral associations were ascertained as were the sizes and distributions of the micro minerals. The use of stereo pairs reveals the interconnectivity of the pores in micro volumes of the macerals indicating a high degree of permeability within those regions.

The finest porosity was observed in vitrinite fragments of both coals and ranged in size from under 2 nm to 20 nm in diameter, with the majority in the smaller end of the size range. On the other hand, inertinite appears to be the most porous maceral and typically contains a broad range of pores from 5 through 50 nm. Much

of the inertinite is granular material varying from fine to coarse grained particles with the former corresponding to micrinite.

Finally, the least porous maceral is exinite which generally appears as a featureless material except for the presence of irregular and tubular pores thought to be initiated by the catalytic action of minerals. The intimate relationship between exinite and inertinite such as exists in durains, where the inertinite contains large amounts of fine mineral matter, may therefore promote the generation of porosity in exinites.

REFERENCES

1. L. A. Harris and C. S. Yust, *Fuel*, 55, 233 (1976).
2. L. A. Harris, D. N. Braski, and C. S. Yust, *Microstructural Science*, 5, 351 (1977).
3. G. R. Hennig, *J. Inorg. Nucl. Chem.*, 24, 1129 (1962).
4. S. P. Gan. H. Nandi and P. L. Walker, *Fuel*, 51, 272 (1972).
5. R. A. Strehlow, L. A. Harris and C. S. Yust, *Fuel*, 57, 185 (1978).
6. J. S. Lin, R. W. Hendricks, L. A. Harris, and C. S. Yust, *J. Appl. Cryst.*, in press, (1978).

By acceptance of this article, the publisher or recipient acknowledges the U.S. Government's right to retain a nonexclusive, royalty-free license in and to any copyright covering the article.



Fig. 1. TEM Splint Coal (Where E = Exinite, V = Vitrinite, GI = Granular Inertinite, OP = Opaque Particles, and P = Pores in Exinites).

Fig. 2. TEM of Illinois No. 6 Coal (Where V = Vitrinite and OP = Opaque Particles).

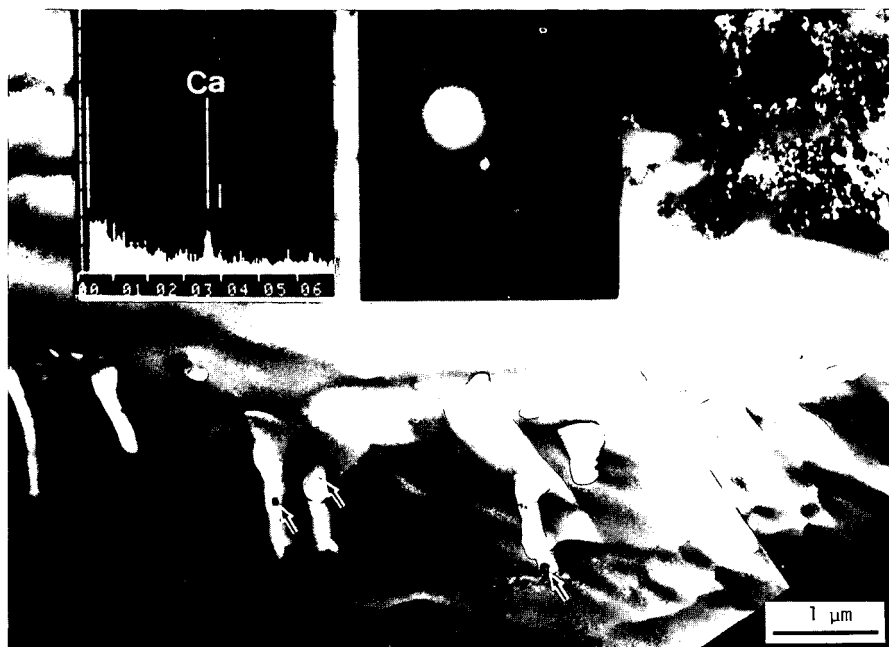


Fig. 3. TEM of Tubular and Irregular Pores in Exinite Showing the Location (See Arrows) and Identity (See Insets) of Spherical Particles.

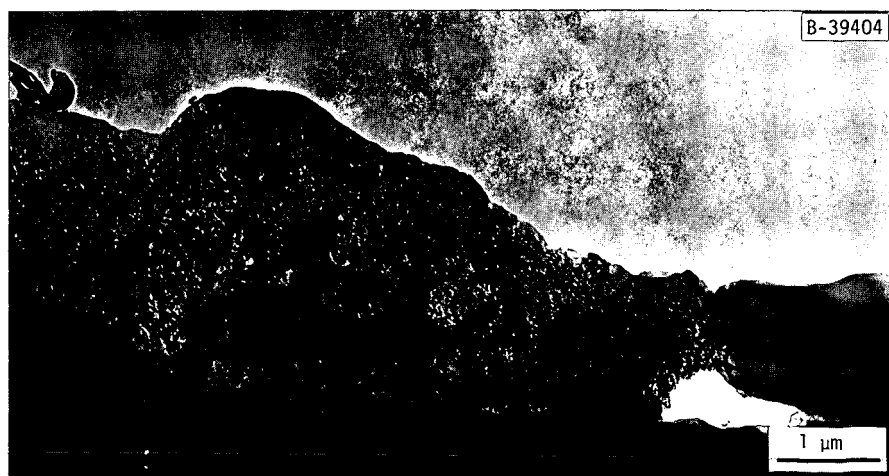


Fig. 4. Fine Porosity Observed in Vitrinite Fragment in Splint Coal by TEM.

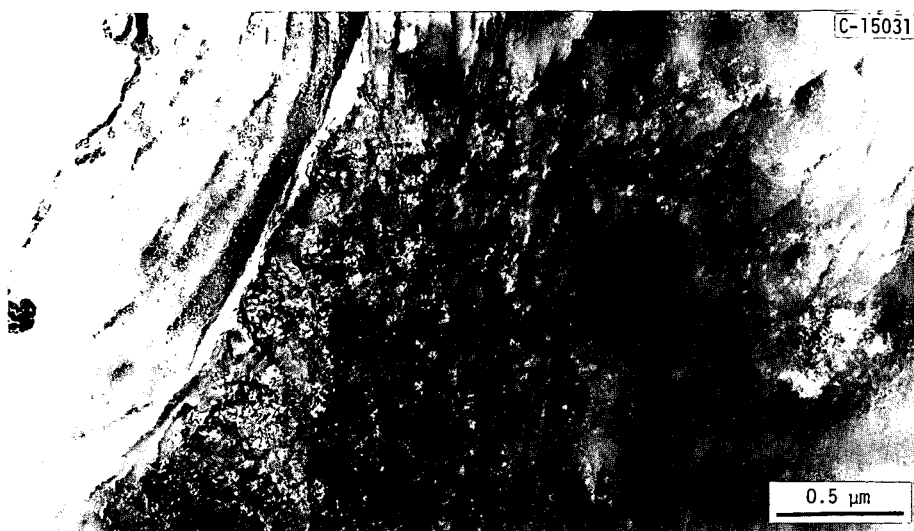


Fig. 5. Fine Porosity Observed in Vitrinite Fragment of Illinois No. 6 Coal by TEM.

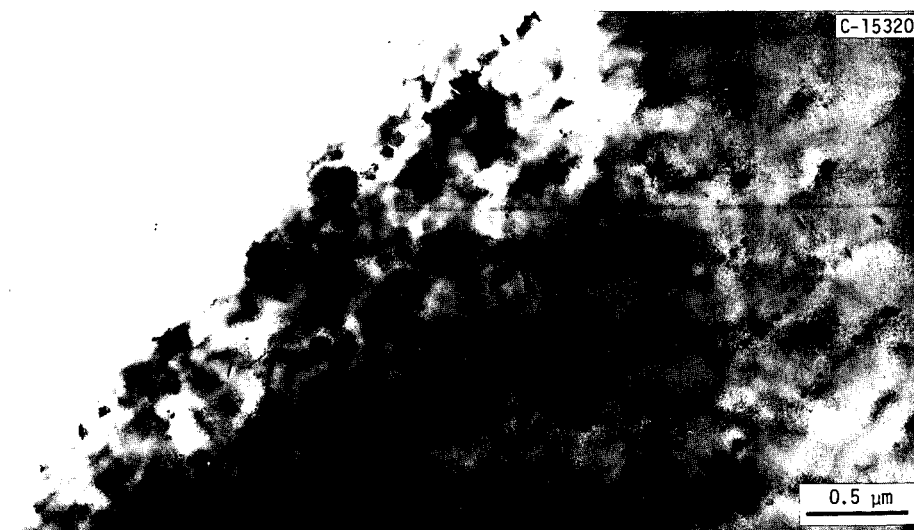


Fig. 6. TEM of Vitrinite of Illinois No. 6 Showing Bands of Minerals.

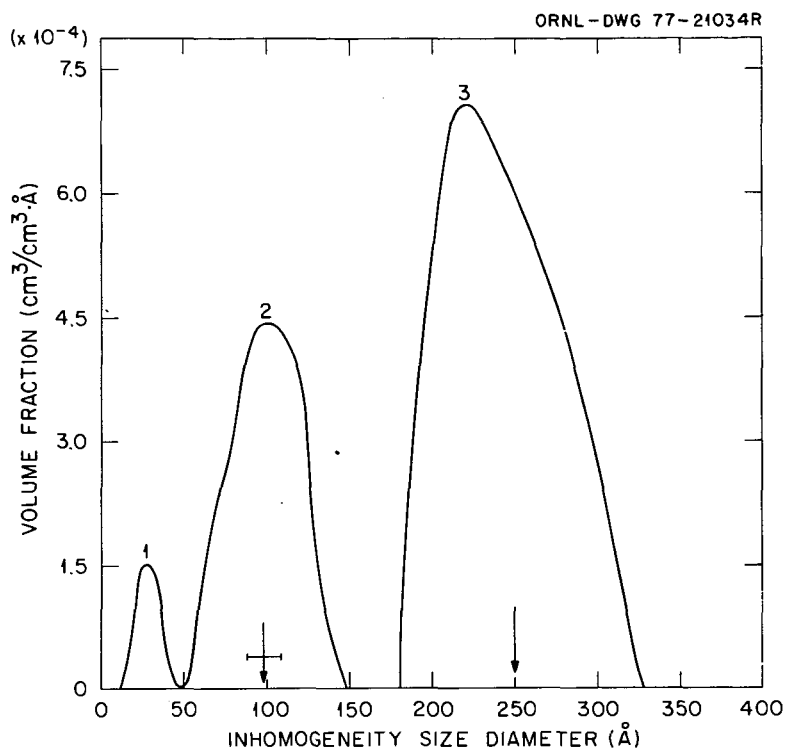


Fig. 7. The Size Distribution of Pores and Minerals from Vitrinite (Illinois No. 6) Obtained by Small Angle X-Ray Scattering (SAXS).

CHARACTERIZATION OF IRON BEARING MINERALS IN COAL

Pedro A. Montano

Department of Physics, West Virginia University, Morgantown, WV 26506

Introduction

Due to the importance of coal as a major source of energy and the environmental hazards involved in its use, considerable research has become necessary in order to a) fully understand the different compounds appearing in the coal and their transformation during processing; and b) know how those compounds contribute to the pollution of the environment, i.e., acidity of water streams near the coal mines and pollution by power plants. Some positive properties can be associated with the mineral matter in coal. For example, recently several researchers have shown that the mineral matter in the coal may play an important role in the liquefaction process (1). Of all the minerals in the coal, the iron bearing minerals seem to be the most important. In most coal utilization techniques the coal is used as raw material, and as a result both the organic and inorganic components may be critical in the acceptance or rejection of a coal for a particular process. Owing to the great importance of iron as a major constituent of the mineral matter in many coals the Moessbauer effect becomes a powerful tool in the characterization of the iron bearing minerals.

The most common use of the Moessbauer effect in mineralogy and geology has been the determination of the oxidation states of iron in various minerals (2). The study of the Moessbauer spectral area also gives valuable information on the concentration of the different minerals in rocks (2). Recently the Moessbauer effect was applied to the study of iron bearing minerals in coal and to determine the amount of pyritic sulfur (3,4,5).

In what follows the application of Moessbauer spectroscopy (^{57}Fe) to determine the iron bearing minerals will be described and a critical view of the advantages and disadvantages of the technique will be presented. In this study more than 200 coal samples were investigated and more than 2000 Moessbauer runs were carried out on those samples. Before going into the experimental results, a brief description of the Moessbauer parameters which give the necessary information to determine the compounds seems appropriate.

Moessbauer Parameters

Isomer Shift (IS): The shift observed in the Moessbauer lines with respect to zero velocity is produced by the electrostatic interaction of the nuclear and s-electrons charge distributions. It is given in the non-relativistic approximation by (6)

$$\text{IS} = \frac{2\pi}{5} ze^2 (R_{\text{ex}}^2 - R_{\text{gd}}^2) \{ |\psi_{\text{ahs}}(0)|^2 - |\psi_{\text{source}}(0)|^2 \} \quad 1)$$

The IS gives valuable and unique information on the valence states of iron, in special for high spin Fe^{2+} and Fe^{3+} .

Besides the IS there exists a shift of the Moessbauer lines due to the second order Doppler effect (7). This shift is given by

$$\delta E_{\text{SODS}} = \frac{E_0}{2} \frac{\langle v^2 \rangle_T}{c^2} \quad 2)$$

where $\langle v^2 \rangle_T$ is the thermal average of the square of the velocity of the Moessbauer atom in the solid. It is a parameter that strongly depends on the lattice dynamical properties of the solid.

The hyperfine interactions affecting the Moessbauer effect are the quadrupole and magnetic interactions (2). The quadrupole interaction exists when the electrons and/or the neighboring atoms produce an inhomogeneous electric field at the nucleus, and when the nucleus possesses a quadrupole moment, Q . This interaction produces a splitting of the Moessbauer lines for ^{57}Fe given by (2)

$$\Delta E_Q = \frac{1}{2} e^2 q Q (1 + \eta^2/3)^{1/2} \quad 3)$$

where q is the electric field gradient, and η the asymmetry parameter. When q arises from the electrons of the Moessbauer atom, the temperature dependence of the QS is very pronounced, like in high spin Fe^{2+} compounds. This temperature dependence is very useful in the identification of the electronic ground state of the ion.

The hyperfine magnetic interaction arises from the interaction of the nuclear magnetic dipole moment with a magnetic field due to the atom's own electrons. In many cases Moessbauer studies at low temperatures are necessary to fully characterize a compound. In such cases one usually applies an external magnetic field. This technique is particularly useful for the study of the electronic ground state of iron ions in minerals (8,9).

A very important Moessbauer parameter is the Debye-Waller factor (DWF). The DWF depends on the temperature and is given in the harmonic approximation by (2)

$$\text{DWF} = \exp(-k^2 \langle x^2 \rangle_T) \quad 4)$$

where $\langle x^2 \rangle_T$ is the mean square displacement of the atom along the direction of the γ -ray emission. The DWF is frequently evaluated in Moessbauer spectroscopy using an effective Debye model. The DWF can be different for the same compound if the particle size is very small. One has to be aware of this problem when using the Moessbauer effect as a quantitative analytical tool.

The Moessbauer effect can be used not only for the identification of mineral species, but also for a quantitative analysis of the mineral contents. The Moessbauer spectral area is given for a single line source and absorber by (10)

$$A = p^{-1} f_s \Gamma_a \frac{\pi}{2} \sum_{n=1}^{\infty} \frac{(-1)^{n+1}}{n!} \frac{(2n-3)}{(2n-2)!} c^n \quad 5)$$

$$p = 1 - B/N(\infty)$$

$$t = n_a \sigma_o f_a$$

where B = background (non-Moessbauer radiation); $N(\infty)$ = counting rate at infinity velocity; Γ = full width of half-height of the absorption line; f_s = DWF of absorber and source; σ = absorption cross-section at resonance; n_a = number of Moessbauer atoms per square centimeter. The above formula has to be corrected for lines splitted by hyperfine interactions (11). When using the Moessbauer effect as a quantitative analytical tool, care must be taken that B , f and f_a are known. A discussion on the quantitative method of analysis will be given at the end of the paper.

Experimental Procedures

The coal samples used in this work were collected following strictly ASTM procedure D2013-72. The samples were mounted in lucite containers that were hermetically sealed. Pressed pellets of the grinded coal were also used as samples. The average surface densities of the samples used were between 150 to 300 mg/cm². Several samples from the same seam were analyzed in order to check for consistency of the results. Some runs were carried out on raw coals (not grinded) as well, for testing purposes. The bulk of the samples used in this study were from West Virginia coals. The Moessbauer spectrometer used in this work was a conventional constant acceleration spectrometer. A 50mC ⁵⁷Co:Pd source was used. The Moessbauer spectra were analyzed using a non-linear least-square fit program and assuming Lorentzian lineshapes. The measurements covered a wide temperature range. Many runs were carried out at low temperatures (4.2 K) and in the presence of an external magnetic field (40 kOe). The velocity calibration is given with respect to α -Fe at room temperature (RT).

Experimental Results and Discussion

The different iron bearing minerals detected in coal using Moessbauer spectroscopy are classified below according to their major groups, i.e., sulfides, clays, carbonates, and sulfates.

Sulfides: Iron disulfide (pyrite) is the most important of the iron bearing minerals in coal. In pyrite the iron ion is in the low spin configuration, Fe^{II}. The six d-electrons are occupying the T_{2g} ground state and no magnetic moment is present at the iron site (8). In pyrite each cation has a distorted octahedral coordination of six nearest neighbors sulfur, the octahedron being slightly compressed along one of the axis. Consequently, the crystalline field at the iron site is lower than cubic and an electric field gradient exists at the ⁵⁷Fe nucleus, producing a characteristic QS in the Moessbauer spectrum.

There is a metastable phase of FeS₂, marcasite, which is the orthorhombic dimorph of pyrite and appears also in several coals. Marcasite has slightly different IS and QS (Table 1). When the amount of marcasite in coal is more than 20% of the total iron disulfide content its detection using Moessbauer spectroscopy is possible. In general, petrographical techniques seem to be more appropriate for identification of marcasite (at least for qualitative measurements). In table 1 a list of the different iron sulfides and their respective Moessbauer parameters is given.

A typical spectrum of a coal is given in figure 1. The sample has been treated with HCl (following ASTM standard D-2492) to get rid of the non-pyritic iron (sulfates). The spectrum is typical of pyrite. All the ca. 2000 spectra run in this work show the presence of pyrite (contents ranging between 7 to 0.1%). While studying several coal macerals a new Moessbauer spectrum associated with pyrite was observed in three different samples (9) rich in framboidal pyrite. The extra Moessbauer doublet showed the same magnetic behavior as pyrite (low spin). However, its Moessbauer parameters are different and the IS suggests a smaller electronic density at the nucleus than for FeS₂. The low temperature measurements indicate that the spectrum cannot be associated with any of the other minerals. It is possible that this phase is highly disordered (or "amorphous") FeS₂.

Other iron sulfides are produced during coal processing. They are mainly pyrrhotites. For compositions varying between FeS (troilite) and Fe₇S₈ (monoclinic pyrrhotite), the compounds are referred to generally as pyrrhotites (12). The Moessbauer spectrum of iron pyrrhotites can be observed in the coal liquefaction

mineral residue. The study of these pyrrhotites is of considerable importance due to their potential use as disposable catalysts in coal liquefaction (1). It is to be noted that the presence of pyrrhotites was observed in some severely "weathered" coal. In studies carried out under a reducing hydrogen atmosphere (between RT and 400°C) the conversion of all the pyrite to pyrrhotites was observed.

Clay minerals: Clay minerals represent a large percentage of the inorganic mineral content in coal. Illite, kaolinite and mixed clays are the major clay minerals present in coal. The crystal structures of the clay minerals are basically derived from two types of sheets. A tetrahedral sheet typically made of SiO_4 units, and an octahedral sheet typically made of $\text{Al}(\text{O}, \text{OH})_6$ units (13). The ideal formula, i.e., for kaolinite is $\text{Al}_2^{3+}\text{Si}_2^{4+}\text{O}_5^{2-}(\text{OH})_4$, but as in all clay minerals, a certain amount of cation substitution is possible. In mica and its derived clay minerals, illites, the octahedral sheet contains only Al^{3+} , but in the tetrahedral sites one quarter of the Si^{4+} is replaced by Al^{3+} . The net negative charge of the layer is balanced by interlayer alkali cations which also bond the layers together. The interlayer in montmorillonite or vermiculite is occupied by H_2O and/or cations, whereas in chlorite there is a complete sheet of aluminum (magnesium) hydroxide, the brucite sheet. Continuous ranges of chemical composition are often possible between the different clays and there is a great variety of mixed layer structures. Iron can be substituted in the octahedral layer in its high-spin ferrous and ferric forms, and occasionally in the tetrahedral layer. However, the iron concentration in clays is relatively small (a few % by weight) for kaolinite and illite, the most frequently found clays in coal (14).

In general the clays appearing in the coal show slightly different Moessbauer parameters than pure clays. The usual method utilized to identify the clay minerals in coal is X-ray diffraction of the LTA, but due to the poor crystallinity of the clays in the coal the technique cannot be used for quantitative measurements. The Moessbauer effect is not much of an improvement due to the small iron content of the clays. A coal rich in clays is shown in figure 2 (about 10% mineral matter). The appearance of two peaks at higher velocity is not due to the presence of two sites in the clay or to two different clays, it is produced by szomolnokite. By treating the sample with HCl, the sulfate was washed away and the clay (possibly illite) could be clearly seen (Figure 3). Treating the coal with HNO_3 dissolves the pyritic iron and the spectrum of the clays can be detected more clearly. Figure 4 shows the Pittsburgh coal (230 mesh) shown in Fig. 1 after treatment with HNO_3 . The spectrum (notice the smaller effect) is identified as that of kaolinite (a small QS is detectable).

In general, to study the clays in coal one should treat the samples as described above, or run the experiments at low temperatures in order to resolve the overlapping lines (measurements in an external magnetic field become necessary) (8,9). Moessbauer parameters for the principal clay minerals, pure and as they appear in coal, are given in table 1.

Sulfates: The iron sulfates were detected in more than 90% of the coal samples studied. The sulfates are considered to be produced by "weathering" of the coal. The amounts detected in this study ranged from 0.2 to 0.005% of total weight.

The standard technique used for detection of sulfates is X-ray diffraction of the LTA. Nevertheless, we have observed that in some cases sulfates are present in the coal and the X-ray does not show any line attributable to them (15). The most abundant divalent iron sulfate observed in the coals studied is $\text{FeSO}_4 \cdot \text{H}_2\text{O}$ (szomolnokite), a monoclinic crystal with a tetramolecular unit cell (16). This compound

orders antiferromagnetically around 10K with an effective interval field of 359 kOe (9). Other sulfate minerals found less frequently are $\text{FeSO}_4 \cdot 4\text{H}_2\text{O}$ (rozenite), and $\text{FeSO}_4 \cdot 7\text{H}_2\text{O}$ (melanterite); anhydrous ferrous sulfate was detected when the coal was stored under vacuum. The ferric sulfates commonly observed in several coals are coquimbite and jarosites.

A word of caution concerning the presence of trivalent sulfates in the coal is appropriate here. These sulfates have in general lines which overlap with the Moessbauer pyrite lines. The result is the detection of a slightly asymmetric pyrite spectrum. If one treats the samples with HCl it will appear as if some of the pyrite has dissolved in HCl, but this is of course not true, and is the result of the presence of the iron sulfates. The ferric sulfates are easily distinguishable from pyrite. When Moessbauer measurements are carried out at 4.2K in the presence of a large external field, the characteristic hyperfine field of Fe^{3+} is detected (about 500 kOe). It was observed also that many of the ferric sulfates are formed during LTA (3).

In figure 5 a Moessbauer spectrum for a mixture of szomolnokite (A) and rozenite (B) is shown. The sample was characterized by X-ray diffraction as well as Moessbauer spectroscopy. After LTA (17) the Moessbauer spectrum shows the presence of szomolnokite (no rozenite) and ferric sulfate. This was observed for all the runs carried on the coal samples studied. In table 1 a list of the iron sulfates and their respective Moessbauer parameters is given.

Carbonates: The Moessbauer spectra of some of the coal samples show the presence of FeCO_3 (siderite). Siderite has a rhombohedral structure with an octahedron of oxygens around the iron with a small trigonal distortion along the c-axis. Siderite is magnetically ordered at low temperatures ($T_N = 38\text{K}$) with a very distinctive Moessbauer spectrum (18). During the study it was observed on several occasions that a Moessbauer spectrum appeared to be that of FeCO_3 ; however, by carrying out low temperature measurements the presence of either clay or ankerite was inferred. Ankerite $[\text{Ca}(\text{FeMg})(\text{CO}_3)_2]$ is another carbonate that appears in some coals. It is nearly impossible to distinguish ankerite from siderite using Moessbauer spectroscopy at room temperature (RT). One has to carry out low temperature measurements. In table 1 the relevant Moessbauer parameters are given for the iron carbonates observed in coal. In all the measurements no more than 0.1% siderite by weight was detected.

Other minerals: In this work no other minerals were detected using Moessbauer spectroscopy, except the ones mentioned above. However, in heavily weathered coals and coal refuse the presence of iron oxides (hematite and to a lesser extent magnetite) were observed. Pyrrhotite was also detectable in some of the heavily weathered coals. Other minerals like spharelite, chalcopyrite and arsenopyrite were not detectable in these experiments. Some of the latter minerals have been identified using scanning electron microscopy, but their presence in the coal is too small to make their contribution to the Moessbauer spectrum significant. Other sulfides like Fe_3S_4 or Fe_2S_3 (19) were not detectable in any of the samples at RT or 4.2K. No evidence of organically bound iron in coal was found for all the studied samples (20).

Moessbauer Spectroscopy as a Tool for Quantitative Determination of Pyritic Sulfur

The use of Moessbauer spectroscopy to determine the amount of iron in a sample presents several serious problems to the experimentalist. One has to know the Debye-Waller factor of pyrite and the background radiation accurately. The DWF of FeS_2 can be determined from the temperature dependence of the spectral area for pure crystals of known thicknesses. However, in many coals pyrite is highly dispersed

and form very small particles which have low crystallinity; consequently, the DWF might differ considerably from that of large FeS_2 crystals. Also, a very important source of error is the determination of the non-resonant radiation background. In all the runs carried out in this study it was observed that variations of 10 to 30% occur in background counting rates for samples of coals with the same weight per unit area. The differences are due to the heterogeneity of the mineral composition of the coals. Both photoelectric scattering (mainly by the 14.4 keV) and Compton scattering of the high energy γ -rays contribute to the background radiation. This, of course, indicates that a full analysis of the γ -ray spectrum for each sample is necessary. Any use of standards to determine the amount of pyritic sulfur will have to take into consideration the problems mentioned above (5). The use of Moessbauer spectroscopy for quantitative analysis has to go hand in hand with the standard chemical procedures (ASTM D 2492-68), as a *complementary technique and not as a substitute*. In general, the most accurate Moessbauer quantitative measurement will give an error of about 10%.

Conclusions

The Moessbauer effect has been used as an analytical tool to characterize the different iron bearing minerals in coal. It has been pointed out that by the use of low temperature measurements (in the presence of a large external magnetic field) and treatment of the coal samples all the iron bearing minerals can be correctly identified. The use of Moessbauer spectroscopy as a quantitative analytical tool presents several experimental difficulties. It is recommended that this spectroscopy be used as a *complement* to and not as a substitute for the standard techniques.

Acknowledgements

The author thanks Drs. A.H. Stiller and J.J. Renton of the West Virginia Geological Survey for their invaluable help in carrying out this investigation. The technical assistant of William Dyson in some of the measurements is gratefully acknowledged.

References

1. Thomas, M.G., Granoff, B., Baca, P.M., and Noles G.T., 1978. Division of Fuel Chemistry, American Chemical Society, 23(1):23.
2. Bancroft, G.M., 1973. Moessbauer Spectroscopy: An Introduction for Inorganic Chemists and Geochemists. New York: John Wiley.
3. Montano, P.A., 1977. Fuel 56:397.
4. Levinson, L.M., and Jacobs, I.S., 1977. Fuel 56:453.
5. Huffman, G.P., and Higgins, F.E., in press. Fuel.
6. Kistner, O.C., and Sunyar, A.W., 1960. Phys. Rev. Letters 4:412.
7. Pound, R.V., and Rebka, G.A., Jr., 1960. Phys. Rev. Letters 4:274; Josephson, B.D., 1960. Phys. Rev. Letters 4:342.
8. Montano, P.A., and Seehra, M.S., 1976. Solid State Communications 20:897.

9. Russell, P., and Montano, P.A., 1978. *Journal of Applied Physics*. 49(3):1573; 49(8):4615.
10. Lang, G., 1963. *Nucl. Instr. Methods* 24:425.
11. Housley, R.M., Grant, R.W., and Gonser, V., 1969. *Phys. Rev.* 178:514.
12. Power, L.F., and Fine, H.A., 1976. *Minerals Sci. Engng.* 8:106.
13. Millot, G., 1970. *Geologie des Argiles*. Paris: Masson.
14. Rao, C. Prasada, and Gluskoter, J. Harold, 1973. *Illinois State Geological Survey, Circular* 476.
15. Stiller, A.H., Renton, J.J., Montano, P.A., and Russell, P.E., 1978. *Fuel* 57:447.
16. Pistorius, C.W.F.T., 1960. *Bull. Soc. Chim. Belg.* 69:570.
17. The LTA was carried out by J.J. Renton at the West Virginia Geological Survey.
18. Ono, K., and Ito, A., 1964. *Journal of the Phys. Soc. of Japan* 19:899.
19. Schrader, R., and Pietzsch C., 1969. *Kristall und Technik* 4:385; Stiller, A.H., McCormick, B., Jack, Russell P., and Montano, P.A., 1978. *Journal of the American Chem. Soc.* 100:2553.
20. Lefelhocz, J.F., Friedel R.A., and Kohman, T.P., 1967. *Geochim. Cosmochim. Acta* 31:2261.
21. Thiel, R.C., and van den Berg, C.B., 1968. *Phys. Stat. Sol.* 29:837.
22. Goncharov, G.N., Ostanevich, Yu. M., Tomilov, S.B., and Cser, L., 1970. *Phys. Stat. Sol.* 37:141; Novikov, G.V., Egorov, V.K., Popov, V.I., and Sipavina, L.V., 1977. *Phys. Chem. Minerals* 1:1; Gosselin, J.R., Townsend, M.G., Tremblay, R.J., and Webster, A.H., 1976. *Solid State Chem.* 17:43.
23. Vaughan, D.J., and Ridout, M.S., 1971. *J. Inorg. Nucl. Chem.* 33:741.
24. Jefferson, D.A., Tricker, M.J., and Winterbottom, A.P., 1975. *Clays and Clay Minerals* 23:355.
25. Coey, J.M.D., 1975. *Proc. Int. Conf. on Moessbauer Spectroscopy* 333, Cracow.
26. Vertes, A., and Zsoldos, B., 1970. *Acta Chim. Acad. Sci. Hung.* 65:261.
27. Greenwood, N.N., and Gibb, T.C., 1971. *Moessbauer Spectroscopy*. London: Chapman and Hall, Ltd.
28. Hryniewicz, A.Z., Kubisz, J., and Kulgawczuk, D.S., 1965. *J. Inorg. Nucl. Chem.* 27:2513.

TABLE 1. MOESSBAUER PARAMETERS OF MAJOR IRON BEARING MINERALS AT RT.

Name	IS (mm/sec)	QS (mm/sec)	Magnetic Hyperfine Field (kOe)	Ref.
SULFIDES:				
Pyrite (FeS ₂)	0.32(2)	0.63(2)	0	*
Marcasite (FeS)	0.28(2)	0.59(2)	0	*
Troilite (FeS)	0.77(4)	0.28	310	(21)
Pyrrhotite (FeS _{1+x})	0.64 - 0.69	-0.14 - 0.32	243 - 310	(22)
	0.70	0.30	322	
Greigite (Fe ₃ S ₄)	0.40 (4.2K)	0	486 (4.2K)	(23)
	0.45	0.4	465	
Fe ₂ S ₃	0.35(6)	0.82(6)		
	0.51(12)	0.88(12)	253 (4.2K)	(19)
Sphalerite (Zn, Fe)S	0.30(2)	0.61(2)	0	*
CLAYS:				
Kaolinite	0.30	0.59	492 (4.2K)	(22)
Chamosite	0.38(5)	0.78(8)		(25)
	1.14(6)	2.57(8)		
Fayalite	1.17(6)	2.85(8)		*
	0.99(7)	1.72(10)		
Montmorillonite	0.38(8)	0.50(13)		(25)
	1.15(6)	2.81(6)		
Muskovite	0.37(5)	0.75(8)	40 (4.2K)	*
	1.17(3)	3.08(7)	500	
Glaucanite	0.36(5)	0.52(12)		(25)
	0.38(3)	1.21(5)		
	1.14(6)	2.30(6)		
Chlorite	0.17(6)	0.78(8)	505 (4.2K)	*
	1.13(4)	2.67(6)	20	
	0.34(3)	0.43(4)	0	
Illite #36 (Morris)	1.24(5)	2.60(6)		*
	1.27(3)	1.92(4)	20 - 30 (4.2K)	
Illite #35 (Fitchian)	0.28(6)	0.60(8)		*
	1.14(7)	2.77(7)		
	1.25(8)	2.54(8)	20 - 30 (4.2K)	
Illite #35 (Fitchian)	0.25(4)	0.58(6)		*
	1.05(4)	2.73(6)		
Illite #35 (Fitchian) after treatment with HNO ₃	1.20(5)	2.51(6)		

TABLE 1. (Cont.)

Name	IS (mm/sec)	QS (mm/sec)	Magnetic Hyperfine Field (kOe)	Ref.
Illite (Coal)	0.3 - 0.4 1.1 - 1.2	0.4 - 0.5 2.6 - 2.8	≈ 0 15	*
SULFATES:				
FeSO ₄				
Szomolnokite (FeSO ₄ ·H ₂ O)	1.28(2)	2.90(2)	185 (4.2K)	*
Rozenite (FeSO ₄ ·4H ₂ O)	1.18(2)	2.69(2)	359 (4.2K)	(9)
Melanterite (FeSO ₄ ·7H ₂ O)	1.32(4)	3.17(4)		*(26)
Coquimbite	1.31	3.20		(26)
Jarosit	0.39(3)	0.60(5)	550 (4.2K)	*(27)
	0.43(2)	1.1 - 1.2	470 - 480 (4.2K)	*(28)
CARBONATES:				
Siderite (FeCO ₃)	1.24(2)	1.87(10)	184 (4.2K)	(18)

(*) This work

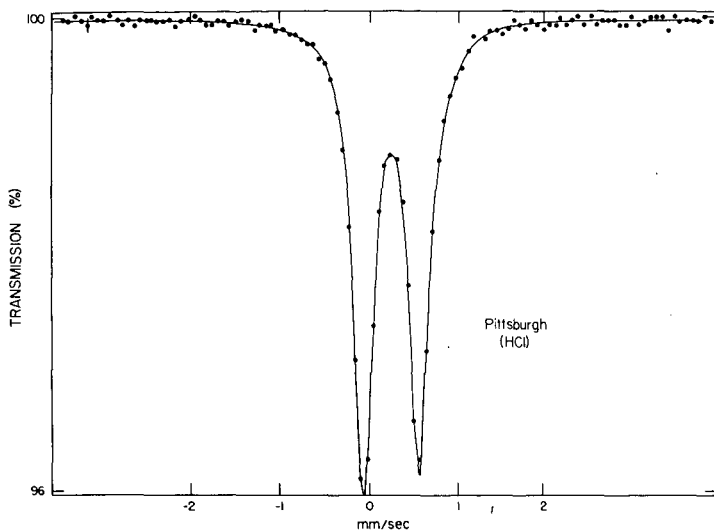


FIGURE 1. Moessbauer spectrum of a Pittsburgh coal (RT) after treatment with HCl.

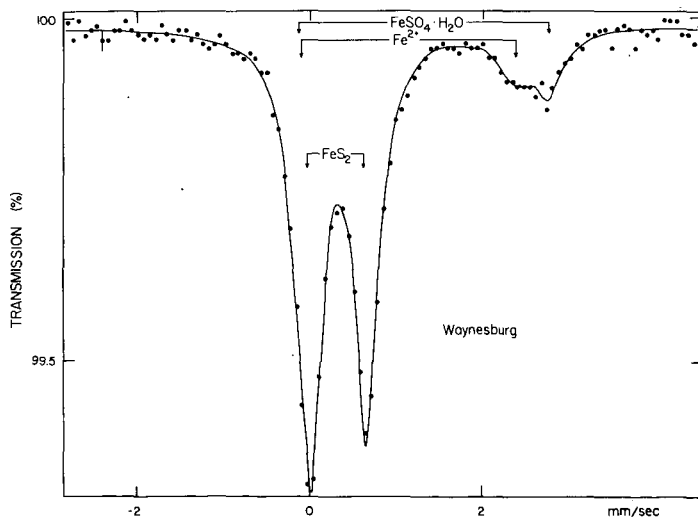


FIGURE 2. Moessbauer spectrum of a Waynesburg coal

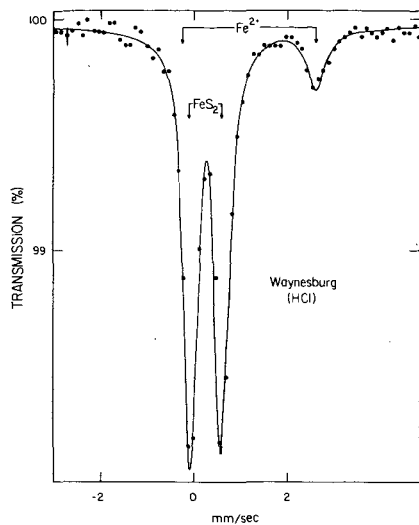


FIGURE 3. Waynesburg coal after treatment with HCl (RT).

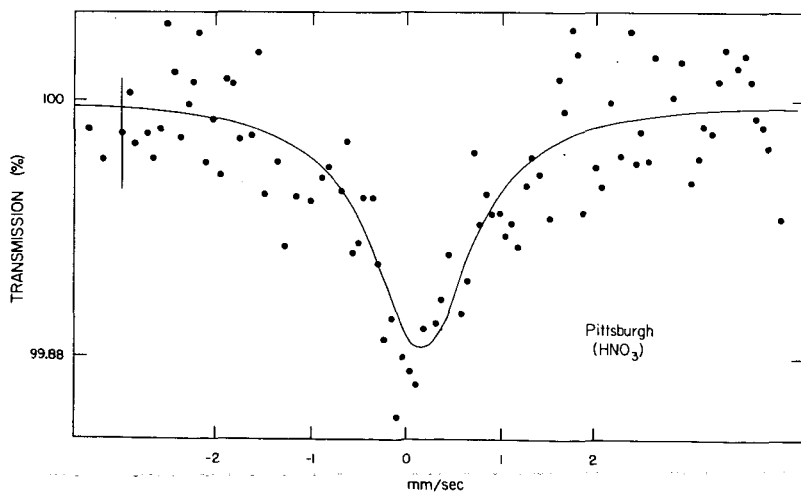


FIGURE 4. Pittsburgh coal (Fig. 1) after treatment with HNO_3

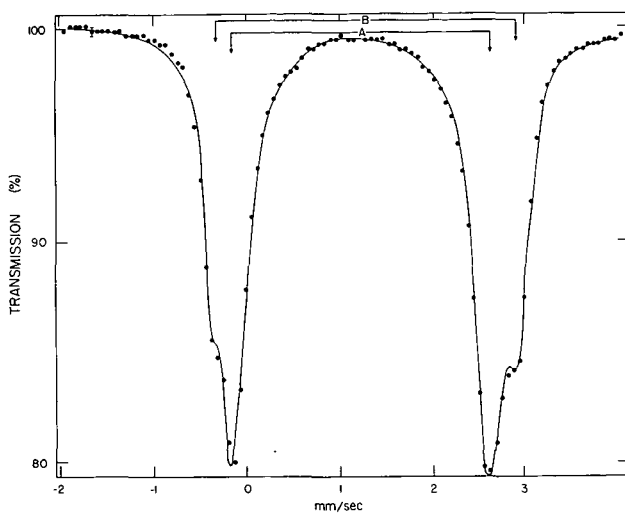


FIGURE 5. Moessbauer spectrum of szomolnokite and rozenite (RT).

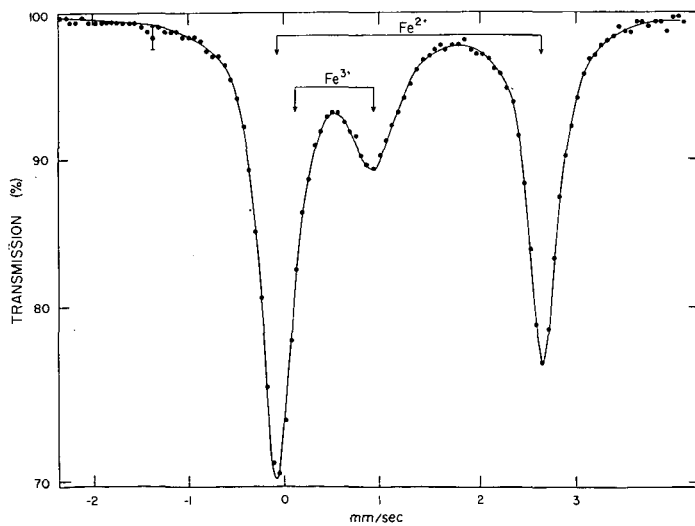


FIGURE 6. Moessbauer spectrum after LTA.